UNIVERSITAT
POLITÈCNICA
DE VALÈNCIA

MI QU ALI
Grupo de Investigación
Microestructura y Química
de Alimentos

Microencapsulation of roasted coffee oil from chitosan nanoparticles-stabilized Pickering emulsions

TESIS DOCTORAL

Presentada por:

Elisa Franco Ribeiro

Dirigida por:

Dra. Vânia Regina Nicoletti (IBILCE/UNESP – Brasil)

Dra. Isabel Hernando Hernando (MiQuAli/UPV – España)

Dra. Amparo Quiles Chuliá (MiQuAli/UPV – España)

Dª. Isabel Hernando Hernando y Dª. Amparo Quiles Chuliá, Catedráticas de Universidad, del Departamento de Tecnología de Alimentos de la Universitat Politècnica de València, y Dª. Vânia Regina Nicoletti, Catedrática de Universidad, del *Departamento de Engenharia e Tecnologia de Alimentos* de la *Universidade Estadual Paulista "Júlio de Mesquita Filho"*,

HACEN CONSTAR QUE:

El trabajo de investigación "Microencapsulation of roasted coffee oil from chitosan nanoparticles-stabilized Pickering emulsions", que presenta Dª. Elisa Franco Ribeiro para aspirar al doble título de Doctora en Ciencia, Tecnología y Gestión Alimentaria por parte de la Universitat Politècnica de València y Doctora en *Engenharia e Ciência de Alimentos* por parte de la *Universidade Estadual Paulista "Júlio de Mesquita Filho"*, y que ha sido desarrollado bajo nuestra dirección en el Grupo de Microestructura y Química de Alimentos de la Universitat Politècnica de València y en el *Instituto de Biociências, Letras e Ciências Exatas* de la *Universidade Estadual Paulista "Júlio de Mesquita Filho"*, reúne las condiciones para su aceptación como Tesis Doctoral.

Valencia, Enero 2021

Fdo. Dra. Isabel Hernando Hernando   Fdo. Dra. Vânia Regina Nicoletti

Fdo. Dra. Amparo Quiles Chuliá

UNIVERSIDADE ESTADUAL PAULISTA "JÚLIO DE MESQUITA FILHO"
Câmpus de São José do Rio Preto

Elisa Franco Ribeiro

Microencapsulation of roasted coffee oil from chitosan nanoparticles-stabilized Pickering emulsions

São José do Rio Preto - SP
2021

Elisa Franco Ribeiro

**Microencapsulation of roasted coffee oil from chitosan
nanoparticles-stabilized Pickering emulsions**

Tese apresentada como parte dos requisitos
para obtenção do título de Doutora em
Engenharia e Ciência de Alimentos, junto ao
Programa de Pós-Gradução em Engenharia e
Ciência de Alimentos, do Instituto de Biociências,
Letras e Ciências Exatas da Universidade
Estadual Paulista "Júlio de Mesquita Filho",
Câmpus de São José do Rio Preto com dupla
titulação em Ciencia, Tecnología y Gestión
Alimentaria pela Universitat Politècnica de
València.

Orientadora (UNESP): Profa. Dra. Vânia Regina
Nicoletti
Orientadoras (UPV): Profa. Dra. Isabel Hernando
Hernando
Profa. Dra. Amparo Quiles Chuliá

São José do Rio Preto - SP
2021

Elisa Franco Ribeiro

**Microencapsulation of roasted coffee oil from chitosan
nanoparticles-stabilized Pickering emulsions**

Tese apresentada como parte dos requisitos
para obtenção do título de Doutora em
Engenharia e Ciência de Alimentos, junto ao
Programa de Pós-Gradução em Engenharia e
Ciência de Alimentos, do Instituto de Biociências,
Letras e Ciências Exatas da Universidade
Estadual Paulista "Júlio de Mesquita Filho",
Câmpus de São José do Rio Preto com dupla
titulação em Ciencia, Tecnología y Gestión
Alimentaria pela Universitat Politècnica de
València.

Comissão Examinadora

Profa. Dra. Vânia Regina Nicoletti
UNESP – São José do Rio Preto
Orientadora na UNESP

Profa. Dra. Isabel Hernando Hernando
UPV – Valência
Orientadora na UPV

Profa. Dra. Amparo Quiles Chuliá
UPV – Valência
Orientadora na UPV

Prof. Dr. Paulo José do Amaral Sobral
USP – Pirassununga

Prof. Dr. Juan Andrés Carcel Carrión
UPV – Valência

Profa. Dra. Milena Martelli Tosi
USP – Pirassununga

Prof. Dr. Ellen Silva Lago Vanzela
UNESP – São José do Rio Preto

São José do Rio Preto
29 de janeiro de 2021

ACKNOWLEDGMENTS

At first, I would like to thank the *Universitat Politècnica de València* (UPV) and the *Grupo de Microestructura y Química de Alimentos* (MiQuAli) for hosting me during my stay in Spain and the *Instituto de Biociências, Letras e Ciências Exatas* (IBILCE) of the *Universidade Estadual Paulista "Júlio de Mesquita Filho"* (UNESP) for all what I have lived and learned there throughout my academic life.

Moreover, a special thanks:

To my supervisor at UNESP, Profa. Vânia Regina Nicoletti, for all her teachings, patience and support. Thank you for being so caring and providing a special working atmosphere.

To Isabel Hernando and Amparo Quiles, my supervisors at UPV, for their support and encouragement throughout these years. Thank you for all pleasant moments in Valencia. I will always be grateful for the amazing experience that I have gained by working with you.

To all other professors I have met both at UNESP (DETA) and UPV (MiQuAli and ASPA), for attention and support in this important stage of my life.

To all of my colleagues from both UNESP and UPV, for companionship, support and mainly for the fun moments. Each friendship has played a significant role at this defining moment of my life.

To Odílio Benedito Garrido de Assis, for the partnership with Embrapa Instrumentação, and for sharing his experience and knowledge.

To my family, for encouraging me throughout this journey. Thank you for all of the unconditionally love I have received, for empowering me to be and to do my best. You have been the biggest and strongest pillars of my life.

To my partner Tiago, for believing in me and for caring about me. Certainly, in the tough times, everything becomes possible with your love and patience. Thank you for being my biggest inspiration.

RESUMO

O processo de emulsificação de óleos ricos em compostos bioativos permite sua melhor aplicação e preservação ao longo do tempo de armazenamento. Dentre os vários mecanismos de emulsificação, o método de Pickering tem se destacado devido à utilização de nanopartículas sólidas naturais, em substituição aos surfactantes artificiais. Estas partículas possuem afinidade tanto pela água quanto pela fase lipídica. Elas se adsorvem na interface óleo/água de forma a estabilizar as gotas de óleo, prevenir sua coalescência e viabilizar a incorporação da fase lipídica em produtos alimentícios hidrofílicos. Entretanto, para que as partículas apresentem propriedades adequadas de adsorção, modificações químicas e/ou físicas devem ser realizadas. Devido a propriedade antioxidante, não-toxicidade e disponibilidade, este trabalho buscou analisar a quitosana e suas modificações como potencial partícula de Pickering. As modificações estudadas foram a autoagregação, ou também chamada de desprotonação, e o intercruzamento com tripolifosfato de sódio. O desempenho destas partículas foi avaliado ao emulsificar óleo de café torrado, um subproduto da indústria cafeeira com alto teor de compostos bioativos e voláteis de interesse. Posteriormente, foram analisadas as propriedades físico-químicas e estabilidade das microcápsulas produzidas após secagem das emulsões por meio das técnicas de spray-drying e liofilização. Emulsões com diferentes concentrações de óleo e de nanopartículas de quitosana foram avaliadas com relação à sua microestrutura, liberação de ácidos graxos e bioativos durante digestão gastrointestinal *in vitro* e sua bioacessibilidade. Todas as emulsões foram caracterizadas com comportamento reológico pseudoplástico, passando por desestruturação ao longo do processo de digestão. As emulsões formuladas com nanopartículas de quitosana desprotonada e menor concentração de óleo demonstraram melhor estabilização e, consequentemente, maior bioacessibilidade aos compostos fenólicos totais. As diferentes nanopartículas de quitosana foram caracterizadas quanto a sua carga superficial, distribuição de tamanho de partícula, microestrutura e afinidade pela água/óleo. Nanopartículas de quitosana desprotonadas tiveram maior tamanho de partícula, o que resultou em emulsões com gotas de óleo também maiores. Na medida em que se aumentou a concentração destas partículas, a viscosidade das emulsões foi positivamente afetada pela formação de uma rede tridimensional na fase contínua. As

nanopartículas obtidas pelo intercruzamento da quitosana com o tripolifosfato de sódio foram menores, originando emulsões com gotas também menores. A viscosidade destas emulsões foi menor e pouco afetada pela concentração de partículas. As imagens obtidas por microscopia permitiram evidenciar a estabilização das gotas pelo método de Pickering. Emulsões de Pickering contendo 10% de óleo de café torrado foram secas por spray-drying e liofilização, utilizando as diferentes nanopartículas de quitosana estudadas e maltodextrina como agentes carreadores. As microcápsulas obtidas apresentaram umidade, atividade de água e solubilidade adequadas para manuseio e estocagem. A presença das nanopartículas de quitosana permitiu maior retenção de óleo nas microcápsulas e eficiência de encapsulação. Enquanto as microcápsulas obtidas por spray-drying tiveram formato esférico mais regular, as micropartículas obtidas por liofilização foram maiores com morfologia irregular. Os compostos bioativos e propriedades antioxidantes foram melhor preservados durante a liofilização. Por outro lado, a secagem por spray-drying permitiu maior proteção destes compostos durante a digestão. As microcápsulas formuladas com nanopartículas desprotonadas foram também submetidas ao ensaio de estocagem durante 30 dias a 25 ºC. Ao longo da estocagem, avaliou-se a sua proteção contra a oxidação lipídica e liberação de voláteis. Para isso, as isotermas de sorção de água destas amostras foram previamente determinadas nas condições de armazenamento. Ambas amostras apresentaram isotermas do tipo II, possibilitando um bom ajuste do modelo de GAB aos dados experimentais. O índice de peróxido e teor de dienos conjugados resultaram em valores adequados ao longo do armazenamento, embora as amostras liofilizadas tenham apresentado ligeira tendência à oxidação devido a maior quantidade de óleo superficial. Estes resultados concordam com os dados de liberação dos compostos voláteis. Apesar de ligeiras diferenças entre as amostras secas, todas mostraram menor perda de aromas totais (~28%) quando comparadas ao óleo não-encapsulado (~51%) ao final da estocagem. Assim, pôde-se concluir que as nanopartículas de quitosana estudadas foram eficientes para encapsular o óleo de café torrado e preservar suas características contra a ação de agentes externos.

Palavras-chave: subprodutos, emulsão de Pickering, encapsulação, estabilidade, compostos bioativos.

ABSTRACT

The emulsification process of bioactive-rich oils makes possible their better application and preservation over the storage time. Among the many emulsification mechanisms, the Pickering method has been highlighted as it uses natural solid nanoparticles in replacement of artificial surfactants. These particles have affinity for both water and lipid phases. They are adsorbed at the oil/water interface in order to stabilize oil droplets, preventing their coalescence and making easier the oil incorporation into food products. However, in order to provide adequate adsorption properties to these particles, chemical and/or physical modifications must be performed. Due to the antioxidant properties, non-toxicity and availability, this work aimed at studying chitosan modifications to produce potential Pickering particles. The studied modifications comprised self-aggregation, also called deprotonation, and crosslinking with sodium tripolyphosphate. The performance of these particles was evaluated in the emulsification of roasted coffee oil, a by-product of the coffee industry with a high content of bioactive and volatile compounds of interest. Subsequently, the physicochemical properties and stability of the microcapsules produced after drying the emulsions using spray-drying and lyophilization techniques were analyzed. Emulsions with different concentrations of oil and chitosan nanoparticles were evaluated with respect to their microstructure, release of fatty acids and bioactive compounds during *in vitro* gastrointestinal digestion, as well as their bioaccessibility. All emulsions were characterized as shear-thinning, being them destabilized over the digestion process. Emulsions formulated with deprotonated chitosan nanoparticles and lower oil concentrations showed better stabilization and, consequently, greater bioaccessibility of to total phenolic compounds. The different chitosan nanoparticles were characterized regarding surface charge, particle size distribution, microstructure and oil/water affinity. Deprotonated chitosan nanoparticles had a larger particle size, which resulted in emulsions with larger oil droplets. As the concentration of these particles increased, the viscosity of the emulsions was positively affected by the formation of a three-dimensional network in the continuous phase. The nanoparticles obtained by crosslinking with sodium tripolyphosphate were smaller, resulting in emulsions with smaller droplets. The viscosity of these emulsions was lower and little affected by the concentration of particles. The images obtained by microscopy showed the stabilization of the oil droplets by the Pickering

method. Pickering emulsions containing 10% roasted coffee oil were spray-dried and freeze-dried, using the different studied chitosan nanoparticles and maltodextrin as carrier agents. The resulting microcapsules showed adequate moisture content, water activity and solubility for subsequent handling and storage. The presence of chitosan nanoparticles resulted in greater oil retention in the microcapsules and higher encapsulation efficiency. Microcapsules obtained by spray-drying had a more regular spherical shape, while the microparticles obtained by freeze-drying were larger with irregular morphology. Bioactive compounds and antioxidant properties were more preserved during freeze-drying. On the other hand, spray drying allowed greater protection of these compounds during the *in vitro* digestion. The spray- and freeze-dried microcapsules formulated with deprotonated nanoparticles were subjected to the storage test for 30 days at 25 ºC. During storage, their protection against lipid oxidation and volatile release were evaluated. The water sorption isotherms of these samples were previously determined under the storage conditions. Both samples presented type II isotherms, which resulted in a good fitting accuracy of the GAB model to the experimental data. The peroxide index and the conjugated dienes content resulted in adequate values during storage, although the freeze-dried samples showed a slightly higher tendency to oxidation due to the higher amount of surface oil. These results were in accordance to the release of volatile compounds. Although slight differences were observed between the dried samples, both of them showed less loss of total volatile compounds (~28%) when compared to the non-encapsulated oil (~51%) at the end of storage. Thus, it was concluded that the studied chitosan nanoparticles were efficient to encapsulate roasted coffee oil and to preserve its characteristics against the action of external agents.

Keywords: Pickering emulsion, encapsulation, spray-drying, freeze-drying, stability, bioactive compounds

RESUMEN

El proceso de emulsificación de aceites ricos en compuestos bioactivos permite su mejor aplicación y conservación durante el tiempo de almacenamiento. Entre los diversos mecanismos de emulsificación, se destaca el método de Pickering ya que utiliza nanopartículas sólidas naturales en sustitución de los tensioactivos artificiales. Estas partículas tienen afinidad tanto por el agua como por la fase lipídica y se adsorben en la interfaz aceite/agua para estabilizar las gotas de aceite, previniendo la coalescencia y permitiendo la incorporación de la fase lipídica en productos alimenticios. Sin embargo, para que las partículas tengan propiedades de adsorción adecuadas, se deben realizar modificaciones químicas y/o físicas. Debido a sus propiedades antioxidantes, no toxicidad y disponibilidad, en este trabajo se estudiaron distintas modificaciones del quitosano para su potencial aplicación como partícula de Pickering. Las modificaciones estudiadas fueron la autoagregación, también denominada desprotonación, y el entrecruzamiento con tripolifosfato de sodio. Se evaluó el comportamiento de estas partículas emulsionando aceite de café tostado, un subproducto de la industria de café con un alto contenido de compuestos bioactivos y compuestos volátiles de interés. Posteriormente, se analizaron las propiedades físico-químicas y la estabilidad de las microcápsulas producidas tras el secado de las emulsiones mediante técnicas de secado por atomización y liofilización. Se prepararon emulsiones con diferentes concentraciones de aceite y nanopartículas de quitosano y se estudió su microestructura, liberación de ácidos grasos y bioactivos durante la digestión gastrointestinal *in vitro* así como su bioaccesibilidad. Todas las emulsiones se caracterizaron por tener un comportamiento reológico pseudoplástico, sufriendo desintegración a lo largo del proceso de digestión. Las emulsiones formuladas con nanopartículas de quitosano desprotonadas y menor concentración de aceite mostraron una mejor estabilización y, en consecuencia, una mayor bioaccesibilidad de los compuestos fenólicos totales. Las diferentes nanopartículas de quitosano se caracterizaron estudiando su carga superficial, distribución del tamaño de partícula, microestructura y afinidad agua/aceite. Las nanopartículas de quitosano desprotonadas tuvieron un tamaño de partícula más grande, lo que dió lugar a emulsiones con gotas de aceite más grandes. A medida que se aumentó la concentración de estas partículas, se afectó positivamente la viscosidad de las emulsiones debido a la formación de una red

tridimensional en la fase continua. Las nanopartículas obtenidas al entrecruzar quitosano con tripolifosfato de sodio fueron más pequeñas, dando como resultado emulsiones con gotas más pequeñas. La viscosidad de estas emulsiones fue menor y poco afectada por la concentración de partículas. Las imágenes obtenidas por microscopía mostraron la estabilización de las gotas por el método de Pickering. Las emulsiones de Pickering que contenían un 10% de aceite de café tostado se secaron por atomización y se liofilizaron utilizando las diferentes nanopartículas de quitosano estudiadas y maltodextrina como agentes portadores. Las microcápsulas obtenidas tuvieron la humedad, actividad del agua y solubilidad adecuada para su manipulación y almacenamiento. La presencia de nanopartículas de quitosano permitió una mayor retención de aceite en las microcápsulas y mayor eficiencia de encapsulación. Las microcápsulas obtenidas por secado por atomización tuvieron una forma esférica más regular, mientras que las micropartículas obtenidas por liofilización fueron más grandes y con morfología irregular. Los compuestos bioactivos y las propiedades antioxidantes se conservaron mejor durante la liofilización. Por otro lado, las microcápsulas obtenidas por atomización presentaron mayor protección de estos compuestos durante la digestión. Las microcápsulas formuladas con nanopartículas desprotonadas fueron sometidas a almacenamiento durante 30 días a 25 ºC. Durante el almacenamiento, se evaluó la protección contra la oxidación de lípidos y la liberación de volátiles. Las isotermas de sorción de agua de estas muestras se determinaron también previamente en las condiciones de almacenamiento. Ambas muestras presentaron isotermas del tipo II, lo que permitió un buen ajuste del modelo de GAB a los datos experimentales. La determinación del índice de peróxido y del contenido de dienos conjugados dio lugar a valores adecuados durante el almacenamiento, aunque las muestras liofilizadas presentaron una ligera tendencia a la oxidación debido a la mayor cantidad de aceite superficial. Estos resultados estuvieron en concordancia con los datos de liberación de compuestos volátiles. Aunque hubo ligeras diferencias entre las muestras secas, todas mostraron menos pérdida de aromas totales (~28%) en comparación con el aceite no encapsulado (~51%) al final del almacenamiento. Así, se concluyó que las nanopartículas de quitosano estudiadas fueron eficientes para encapsular el aceite de café tostado y preservar sus características frente a la acción de agentes externos.

Palabras clave: subproductos, emulsión de Pickering, encapsulación, estabilidad, compuestos bioactivos.

RESUM

El procés d'emulsificació d'olis rics en compostos bioactius permet la seua millor aplicació i conservació durant el temps d'emmagatzematge. Entre els diversos mecanismes d'emulsificació, destaca el mètode de Pickering, ja que utilitza nanopartícules sòlides naturals en substitució als tensioactius artificials. Aquestes partícules tenen afinitat tant per l'aigua com per la fase lipídica. Les partícules s'adsorbeixen a la interfase oli/aigua per a estabilitzar les gotes d'oli, prevenint la coalescència i permetent la incorporació de la fase lipídica en productes alimentaris. No obstant això, perquè les partícules tinguen propietats d'adsorció adequades, s'han de realitzar modificacions químiques i/o físiques. A causa de la seua propietat antioxidant, de la no toxicitat i de la disponibilitat, aquest treball va buscar analitzar el quitosà i les seues modificacions com potencials partícules de Pickering. Les modificacions estudiades van ser la autoagregació, també anomenada desprotonació, i l'entrecreuament amb tripolifosfat de sodi. Es va avaluar el comportament d'aquestes partícules emulsionant oli de cafè torrat, un subproducte de la indústria del cafè amb un alt contingut de compostos bioactius i volàtils d'interès. Posteriorment, es van analitzar les propietats fisicoquímiques i l'estabilitat de les microcàpsules produïdes després de l'assecat de les emulsions mitjançant tècniques d'assecatge per atomització i liofilització. Es van avaluar emulsions amb diferents concentracions d'oli i nanopartícules de quitosà, estudiant la seua microestructura, alliberament d'àcids grassos i bioactius durant la digestió gastrointestinal in vitro així com la seua bioaccesibilitat. Totes les emulsions tenien un comportament reològic pseudoplàstic, sofrint desintegració al llarg del procés de digestió. Les emulsions formulades amb nanopartícules de quitosà desprotonades i menor concentració d'oli van mostrar una millor estabilització i, en conseqüència, una major bioaccesibilitat als compostos fenòlics totals. Les diferents nanopartícules de quitosà es van caracteritzar estudiant la seua càrrega superficial, distribució del tamany de partícula, microestructura i afinitat aigua/oli. Les nanopartícules de quitosà desprotonades van tindre un tamany de partícula més gran, el que va resultar en emulsions amb gotes d'oli més grans. A mesura que es va augmentar la concentració d'aquestes partícules, es va afectar positivament la viscositat de les emulsions a causa de la formació d'una xarxa tridimensional en la fase contínua. Les nanopartícules obtingudes a l'entrecreuar quitosà amb tripolifosfat de sodi van ser

més menudes, donant com a resultat emulsions amb gotes més menudes també. La viscositat d'aquestes emulsions va ser menor i poc afectada per la concentració de partícules. Les imatges obtingudes per microscòpia van mostrar l'estabilització de les gotes pel mètode de Pickering. Les emulsions de Pickering que contenien un 10% d'oli de cafè torrat es van assecar per atomització i es liofilitzaren utilitzant les diferents nanopartícules de quitosà estudiades i maltodextrina com a agents portadors. Les microcàpsules obtingudes van obtenir una humitat, activitat de l'aigua i solubilitat adequada per a la seua manipulació i emmagatzematge. La presència de nanopartícules de quitosà va permetre major retenció d'oli en les microcàpsules i major eficiència d'encapsulació. Les microcàpsules obtingudes per assecat per atomització van tindre una forma esfèrica més regular, mentre que les micropartícules obtingudes per liofilització van ser més grans i amb morfologia irregular. Els compostos bioactius i les propietats antioxidants es van conservar millor durant la liofilització. D'altra banda, les microcàpsules obtingudes per atomització presentaren major protecció d'aquests compostos durant la digestió. Les microcàpsules formulades amb nanopartícules desprotonades també van ser sotmeses a la prova d'emmagatzematge durant 30 dies a 25°C. Durant l'emmagatzematge, es va avaluar la seua protecció contra l'oxidació de lípids i l'alliberament de volàtils. Per això, les isotermes de sorció d'aigua d'aquestes mostres es van determinar prèviament en les condicions d'emmagatzematge. Les dues mostres van presentar isotermes de tipus II, el que va permetre un bon ajust del model de GAB a les dades experimentals. L'índex de peròxids i el contingut de diens conjugats van resultar en valors adequats durant l'emmagatzematge, encara que les mostres liofilitzades van presentar una lleugera tendència a l'oxidació a causa de la major quantitat d'oli superficial. Aquests resultats van estar d'acord amb les dades d'alliberament de compostos volàtils. Encara que va haver lleugeres diferències entre les mostres seques, totes van mostrar menys pèrdua d'aromes totals (~28%) en comparació amb l'oli no encapsulat (~51%) a la fi de l'emmagatzematge. Així, es va concloure que les nanopartícules de quitosà estudiades van ser eficients per encapsular l'oli de cafè torrat i preservar les seues característiques enfront de l'acció d'agents externs.

Paraules clau: subproductes, emulsió de Pickering, encapsulació, estabilitat, compostos bioactius.

FIGURE LIST

emulsions formulated with the lowest concentration of chitosan (0.9 g /100 g).

TABLE LIST

SUMMARY

1. Introduction

Many food products are produced by immiscible ingredients, such as water and oil. However, their adequate incorporation is often dependent on a previous emulsification process. In the emulsified systems, surfactants are used in order to avoid phase separation and to increase stability. Conventional emulsions are usually stabilized by molecules that present at least one (non-polar) hydrophobic region and at least one (polar) hydrophilic region. This is a common structural feature of surfactants, or also called surface-active substances. Their amphiphilic nature provides the ability to decrease the interfacial tension when adsorbed at the oil-water interface.

Althoug the use of stabilizers is important for homogenizing two different phases, the stability of an emulsion is determined according to its resistence to changes in its physicochemical properties over time. Emulsions may typically break down and become unstable during storage due to different mechanisms, such as gravitational separation (creaming or sedimentation), flocculation, coalescence and Ostwald ripening.

Gravitational separation processes occur by the action of the gravity and depend upon the emulsion droplets density. Droplets move upward ("creaming") or downwards ("sedimentation") when their density is, respectively, lower or higher than that of surrounding liquid. Flocculation is the adhesion of two or more droplets forming an aggregate. As well as gravitational separation, flocculation does not lead to changes in the integrity of individual droplets. Coalescence, in turn, is the process by wich several droplets merge together and form a single larger droplet. Ostwald ripening is a diffusional mass transfer process that is linked to the difference of solubility between dispersed and continuous phase of emulsion. It occurs in a polydisperse emulsions in wich small droplets disappear by dissolution and deposition on the larger droplets (McClements, 2007; Liu et al., 2019).

Alternatively to the artificial surfactants, emulsions can be stabilized by solid colloidal particles. They can be inorganic or organic particles with partial wetting property by both oil and water. It results in the so-called Pickering emulsions, a different approach to replace surfactants by solid particles that strongly adsorb the oil-water interface. This technique enables the Pickering stabilizers to form a rigid barrier around the droplets that reduces their mobility, resulting in a steric hindrance at the oil/water (O/W) interface. The wettability of a particle is characterized by how intense is the particle affinity for one phase or other. In addition, particles with an

equal affinity for both phases require high desorption energy at the interface – making them responsible for the physical barrier that prevent the coalescence of the droplets (Berton-Carabin e Schroën, 2015).

Natural sources for producing such particles are widely reported in literature, such as zein, soy protein, pea protein, starches, cellulose derivatives, chitin and chitosan. They have been used in Pickering emulsion formulations after modifications to achieve suitable properties to act as Pickering stabilizers (Jiang, Sheng & Ngai, 2020; Sarkar & Dickinson, 2020)

Chitosan is included in the group of commonly used polyssacharides for emulsions stabilization. Physicochemical changes are produced in its structure to obtain the expected binding properties at the oil-water interface. Chitosan presents free amine and hydroxyl groups along its structure, being them susceptible to changes depending on the pH of the medium. In acid aqueous solutions the protonation of the amino groups makes the chitosan soluble as a polycationic polymer. As the pH solution increases, chitosan aggregates with favorable properties are formed for acting as particulate emulsifiers to produce Pickering emulsions.

Chitosan particles can also be formed throught its interaction with a polyelectrolyte complex with polyanions such as sodium tripolyphospate (TPP). The intermolecular bounds between phosphate groups of TPP and positively charged amino groups of chitosan give rise to the crossliked chitosan particles to be adsorbed onto the oil-water interface of Pickering emulsions.

The development of emulsions by well-defined templates has been extensively explored to produce systems with adequate release of functional compounds, protection against chemical degradation and increased bioaccessibility during gastrointestinal digestion (Araiza-Calahora, Akhtar, & Sarkar, 2018; Low et al., 2019; Lamothe, Guérette, & Britten, 2020; Singh, Lim, & Chan, 2021). The stabilization of emulsions by biopolymers, such as chitosan, has been studied as a potential method for encapsulation, oxidative stability and release systems for bioactive compounds. However, little information is reported about the mechanisms of particle synthesis and their role in the release of bioactive compounds and storage stability.

Recent studies have been carried out to produce microcapsules from Pickering emulsions by drying methods. In addition to the lower volume and water content, the microcapsules form a protective barrier to the sensitive components found into the core (Stasse et al., 2020; Singh, Lim, & Chan, 2021). These

compounds can be sensitive to moisture, light and oxygen. Encapsulation, therefore, results in products with a longer shelf life and has a wide variety of applications, from flavors and fragrances to bioactive and probiotic compounds.

There are several microencapsulation techniques, such as spray-drying, spray chilling, coacervation, lyophilization, extrusion and emulsification. The choice of the technique depends on the type of material to be encapsulated, the application of the microcapsule, the required size of the particles to be obtained, the physical and chemical properties of the core and the wall material as well as the release mechanism of the encapsulated compound. Thus, the control of the structure, permeability, mechanical resistance and compatibility must be taken into account to make them compatible in many applications with controlled release and protection of the components against adverse conditions.

The spray-drying technique is one of the most used for microencapsulation and has been used to encapsulate lipophilic and hydrophilic compounds in order to protect them from degradation. In this technique, the liquid containing the material of interest is dispersed in droplets that come into contact with a flow of heated air, quickly removing the solvent and forming solid particles. However, although it is considered a technique with fast processing and low cost, there is a need to use high temperatures, which can compromise the integrity of bioactive compounds present in the material.

On the other hand, freeze-drying is used for the dehydration of heat-sensitive products. This method is based on water sublimation from the solid phase to the gas phase under low temperatures and low pressure. In spite of its high production costs and long processing time, freeze-drying has been an efficient method to protect flavorings products and suscetibles to oxidation.

Regardless the type of microcapsules obtained, the release of the encapsulated material can be evaluated by several mechanisms: solvent addition, changes at pH and temperature, mechanical break during food processing and storage or its absorption in specific sites of the body. During digestion, structural changes in the food provide important information about the digestibility and bioaccessibility of compounds present in the food matrix. In this way, the mechanical and chemical transformations that occur during digestion are considered ways of releasing an encapsulated compound.

Among the most diverse source of bioactive compounds, there is an increasing trend by using ingredients from food co-products. Coffee oil from roasted coffee beans is an example of bioactive-rich co-product. The coffee bean consists of around 17% of oil depending on the species (*C. Arabica* and *C. Canephora*), and the lipid fraction is composed of about 75% of triacylglycerides (Speer, 2006). The fatty acids are represented mainly by palmitic, stearic, linolenic acids and by essential acids such as oleic and linoleic, corresponding to 7% - 14% and 43% - 54% of the whole fraction, respectively. Tocopherols, caveol and cafestol diterpenes, sterols and other minority components in the unsaponifiable fraction have been highlighted for their antioxidant, antimicrobial and anticarcinogenic activities (Raba et al., 2015; Cárdenas et al., 2015; Hatzold et al., 2012), in addition to provide emollient properties and protection agaist UV radiation (Wagemaker et al., 2015).

The global coffee production is estimated at 170 million 60-kilogram bags annually. Brazil is the largest world´s coffee producer, being responsible for around 30% of the world suplly. The quality of coffee beans is the main concern of producers, since harvesting and pre-processing operations can affect their chemical composition. About 20% of coffee production consists of defective beans such as irregularly-shaped, immature, insect-damaged and broken beans that dramatically affect the taste in the cup (Casas et al., 2017). An alternative for adding value to the defective coffee beans is the extraction of oil, making it a value-added co-product.

Although still little exploited, roasted coffee oil has shown great potential for the food industry due to the presence of large amounts of essential fatty acids and phenolic compounds. Moreover, the aromatic compounds found in the roasted coffee beans are fat-soluble substances that can be used as flavoring ingredients in most diverse food formulations. In addition, studies report that the roasting process of grains does not affect the oxidation level of the oil, but confers stability due to the antioxidant characteristics of the Maillard reaction products (Anese et al., 2000).

Due to its composition, coffee oil has potential for application in formulations of food products, such as ice cream, chocolates, instant beverages, confectionery, and nutraceutical foods. However, the insolubility in water is one of the factors that possibly hinder its use. Therefore, emulsion-based encapsulation can be regarded as one of the most promising techniques to protect the oil against oxidative degradation and also make it easier to be applied in matrices of food products.

In this way, this work was aimed at considering different chitosan nanoparticles as Pickering stabilizers to protect the bioactive and aromatic compounds of roasted coffee oil in emulsions and/or in the resulting dried microcapsules.

2. Objectives

2.1. General

The general objective of this thesis was to produce chitosan-based emulsions of roasted coffee oil and to evaluate the efficiency of spray-drying and freeze-drying in the protection of interest compounds.

2.2. Specifics

In order to attain the general objective, it was intended specifically:

1. To produce chitosan nanoparticles able to stabilize o/w emulsions of roasted coffee oil.
2. To evaluate the crosslinking method on the production of chitosan nanoparticles to stabilize the emulsions.
3. To evaluate the effectiveness of chitosan nanoparticles by investigating changes in the emulsion structure during *in vitro* digestion.
4. To characterize the physical properties of chitosan nanoparticles and to evaluate their role on the stabilization of emulsions.
5. To produce dryed microcapsules from emulsions using spray-drying and freeze-drying methods.
6. To characterize the effect of drying methods and wall material on the physical properties and digestibility of microcapsules.
7. To evaluate the oxidative stability of microcapsules as indicated by peroxide index, conjugated dienes and volatile compounds.

3. Thesis structure

This section describes the work packages (Figure 3.1) followed in the present thesis, in order to achieve the previously established objectives. The thesis consists of five main chapters that address the use of chitosan particles as emulsion stabilizers and further as wall material of roasted coffee oil dried microcapsules. In order to provide information for food industry, each chapter reports different steps used for developing the final product. The specific matherials and methods used are widely described in each chapter.

Chapter 1 addresses a review about Pickering particles, an alternative system to surfactant-stabilized emulsions.

In Chapter 2, changes in the structure of emulsions during *in vitro* digestion were studied. A simulated gastrointestinal model consisting in mouth, stomach and intestine was used to mimic the human digestion and the effectiveness of chitosan nanoparticles was evaluated based on bioaccessibility of phenolic compounds of roasted coffee oil.

Chapter 3 was focused on characterizing the chitosan nanoparticles able to stabilize o/w emulsions as well as the physical properties of the emulsions. Chitosan nanoparticles were produced by two different methods: deprotonation and ionic gelation with crosslinking agent. Deprotonated particles were produced by modifying the pH of chitosan solution to pH > pKa, resulting in self-aggregation particles. Crosslinked nanoparticles were formed through electrostatic interaction between negative groups of sodium tripolyphosphate (TPP) and the positively charged amino groups of chitosan. Chitosan nanoparticles were characterized according to surface charge, particle size distribution, chemical structure, wettability and microstructure imaging whereas physicochemical, microscopic and rheological assays were carried out to evaluate the emulsions stabilized by the nanoparticles.

Chapter 4 addresses on the production of microcapsules from previously prepared emulsions using two different drying methods: spray-drying and freeze-drying. The microcapsules were characterized in relation to moisture content, water activity, solubility, particle size distribution and oil retention. Powder morphology was evaluated by microscopic images. In addition, microcapsules were subjected to *in vitro* digestion to evaluate the effect of the drying method and wall material on the recovery index and bioaccessibility of phenolic content and antioxidant activity.

Finally, the stability and volatile composition of roasted coffee oil microcapsules during storage were evaluated in Chapter 5. Sorption isotherms were

experimentally determined and modeled for samples obtained by spray-drying and freeze-drying. Lipid oxidation and volatile compounds were evaluated over 30 days of storage under controlled relative humidity.
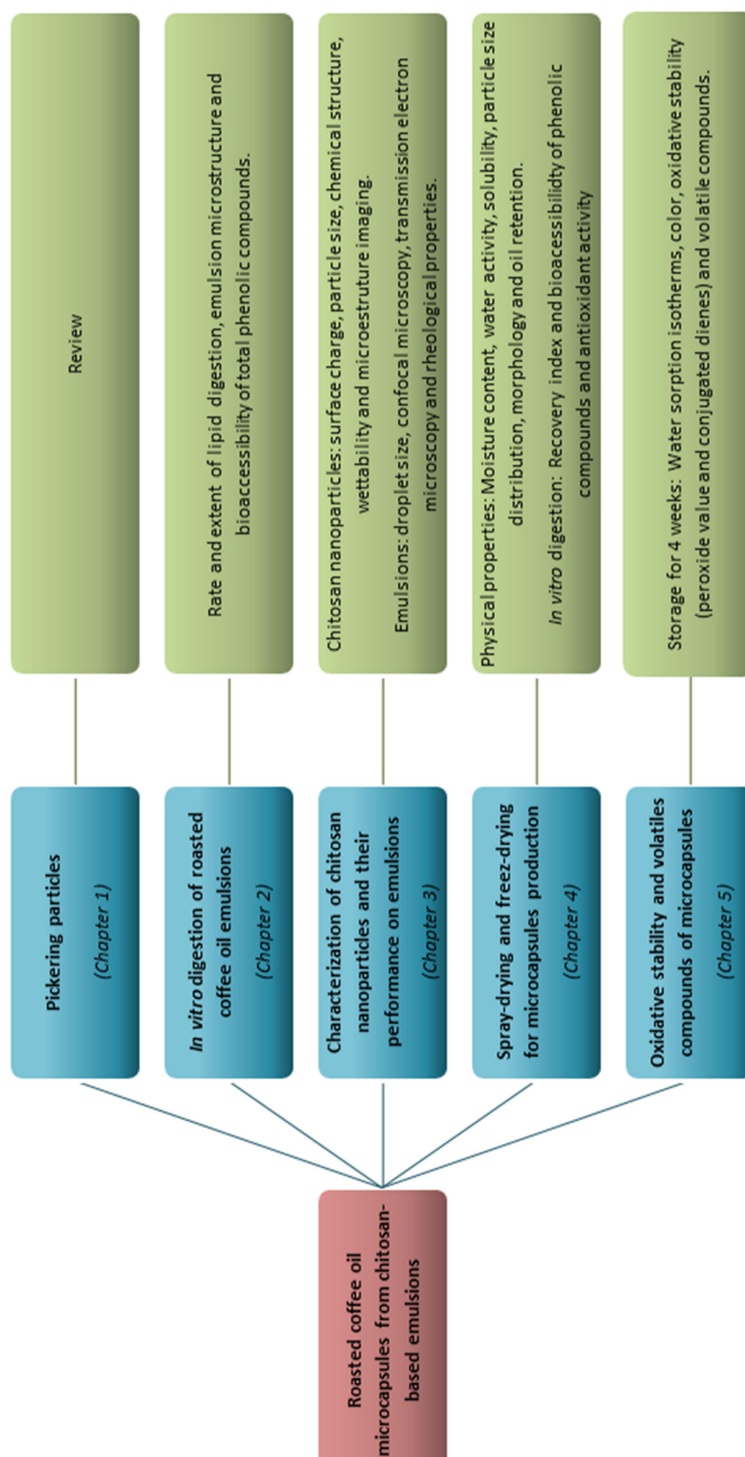
Figure 3.1. Thesis structure

4. Results

4.1. CHAPTER 1

Pickering particles

Protein- and polysaccharide-based particles used for Pickering emulsion stabilisation

Ribeiro, E. F.[1,2], Morell, P.[1], Nicoletti, V. R.[2], Quiles, A.[1], Hernando, I.[1,*]

[1] **Grupo de Microestructura y Química de Alimentos. Departamento de Tecnología de Alimentos. Universidad Politécnica de Valencia,** Camino de Vera, s/n, 46022, Valencia, Spain

[2] **São Paulo State University (Unesp), Institute of Biosciences, Humanities and Exact Sciences,** Campus São José do Rio Preto, SP, 15054-000, Brazil

Abstract: Food science researchers have been motivated to investigate novel Pickering emulsions templates stabilised using food-grade solid particles. Protein- and polysaccharide-based particles can function as effective stabilisers and thickening agents, respectively, in multi-phase food systems. Studies have shown that using protein-based particles may lead to aggregation and structural instability, whereas using polysaccharide-based particles can cause poor emulsifying performance and interfacial activity. Thus, the purpose here is to show those studies highlighting using amphiphilic protein-polysaccharide particles that can function as outstanding copolymer stabilising agents. Combining protein- and polysaccharide-based particles and tailoring the multi-phase systems results in particle-stabilised emulsions with higher stability against coalescence. The current challenges and emerging research trends are exploring renewable, sustainable, clean-label, and eco-friendly biopolymer particles that are effective as Pickering stabilisers.

4.1.1. Introduction

The use of solid particles as stabilisers for oil droplets in water dates back over a century ago (Binks, 2002). The first studies documenting the particle-stabilised emulsions, also referred to as Pickering emulsions, were reported by Ramsden and Pickering and have had an increasing interest in recent years (Berton-Carabin and Schroën, 2015). Despite the well-established theories on inorganic and synthetic polymer-based Pickering emulsions, research about emulsions stabilised using edible colloidal particles is increasingly attractive (Xiao, Li, and Huang, 2016). The current challenges and emerging research trends address using renewable, sustainable, clean-label, and environmentally friendly biopolymer particles that are not only effective as Pickering stabilisers but also acceptable as food-grade materials (Rayner et al., 2014).

In multi-phase food systems, protein and polysaccharide particles have the ability to function as stabilizers and thickening agents, either in the form of nano- or micro-particles (Dickinson, 2012). In addition to its surface activity, proteins have fast interfacial adsorption kinetics, whereas the polysaccharide moieties form a thick steric layer because they protrude into the aqueous phase providing electrostatic repulsive forces against droplet aggregation (Chen et al., 2018). Nevertheless, modification of the particles' surface hydrophobicity and formation of protein-polysaccharide complexes have been recommended, as protein particles may cause aggregation and structural instability in Pickering emulsions, and polysaccharide-based particles give poor emulsifying performance and surface activity (Ashaolu and Zhao, 2020).

Physical stability and textural characteristics of colloidal systems (dispersions, emulsions, foams, gels, and their mixed variants) in food manufacture can be improved using well-known and efficient methods of associative interactions between proteins and polysaccharides (Dickinson, 2017). There is a great diversity of possible interactions between these types of macromolecules, including non-covalent attractive forces such as electrostatic, hydrogen bonding, hydrophobic, and van der Waals. In addition, covalent bonds are mostly formed between side-chain-exposed functional groups resulting in an irreversible binding (Semenova, 2017).

Flexible biopolymers such as protein and polysaccharide form thick interfacial layers, which possess high viscoelastic moduli, and therefore can provide excellent

stability for emulsion droplets (Gao et al. 2017). However, a required dual wettability of the particles by oil and water is a critical factor for obtaining emulsions with long-term stability (Gao et al. 2014). Therefore, not all food biopolymers are suitable as Pickering stabilisers for emulsions due to the limited wettability and interfacial properties.

Novel opportunities for the stabilisation of food emulsions using solid biopolymer nanoparticles and microparticles are emerging. The major advantage of such stabilisation is its longevity, regarding coalescence, with no significant structural change over storage. Due to the effective steric structural barrier formed by the adsorbed solid particles, only slight coarse droplets might be formed after several months (Dickinson, 2013; Semenova, 2017).

Regarding to the advances in the use of Pickering emulsions, gel-like emulsions obtained from Pickering systems are an emerging trend. Emulsion gels are achieved by modulating the gelling agents' concentration, oil volume fraction (Φ), and magnitude of triggering forces (Mao et al. 2018). In addition to the high physical stabilisation and oxidative stability due to a strong gel-like network, Pickering emulsion gels also represent a novelty for delivering bioactive compounds (Li et al. 2020; Mao et al. 2019). Zhu, Ya, Huan, et al. (2020) named these emulsions as Pickering high-internal-phase emulsions (HIPEs).

This review focuses on recently achieved insights concerning the contribution of proteins and polysaccharides and their associative interactions, considering many functions. (i) The characterisation of the most common biopolymer (protein and polysaccharide) micro and nanoparticles for emulsion stabilisation). (ii) The review and analysis of the relevant studies of emulsion stabilisation using biopolymeric particles. (iii) The ongoing challenges and novel techniques to achieve and assess biopolymer associations. Moreover, to meet the novel demand of this review's topic, literature references were limited to the past decade. Table 4.1 provides a list of recent investigations regarding protein- and polysaccharide-based particles used for Pickering emulsion stabilisation.

4.1.2. Food-grade particles for emulsion stabilisation

4.1.2.1. Polysaccharide-based particles

Natural biopolymers, such as polysaccharides, can be an attractive source of particulate material for potential use in foods. Significant research have shown that

modified starches, cellulose-based, and chitin-based particles could be used as Pickering stabilisers in food-grade emulsions (Table 4.1) (Dickinson, 2017; Murray, 2019).

Increasing storage stability can be achieved when small starch particles are used, as decreasing starch particle size decreases droplet size of Pickering emulsions. Therefore, different methods have been reported for producing starch nanoparticles and nanocrystals: acid hydrolysis, high pressure homogenisation, ultrasonication, reactive extrusion, γ-irradiation, steam jet cooking, nanoprecipitation, enzymatic debranching and recrystallisation, polyelectrolyte complex formation, electrospinning, electro spraying, and self-assembly (Sun, 2018; Zhu, 2019).

Modified starch particles of various biological sources play the major role as food-grade particles with potential to be used as Pickering stabilisers for oil-water (O/W) emulsions (Murray, 2019). Because these particles are generally highly hydrophilic, chemical modifications are to make them more hydrophobic to confer higher affinity for the O/W interface (Berton-Carabin and Schroën, 2015). The particles remain intact even after the hydrophobic modification, thus presenting proper wettability by the aqueous phase and being able to be used as a stabiliser in Pickering emulsions (Song et al. 2020; Wang et al. 2017). Starch esterification with OSA is the most widely used modification. It consists of a partial substitution of the hydroxyl groups by hydrophobic substituents. The degree of starch granule derivatisation can be performed differently to provide them an amphiphilic character and interfacial activity (Altuna, Herrera, and Foresti, 2018; Li et al., 2019; Saari, Wahlgren, Rayner, et al. 2019; Wang, Luo, Chun-Chen, et al. 2020). It is important to highlight that in addition to the properties of the starch raw material, other factors may influence the physicochemical properties of OSA-modified starches: the processing conditions used not only during, but also before and after the modification in case pre-/post-treatments are applied; the extent of derivatisation; and the distribution of the introduced groups within the starch granules (Altuna et al., 2018). Other chemicals used to increase the hydrophobicity of starch granules include acetic anhydride and phthalic anhydride. However, starch particles produced using chemical modifications may not be appealing to consumers in the rising clean-label ingredients market (Zhu, 2019).

Another important group is formed by cellulose derivatives. Native cellulose is a hydrophilic polysaccharide lacking good emulsifying ability. However, studies have

demonstrated that stable Pickering emulsions can be formed using various cellulose particulate materials which act as emulsifiers by adsorbing at the O/W interface (Kalashnikova et al. 2013; Kalashnikova, et al. 2011). Structurally, both amorphous and crystalline regions are found in native cellulose. Cellulose crystals with different shape and size can be produced by isolating crystalline zones by chemical, mechanical and/or biological techniques in order to develop several functional ingredients. Depending on the preparation methods and sources, examples include microcrystalline cellulose, microfibrillated cellulose, regenerated cellulose, nanocrystalline cellulose, nanofibrillated cellulose, and bacterial cellulose (Nsor-Atindana et al., 2017).

Micro/nanoscale cellulose crystals can stabilise emulsions by taking advantage of their amphipathic nature, since hydrophilic points correspond to the free hydroxyl groups on the material surface, while the crystalline portion can function as the hydrophobic edge, giving amphiphilic character (Kalashnikova et al., 2011; Nsor-Atindana et al., 2017). Cellulose nanocrystals are regarded as an ideal biomaterial due to their low density, low carbon footprint, chemical tenability, environmental sustainability, and anticipated low cost. The preparation processes are simple and easy to handle because they are conducted in aqueous solutions, in which nanocelluloses are well dispersed and do not require any time-consuming solvent exchange process (Fujisawa, Togawa, and Kuroda, 2017). Modifying and functionalising cellulose nanocrystals is an attractive prospect since new or improved properties can be found in the final product such as good mechanical properties and environmentally friendly characteristics (Tang et al. 2017).

Besides cellulose derivatives, chitin and its derivatives represent another interesting group of biopolymers suitable for Pickering stabilisers. Chitin is a linear polysaccharide that works as a major structural component in the exoskeleton of various marine invertebrates. It is extracted from marine shell waste streams on an industrial level (Muxika et al. 2017). Chitin has garnered considerable interest due to its non-toxicity, biocompatibility, and biodegradability. To extend its applications, chitin has been converted into chitosan, chitin nanocrystals, chitin nanoparticles, and/or chitin nanofibers by mechanical processing, acid, and enzymatic hydrolysis (Sun et al. 2019). Chitin nanocrystals and nanofibers have produced Pickering emulsions by adsorbing on the O/W interface, exhibiting good emulsifying ability and stability (Barkhordari and Fathi, 2018).

Despite being abundant and having exceptional functional features, chitin has limited utility due to its poor solubility. Chitin can be converted into chitosan through enzymatic or chemical processes, thus improving its solubility and providing opportunities to be converted to many forms, such as films, nanofibers, hydrogels, and pastes. In addition, its functional properties such as antibacterial activity also include it in a wide variety of applications (Muxika et al., 2017).

4.1.2.2. Protein-based particles

Proteins have long been recognised as excellent natural building blocks to prepare micro and nanoparticles due to their versatility in tuneable conformations (Xiao, Li and Huang et al. 2016). As the globular protein is heated, aggregates with varied morphologies may arise depending on the protein concentration and thermal conditions. As a consequence, it can generate spherical particles, flexible or rigid fibrils, and fractal clusters (Nicolai and Durand, 2013). Different kinds of protein-based particles have been reported to successfully stabilise O/W emulsions by the Pickering method (Table 4.1). Proteins stabilise emulsions not only by the creation of a physical barrier but also by the presence of repulsive steric and electrostatic interactions between the oil droplets (Tavernier et al. 2016). The main protein-based particles can be classified according to their source; from plant origin (zein, kafirin, gliadin, vicilin, and legumin) and animal origin (gelatin, dairy protein such as whey protein, bovine lactoglobulin, bovine serum albumin, α-lactalbumin, and lactoferrin).

Proteins from plant sources exhibit an excellent Pickering stabilisation. In general, the emulsifying properties of plant proteins depend on their amino acid composition, pH, concentration, and lipid content in the resulting emulsion (Liang and Tang, 2014). Prolamins are plant storage proteins with potential application as O/W stabilisers as they are naturally insoluble in water and hydrophobic. Good stabilisation of O/W emulsions has been reported that the hydrophobicity of the prolamin particles can be moderate in combination with other water-soluble polymers (Murray, 2019). Among prolamins, of paramount interest regarding their stabilisation ability are zein from maize (Kasaai, 2018) and gliadins from wheat (Zhu, Chen, McClements, et al. 2018), which are major cereals crops, but kafirin from sorghum has also been studied extensively (Xiao et al., 2015; Xiao, Lu, and Huang, 2017; Xiao, Wang, Perez Gonzalez et al. 2016).

Zein, the major storage protein in maize, is an environmentally friendly material, recognised as safe for food applications (Weissmueller, 2016). Zein has a significant amount of non-polar amino acids (about 50% of total amino acids including leucine, alanine, and proline) and can form relatively hydrophobic nanoparticles due to its self-assemble capability (Kasaai, 2018). Moreover, zein-based complex particles, e.g. zein-polysaccharides and zein-polyphenols, have been successfully prepared via an antisolvent approach, which provides the self-assembly behaviour and changes the interfacial wettability, thus forming different stable zein-based complexes that could be used at the droplet interface in Pickering emulsions (Sun et al. 2019; Wang et al. 2015).

Kafirin, a sorghum protein, belongs to the prolamin family with the highest hydrophobicity – which makes them insoluble in water and soluble in alcohol. Although it resembles zein in its solubility, molecular weight, amino acid composition, and structure of polypeptides, kafirin is more hydrophobic than zein (Xiao, Wang, Perez Gonzalez et al. 2016). It enables the production of more stable films with better gas and water vapour barrier characteristics (Xiao et al. 2015).

Self-assembled structure can be also found in gliadins – the major constituent of wheat protein. The nanoparticles that result from this natural process are due to both hydrophobic and hydrophilic regions on gliadin surface that support Pickering stabilization (Zhu, Chen, McClements, et al. 2018). In addition, intramolecular and intermolecular disulphide bonds may be formed by the numerous residues of cysteine in the chain. Gliadin colloidal particles have been proved as effective particle-stabilisers of O/W emulsions and Pickering HIPEs with the advantage of being biocompatible, edible, and based on fully natural renewable resources (Hu et al. 2016).

Among plant proteins, legume proteins are of great interest for the food industry. In addition to their widespread abundance and good functional attributes, they are low cost, sustainable, and impact customer perceptions in a positive way. Globulins consist in around 70% of the legume proteins and are represented mainly by vicilin and legumin. Due to its low molecular weight and more flexible tertiary structure, vicilin shows the best surface-active properties (Gumus, Decker, and McClements, 2017). The most important sources of legume protein for Pickering stabilisation are soy and pea.

Soy protein isolate is produced by a conventional process that consists of an alkali extraction followed by an acid precipitation. Soy proteins act as effective emulsifiers to form and stabilise O/W emulsions diffusing and adsorbing at the interface of oil droplets due to their amphipathic nature (Tang et al. 2017). Although most proteins in soy protein isolate are in an aggregated state, nanostructured particles can be obtained if an appropriate pre-treatment is applied, e.g., shearing homogenisation, ultrasonication, or micro fluidisation (Benetti, do Prado Silva, and Nicoletti, 2019; Tang, 2019).

The increasing knowledge of the emulsifying properties of purified globulins, vicilin, and legumin from pea protein fractions can greatly extend their application in the food industry, as they present emulsifying capacity with the possibility of foaming and gelling. Extensive studies have indicated that the emulsifying ability of pea protein isolate is better at acidic conditions (pH 3.0) than at neutral or alkali pH (Liang and Tang, 2014; Vélez-Erazo et al. 2020).

Concerning animal protein, gelatin is the denaturation product of collagen under different conditions (e.g., the action of acid, alkali, enzyme, or high temperature). Collagen is commonly found in animal products and by-products, as skin, bones and tendons. Gelatin is cheap, easy to obtain, and theoretically suitable for preparing Pickering soft particles because of its good gelling properties. However, due to its strong hydrophilicity and thermal dissolution, gelatin nanoparticles able to stabilise Pickering emulsions are difficult to obtain (Feng et al. 2019; Jin et al. 2017). Furthermore, taking into account that insects are a promising alternative for meat-like products, recent studies have shown comparable properties of cricket flours and protein isolates regarding emulsifying activity and foaming capabilities of legume flours (Stone, Tanaka, and Nickerson, 2019; Zielińska, Karaś, and Baraniak, 2018).

Dairy protein fractions, as whey proteins and caseins, are the major natural food emulsifiers, but there is a scarcity of reports on their application in Pickering emulsions (Destribats et al. 2014). Specifically, isolated globular proteins (e.g. β-lactoglobulin) denatured under specific conditions of pH and temperature have been used to prepare well-defined particles with emulsion stabilising ability (Su et al. 2020). However, dairy proteins are a chemically interesting source for emulsion stabilisation due to their ability to turn into protein microgels.

Microgels are deformable and soft polymer-based particles that, in contrast to an individual macromolecular species, possess a more complex structure and

functionality acting as an emulsifier, thickener, or steric stabiliser. It is a colloidal entity with definite particle-like features, and comprises a crosslinked network of polymer molecules. Its particular features enable the microgel particle to rapidly swell and deswell reversibly in response to various external stimuli, including changes in pH, temperature, ionic strength, as well as following the addition of cosolvents, polymers, and surfactants. They are surface active and its emulsion stability is attributable to the thickness, coherence, and elasticity of the adsorbed layer. Many food proteins and polysaccharides can form edible microgel ingredients, such as casein micelles, whey proteins, legume proteins, and even starch granules (Dickinson, 2015b).

4.1.2.3. Protein-polysaccharide particles

Protein-polysaccharide interactions are well-known basic constituents of food structures. These interactions could lead to particle formation that includes composite protein-polysaccharide nanoparticles and microparticles, protein-polysaccharide complex coacervates, and protein-polysaccharide multilayer Pickering emulsions (Table 4.1) (Dickinson, 2010; Li and de Vries, 2018).

Proteins rarely provide optimal amphiphilicity (balance between hydrophobicity and hydrophilicity) for interfacial stabilisation since they are generally too hydrophobic. Moreover, their hydrophobicity may be too high to be used as efficient Pickering stabilisers. However, using complexation or conjugation with polysaccharides provides a hybrid stabilisation that has the right amphiphilicity (Li and de Vries, 2018).

Complexation can be obtained through controlled association of protein and polysaccharide molecules. One of the possible methods is driven by electrostatic interactions (Figure 4.1). Proteins and polysaccharides can associate with each other under conditions of opposed electrical charge. Proteins possess a net negative charge above their isoelectric point (pI) and a net positive charge below this pH. Proteins that possess a high net negative charge (pH > pI) have a repulsive force between proteins and anionic polysaccharides. However, when the solution is adjusted to around the pI of the protein (pH $\cong$ pI), localised cationic segments on the protein interact with anionic groups on the polysaccharide leading to weak electrostatic complexation and formation of complexes. Further pH reduction (pH < pI) induces greater interaction between the protein and polysaccharide, eventually

resulting in phase separation of the fully neutralised complex, which is also termed a coacervate (Figure 4.1). Complex coacervation is the association of the initially soluble protein-polysaccharide complexes into larger particles (coacervates) generally by reducing pH beyond the pI of the protein. This process results from both entropic and enthalpic factors and depends on compositional and environmental variables, such as polymer type, pH, temperature, and ionic strength (Jones and McClements, 2010; Wu and McClements, 2015).
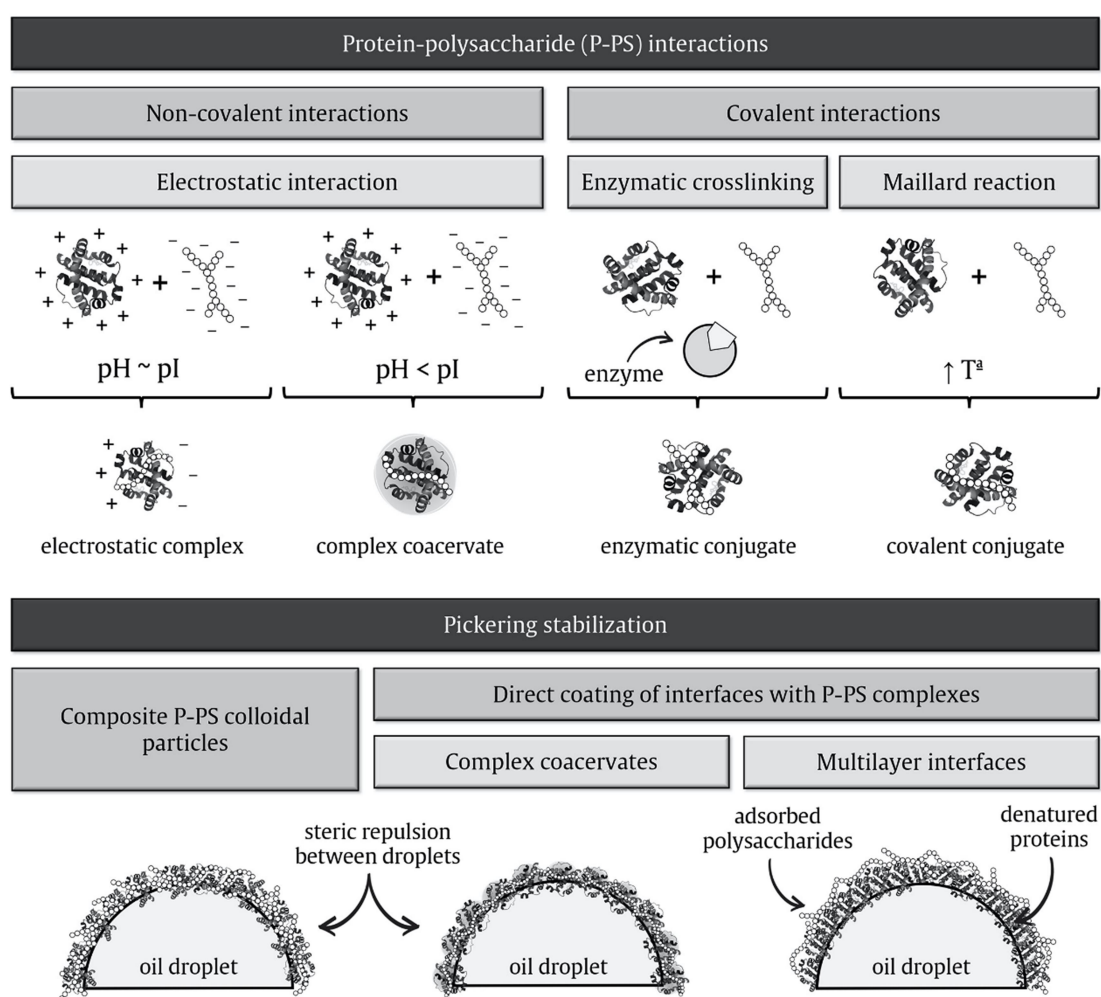
Figure 4.1 Schematic representation of both protein-polysaccharide non-covalent and covalent interactions and the different processes of Pickering stabilisation of these complexes and conjugates.

An alternative electrostatic particle formation mechanism involves heating the protein, thus inducing denaturation and aggregation to form the protein nanoparticle core. Then, desirable pH adjustment is required to coating the protein nanoparticles with polysaccharides through electrostatic interaction. The nucleation and growth of

the biopolymer particles can be managed by controlling conditions such as the holding temperature, holding time, concentration, pH, and ionic strength, giving rise to different biopolymer nanoparticle's size (Dickinson, 2015a; Jones and McClements, 2010; Xiao, Li and Huang. 2016).

These stable inter-biopolymer electrostatic complexes are generally known to form and stabilise emulsions effectively, although many parameters including salt concentration, pH values, and protein to polysaccharide ratio can influence the protein-polysaccharide interaction. In contrast, covalent crosslinking results in permanent and firmer complexes than those formed by electrostatic interactions (Chen et al., 2018).

The Maillard reaction and enzymatic crosslinking can give protein-polysaccharide conjugates (Figure 4.1). Maillard reaction is a sequence of non-enzymatic browning reactions, which begins by linking protein amino groups to the reducing end carbonyl groups of polysaccharides. Energy in the form of heat is necessary for the Maillard reaction to take place, and a higher reaction velocity is reached as the temperature increases. Moreover, the capacity of Maillard reaction products to enhance emulsifying properties has been verified, and, in addition, they are environment friendly compounds for food industry uses. Protein-polysaccharide conjugates can also be produced by enzymatic methods. Using enzymes to structure foods is an ecologically and economically viable alternative. Crosslinking enzymes such as transglutaminase and laccase promote intra- and intermolecular bond formation between biopolymers to improve stability and functionality (Zeeb, McClements, and Weiss, 2017).

The solubility of native proteins can be improved by the covalent coupling of proteins and polysaccharides under unfavourable conditions, due to the attached hydrophilic polysaccharide moieties (Akhtar and Ding, 2017). To function as a copolymer stabilising agent, the conjugate should be strongly adhered to the oil-water interface via the protein's hydrophobic regions at the same time the nonadsorbing polysaccharide region is extended away from the interface to enhance steric stabilisation. It provides an amphiphilic conjugate, which is the main concept underlying this strategy (Dickinson, 2008).

Therefore, Pickering stabilisation can be obtained using protein-polysaccharide composite colloidal particles, or by a direct coating of interfaces either

with complex coacervates of proteins and polysaccharides or multilayers formed by complexation (Figure 4.1) (Li and de Vries, 2018).

4.1.3. Pickering emulsions

4.1.3.1. Pickering emulsions with polysaccharides

Starch can be modified to become suitable for Pickering emulsion fabrication, and a range of chemical and physical modifications, plus their combinations have been investigated as suitable to tune starch particles for Pickering emulsion formulations (Zhu, 2019). Wang et al. (2020) prepared OSA-modified rice starches with the same degree of substitution using different percentages of sodium hydroxide (NaOH) as catalyst. The stability of Pickering emulsions formulated by OSA-modified starch particles was greatly affected by the OSA group's distribution, which was related to NaOH concentration. The results indicated that high concentration of NaOH affected the structure of starch granules and induced OSA groups to distribute more uniformly in the granule. Rheological analysis indicated that these Pickering emulsions displayed a good shear stability with shear-thinning behaviour, providing a novel particle stabiliser for improving the viscoelastic properties and flow behaviour of Pickering emulsions.

Saari, Wahlgren, Rayner, et al. (2019) investigated the stability of emulsions prepared by OSA-modified waxy maize starch in three different forms: granules, dissolved starch, and non-solvent precipitated starch. The varied sizes and shapes of the waxy maize-based emulsifiers could influence the resulting emulsion droplet size and stability. Optimum emulsifying properties were obtained with the non-solvent precipitates, which allowed the emulsions to remain stable after one year of storage. Thus, this study showed the high potentiality of non-solvent precipitated starch as emulsifier.

Sánchez de la Concha et al. (2020) compared waxy maize and amaranth starch nanocrystals chemically modified with OSA. OSA treatment modified the structure of nanocrystals by conferring superficial charge, which increased the repulsion forces between oil droplets incorporated with nanocrystals. Amaranth nanocrystals exhibited superior emulsification ability than waxy maize nanocrystals, which was preserved under storage conditions. The results in this study showed that the combination of nanocrystals and OSA treatment is a relatively simple and effective approach for stabilisation of O/W emulsions.

Particle-stabilisers and surfactants are required to produce stable systems in commercial applications. Song et al. (2020) fabricated sunflower O/W Pickering emulsions using OSA-modified starch particles and small molecular surfactants as stabilisers, and showed that starch particles were compatible with anionic surfactants, in this case sodium dodecyl sulphate, and could enhance the stability of Pickering emulsions.

Cellulose-based Pickering emulsions were conceived as a promising alternative for surfactant-based systems on account of their non-toxicity, safety, biodegradability, and sustainability. The physicochemical properties, which define the functionality of microcrystalline cellulose, are determined by both the raw material and the preparation technique. Modified microcrystalline celluloses can be prepared by surface modification through polymer adsorption using no organic or harmful solvents. The polymer adsorption of sodium carboxy methyl cellulose on microcrystalline cellulose provided an important green method for potential use in the fabrication of eco-friendly Pickering emulsions (Ahsan et al. 2019).

Surface charges of nanocelluloses can tailor the wettability of these fine particles, playing a key role in the stability of the emulsions. Different crystalline allomorphs result in differences in properties of cellulose nanocrystals, such as their morphology, crystal structure, degree of hydrogen bonding, surface potential, and thermal and dispersion stability (Gong et al. 2017). Li, Xia, Li, et al. (2018) obtained two nanocelluloses with different crystalline allomorphs. The performance of crystalline nanocelluloses-I (CNCs-I; needle-like particles) to stabilise Pickering emulsions were higher than crystalline nanocelluloses-II (CNCs-II; ellipsoid-shape particle). Pickering emulsions stabilised by CNCs-I presented droplet sizes about two times smaller and were more stable after centrifugation. Therefore, it is possible to conclude that different crystalline allomorphs resulted in differences in the hydrophilicity and morphologies of nanocelluloses.

Nanofibrillated cellulose has partially disintegrated nanofibrils with a lateral dimension in the scale of tens of nanometres and lengths of several micrometres. It has similar properties to crystalline nanocelluloses and can be used as a thickener or emulsifier in food technology (Grishkewich et al. 2017). Winuprasith et al. (2018) and Mitbumrung et al. (2019) encapsulated vitamin D3 within O/W Pickering emulsions stabilised by nanofibrillated cellulose, and found it an effective Pickering emulsifier while protecting the vitamin D3 from environmental stresses. This effect was

attributed to the ability of the nanofibrillated cellulose to form a thick interfacial coating around the oil droplets, which provided strong steric and electrostatic stabilisation. The non-adsorbed nanofibrillated cellulose increased the viscosity of the continuous phase and promoted the formation of a network of aggregated oil droplets, improving emulsion stability.

Another potential cellulose derived stabiliser is bacterial cellulose. The supramolecular structure of bacterial cellulose nanosized fibrils (BCNFs) can be altered through mechanical treatment. Li, Wang, Wu, et al. (2019) used high pressure homogenisation to modulate the morphology and size of bacterial cellulose. The content and particle size of the BCNFs had significant influence on the O/W interface, being associated with the strengthened intermolecular crosslinking and the increased steric barrier. The physical modification process can provide an easy green method for fabricating a potential BCNFs-based eco-friendly food-grade stabiliser for Pickering emulsion production.

In addition to cellulose-based solid particles, crystalline parts of chitin can be obtained by chemical or physical treatments, and chitin nanocrystals can be used for encapsulation and production of Pickering emulsions. Barkhordari and Fathi (2018) produced chitin nanocrystals by hydrolysing chitin from prawn shells and used them for producing Pickering emulsions. The developed nanocrystals were biodegradable and biocompatible ingredients that could be used for producing stable Pickering emulsions during four weeks of storage. The results showed that the mean diameter of oil droplets in the nanoparticle stabilised emulsion was smaller than in a lecithin containing emulsion with the same concentration (4.5 versus 10.9 µm, respectively). Kaku et al. (2020) and Zhang et al. (2015) also prepared chitin nanofibers with diameters around 50 nm, which formed stable Pickering emulsions through a simple dissolution and regeneration process.

Highly charged chitin nanoparticles of three different average aspect ratios (≈ 5, 25, and > 60 nm) were obtained using low-energy deconstruction of partially deacetylated chitin. Bai et al. (2019) observed that these nanoparticles were effective at reducing the interfacial tension and stabilised the O/W interface via network formation, thus becoming effective at stabilising Pickering systems, depending on the nanoparticles size, composition, and formulation. In addition, an increase in the interfacial wettability could have occurred from a deacetylation process before chitin transformation into the nanoparticles, enabling high electro-steric stabilisation. Then,

the nanoparticle's surface coverage on the oil droplets as well as their ratio and long-term stability against coalescence could be easily controlled.

Ground crickets contain a significant amount of protein and chitin particles, and both could contribute towards emulsification. Hirsch et al. (2019) determined the interfacial and emulsifying properties of the two cricket-derived particles: aqueous protein suspensions and finely milled chitin particles. Both water-soluble protein and milled chitin particles could contribute towards stabilisation of O/W emulsions. Cricket protein fractions enabled better emulsifying capacity than the source cricket powder and demonstrated that the decreased interfacial tension at the droplet surfaces was dependent on the concentration. On the other hand, in addition to weaker adsorption behaviour of chitin fractions, only the smallest of the milled chitin was useful for emulsification, limiting their availability as industrial emulsifiers. Thus, a partial deacetylation of chitin particles would be a potential mean to improve interfacial characteristics of the whole flour or chitin fraction and increase hydrophilicity.

Chitosan which, in turn, is a highly hydrophilic biopolymer, requires surface modification or complexation with other polymers, to improve its emulsification properties. As an alternative to encapsulate roasted coffee oil, Ribeiro et al. (2020a; (2020b) investigated the ability of chitosan nanoparticles obtained by deprotonation and by ionic crosslinking to produce emulsions with different lipid phase fractions. Better droplet stabilisation was achieved using the deprotonation method when lower oil content was used. Chitosan nanoparticles could adsorb onto oil droplet surfaces, providing efficiency in encapsulating and protecting bioactive compounds. Moreover, deprotonated chitosan was able to create a three-dimensional network that entrapped the oil droplets while the crosslinked nanoparticles stabilised oil droplets along the continuous phase.

Complexation of chitosan with other biopolymers is considered an easy alternative to the currently used chemical surface modification strategies. Atarian et al. (2019) prepared different Pickering emulsions stabilised with different chitosan and stearic acid ratios, and at different pH values. More stable emulsions were obtained using chitosan-stearic acid nanogels with higher stearic acid to chitosan ratios and at alkaline pH.

Chitosan and gum arabic nanoparticles have been synthesised and their use as novel stabilisers for Pickering emulsions was tested by Sharkawy, Barreiro, and Rodrigues (2019). Arabic gum, with its hydrophobic moieties, had an important

function in modifying the wettability of the obtained particles. The nanoparticles formed an effective layer around the oil droplets, which prevented droplets from coalescence and assured emulsion stability. Moreover, an inhibition of gravitational separation on long-term storage has been shown by increasing the oil volume fraction and the nanoparticles concentration in the produced Pickering emulsions.

4.1.3.2. Pickering emulsions with proteins

The requirements to serve as a particle stabiliser, such as insolubility in both fluid phases and intermediate wettability, are so challenging that few available natural materials can fulfil them. A limitation in using protein particles to stabilise Pickering emulsions alone include aggregation and structural instability. Water insoluble proteins such as prolamins have been used as a platform for water continuous emulsion stabilisation (De Folter, Van Ruijven, and Velikov, 2012; Donsì et al. 2017), however, most prolamins studies involve modification of the protein or association with other molecules. The use of zein specifically involves complexing the protein with a more water-soluble polysaccharide (Gao et al. 2014), with a second protein (Zhu, Chen, McClements, et al. 2018), or an organic acid (Zou, Yang, and Scholten, 2018) to aid its dispersion in water and therefore adsorption at the O/W interface.

Rutkevičius et al. (2018) showed that zein particles can stabilise W/O emulsions to a limited extent due to its high hydrophobicity. This fundamental research showed that, although zein is a good Pickering stabiliser for O/W emulsions, the protein alone is a poor W/O Pickering stabiliser. Modification of zein particles with other surfactants or addition of a higher fraction of oil soluble lecithin allowed additional water incorporation into the emulsions. The results showed that zein particles function as a stabiliser that requires adjustment prior to emulsification to form W/O emulsions.

Li, Zhu, Meng, et al. (2019) aimed at using gliadin nanoparticles from gluten after chemical modifications to improve their amphiphilic characteristics and emulsifying properties. For this, the amino groups of gliadins were replaced by succinylation reaction under alkaline conditions. The octenyl succinic anhydride (OSA)-modified gliadin nanoparticles were used to improve O/W emulsification efficiency and stability, mainly at higher nanoparticle concentration and lower pH value (higher electrostatic repulsion). The good storage stability can be attributed to the adsorption of modified gliadin nanoparticles onto the O/W interface in order to

create a dense packed layer on the oil droplet surface. The results of this study provide interesting alternative to stabilise Pickering emulsions at the same time the protein content is increased in food products.

Liu et al. (2017) demonstrated a novel technology to construct structured algal oil products with no thermal or chemical treatment. Crosslinking was initiated by hydrophobic interaction under mild alkaline conditions, and interfacial disulphide crosslinking of gliadins was triggered by microfluidisation. The interfacial covalent crosslinking of emulsions can contribute positively to withstand environmental stress and provide the formation of a new class of food products.

Although gliadin and zein are both cereal prolamins, gliadin is relatively more hydrophilic than zein. Liu et al. (2019) synthesised zein-gliadin complex particles (ZGCP) using an antisolvent approach and investigated their efficiency as stabilisers to fabricate Pickering emulsions. Adding gliadin affected the self-assembly, aggregation, and wettability of ZGCP. ZGCP form a dense interfacial layer around droplet and smaller droplet sizes than those obtained by zein or gliadin. Thus, ZGCP-stabilised emulsions demonstrated higher viscoelastic attributes and much better stability against coalescence.

Xiao et al. (2015, 2017) and Xiao, Wang, Perez Gonzalez, et al. (2016) reported the first attempt of using the major prolamin from sorghum, kafirin, as a fully natural Pickering emulsion stabiliser. Kafirin was fabricated into spherical nanoparticles using antisolvent precipitation and was introduced as stabiliser for Pickering emulsions. The kafirin nanoparticles exhibited water over oil wetting preference, and the resultant Pickering emulsion manifested its superiority in storage and exhibited resistance against coalescence.

Most proteins in soy protein isolate are in the aggregated state, and with the appropriate pre-treatment, e.g. heat-induced aggregation, the aggregated state can be transformed into nanostructured particles (Tang, 2019). In a series of studies, Liu and Tang (2013, 2014, 2016a, 2016b, 2016c) demonstrated that a heat treatment (above protein denaturation temperatures) of soy proteins can readily transform them into effective Pickering nanoparticle stabilisers for O/W emulsions. The heating remarkably strengthens the intraparticle interactive forces, and the internal structure of these heat-induced nanoparticles is mainly maintained by both hydrophobic interactions and disulphide bonds. Zhu et al. (2017) evaluated the freeze-thaw stability of Pickering emulsions stabilised by nanoparticles from heated soy protein

isolate and whey protein regarding flocculation, coalescence, and creaming index. The enhanced freeze-thaw stability of these emulsions seemed to be a consequence of the Pickering steric stabilisation, and the gel-like network formation. Soy protein isolate microgel particles produced by heat denaturation, followed by high pressure homogenisation or sonication, with different NaCl contents, could stabilise O/W emulsions by acting as a wall material for microencapsulating soybean oil by spray drying (Benetti et al., 2019). The presence of NaCl slightly affected the droplet size of the emulsions but led to an increase in flocculation and induced shear-thinning behaviour in the system. Spherical microcapsules with high oil retention (>80%) could be produced by spray drying the emulsions.

Ju et al. (2020) fabricated a novel Pickering emulsion stabilised by covalently bonded soy protein isolate-anthocyanin nanoparticles. The improved oxidative stability, resistance to *in vitro* digestion and noticeable emulsion stability reported in this study could be attributed to the intrinsic properties of Pickering emulsions.

The investigation of biopolymer-based microgels as potential stabilisers in Pickering emulsions offers new opportunities for food technologists. Zhang, Holmes, Ettelaie, et al. (2020) designed plant protein-based microgel particles to create Pickering emulsions. Adjusting the pH of the emulsions to pI made the pea protein microgels adsorbed at the interface to aggregate, providing a higher degree of adsorption and enhanced interdroplet flocculation with shear-thinning character. Findings from this study provide opportunities for applying this protein microgels in food products, focusing on the growing demand by plant-based sustainable stabilisers.

Regarding animal protein, Chevallier et al. (2018, 2019) showed that it is possible to prepare heat-stable emulsions by using whey protein microgels and a sufficient amount of caseins to fully cover a fat droplet surface. Whey protein microgels were highly stable against heating and are able to produce Pickering emulsions with long-term resistance to coalescence. However, the heat stability was reported to depend on the emulsion characteristics (concentration and presence of non-microgel proteins such as caseins). When compared to other polymers used for microgel production, whey protein does not require additional crosslinking agents (Schmitt et al., 2010).

Fibrillar proteins could also interact with polyphenols improving its emulsifying properties. Su et al. (2020) prepared composite nanoparticles with antioxidant

capacity using β-lactoglobulin nanoparticles and epigallocatechin-3-gallate (EGCG) and applied them as Pickering emulsifiers to stabilise a model lutein emulsion. Forming composites between β- lactoglobulin and EGCG was due to the hydrogen bonds and hydrophobic effects. β-lactoglobulin-EGCG composite nanoparticles exhibited stronger antioxidant activity and can exert their effects as particulate emulsifiers with partial wettability, which can produce a thicker interfacial layer around the droplets and repel the aggregation of the droplets through steric repulsion.

Gelatin particles, including microgels and gelatin-containing nanocomplexes, have been also reported to fabricate Pickering emulsions. However, few studies address their feasibility, as the unstable structure and potential toxicity of glutaraldehyde and acetone used to obtain rigid microspheres can limit their usage in edible Pickering emulsions (Zhu, Li, Li, et al. 2020). Ding et al. (2019, 2020) successfully prepared a crosslinked gelatin nanoparticle with good layer formation ability using a two-step desolvation method from bovine bone gelatin granules and used them to prepare Pickering emulsions. The authors explored the variables of the preparation method and storage temperature on the microencapsulation of fish oil by crosslinked gelatin nanoparticles in Pickering emulsions. The results demonstrated that gelatin molecular structure affected droplet size and creaming stability, but not the droplet size. Another work by Feng et al. (2019) also prepared food-grade gelatin nanoparticles (GNPs) using a two-step desolvation method to stabilise O/W Pickering emulsion. The results showed that GNPs with narrow size distribution and good dispersion could only be obtained at pH 12. The Pickering emulsions stabilised by the GNPs had good uniformity and stability, with no obvious phase separation even after 30 days of storage – highlighting their potential to be used as food-grade Pickering stabilisers.

Zhu, Li, Li, et al. (2020) assessed the feasibility of using acid-soluble collagen as a stabiliser to fabricate O/W Pickering emulsions. The stability of Pickering emulsions was enhanced as the acid-soluble collagen concentrations increased. A diminution of particle size and a gel-like structure formed in the emulsion is the main reason that enables an effective adsorption of acid-soluble collagen at O/W interface. Collagen has excellent mechanical properties to prepare viscoelastic emulsions with solid-like appearance. This fact makes possible the use of collagen to produce fat mimetics aiming at designing reduced-fat products as breads and chocolates.

However, factors such as the risk of pathogen contamination, cultural dietary, and price are the main limiting reasons to be overcome for real application of animal-based protein particles in food industries.

4.1.3.3. Pickering emulsions with protein-polysaccharide complexes and conjugates

An additional interesting approach for producing Pickering emulsifier candidates involves the utilisation of protein-polysaccharide complex-based nanoparticles (Table 4.1). These complexes are perfect to create distinct types of colloidal systems with unique properties that result in higher stability than using individual biopolymers. Complexes of zein with different polysaccharides have been used by several authors. Sun et al. (2019) produced stable Pickering emulsions using spherical zein colloid particles and fibrous chitin nanofiber complexes as stabilisers. Chitin nanofiber aggregations were found on the O/W interface, providing steric hindrance among oil droplets, but zein colloid particles played a dominant role in stabilising oil droplets. The chief driving forces between them were hydrogen bonds and hydrophobic interaction, thus, regulating the interaction between these two components is an effective method to modulate the physicochemical properties of emulsions. Shi et al. (2016) fabricated novel film-forming emulsions based on zein-chitosan colloid particles; the Pickering emulsions were extremely stable, evidenced by the similar droplet sizes and size distribution in the film matrix. Interestingly, emulsion films exhibited excellent oxygen-barrier efficiency. This study opened a promising pathway for producing emulsion films with excellent oxygen-barrier capability via the manipulation of the film-forming emulsion's interfacial nanostructure using the Pickering stabilisation principle.

Dai et al. (2018) successfully prepared zein-gum arabic complex colloidal nanoparticles (ZGAPs) with a core-shell structure through hydrogen bonding and electrostatic interactions. The resulting emulsions were adequately obtained with high oil volume fractions (0.5-0.7). ZGAPs absorbed efficiently at the O/W interface, forming steric barriers. Consequently, Pickering emulsion gels could be obtained with long-term storage stability.

Another vegetal protein often used to form protein-polysaccharide complexes and conjugates is soy protein. Zhang, Zhou, Chen, et al. (2020) presented an easy method for making edible solid foams using Pickering emulsion technology. The O/W Pickering emulsions, stabilised by soy protein isolate and bacterial cellulose,

exhibited smaller droplet sizes and better physical stability with increasing contents of complexes or with increased oil volume. Further, the nanoscale soy protein isolate aggregates could adsorb on the bacterial cellulose nanofibril networks. Dynamic rheology results showed that all emulsions presented gel-like rheological behaviour, and both the shear viscosity and viscoelastic moduli increased with the increasing content of complexes or oil volume fractions.

Ashaolu and Zhao (2020) prepared a conjugate of soy protein isolate with okara dietary fibre by crosslinking using the Maillard reaction. The resulting soy protein isolate-okara dietary fibre conjugates were thermally stable, hydrophilic, and exhibited excellent Pickering emulsion stabilisation potential. In addition, the conjugates' structure and function relationships, amino acid profile, and emulsifying potential were favourable for formulating of emulsion-based foods.

A promising protein-polysaccharide complex was designed between gliadin and chitosan. Li, He, Li, et al. (2019) studied Pickering emulsions stabilised by gliadin-chitosan nanoparticles (GCNPs). Three types of GCNPs structures, including primary complexation, soluble complexes, and coacervates were obtained by simply altering pH to produce different interaction levels. The reinforcement in gliadin-chitosan interactions reduced the surface charges of the particles and improved their wettability to absorb at the O/W interface. The gliadin-chitosan soluble complexes and coacervates stabilised more oil bridging droplets together, producing a strong network structure against coalescence. Moreover, the coacervate-stabilised Pickering emulsion had the highest viscoelasticity and solid-like behaviour. The findings showed such interactions can regulate either the stability, as the rheological, and antioxidant properties of GCNPs stabilised Pickering emulsion through changing the pH.

Khemissi et al. (2018) obtained protein microgels by heating whey protein isolate and mixed them with anionic or cationic polysaccharides; κ-carrageenan or chitosan, respectively. They found that small stable complexes can be formed with κ-carrageenan between pH 4.3 and 5.5 and with chitosan between pH 4.1 and 6.5, both below and above the isoelectric point of the microgels (pI = 5.0). The droplet size was found to be larger with κ-carrageenan than chitosan. Complexation of protein microgels with polysaccharides is a versatile method of modifying the properties of protein particles. Iqbal et al. (2019) studied the influence of oppositely charged protein and polysaccharide microspheres on the rheological properties of

W/O emulsions. Three kinds of polysaccharides (high methoxyl pectin, κ-carrageenan, and sodium alginate) were mixed with whey protein isolate separately in acidic aqueous solutions. The rheological properties suggest denser gel network formation between opposite charged emulsion droplets, especially in the whey protein isolate-high methoxyl pectin mixed system. The three-dimensional networks were formed through the exposure of positive and hydrophobic regions caused by denaturation in whey protein isolate molecules when subjected to heating. Thus, anionic polysaccharides could be bonded with greater efficiency than in single droplet emulsion systems. Potential applications in the food industry are enabled for these structured emulsions, since they may have reduced levels of saturated, trans, and total fat content.

4.1.3.4. Pickering high-internal-phase emulsions (HIPEs)

Pickering stabilisers, which typically comprise solid or semi-solid particles, can be used to form stable HIPEs (Zamani et al. 2018). HIPEs are highly concentrated gelled emulsions with an internal phase volume fraction (Φ) exceeding 0.74 (Cameron and Sherrington 1996). An internal phase volume fraction exceeding this value results in the dispersed droplets reaching their maximum packing density, giving rise to highly viscoelastic flow behaviour. When the highest geometric limit for packing of rigid spheres is exceeded, the liquid droplets in HIPEs are squeezed tightly together and typically develop polyhedral geometries. Texturally, HIPEs are highly viscous or gelled soft solid materials (Zamani et al. 2018). A high resistance to Ostwald ripening, coalescence, and phase separation is one of the advantages found in Pickering HIPEs over the conventional. This kind of HIPE has become a popular research topic due to their applicability in commercial products (Table 4.1) (Xiao, Li, and Huang 2016).

Native proteins have been used as Pickering particles in HIPEs. Recently, Xu, et al. (2018) reported that native ovalbumin of several nanometres is an outstanding Pickering stabiliser for O/W HIPEs, thanks to its strong intramolecular structural stability that ensures its particulate nature when adsorbed at an interface. These Pickering HIPEs exhibit an extraordinary stability against heating and long-term storage, unique responsiveness to freeze-thawing, and reduced volatile oil vaporization. In another recent study, Xu, Liu and Tang (2019) demonstrated that native soy β-conglycinin (a major storage globulin in soybean), possessing similar

structural features to ovalbumin, is another effective Pickering nanostabiliser for HIPEs.

However, some native proteins need modifications to improve their emulsifying ability. Xu, Tang, and Binks (2020) reported that bovine serum albumin glycated with galactose possessed a much stronger structural integrity and higher refolding ability. The authors showed improved HIPE emulsification and stabilisation when compared to native bovine serum albumin. A core-shell nanostructure formed with a hydrophilic galactose shell surrounding the protein core in glycated bovine serum albumin is the result of the underlying mechanism for improving emulsification performance. These HIPEs presented a self-supporting gel network that contributes to an enhanced stability under long-term storage, resistance to drastic heating and good freeze-thaw reversibility.

Yang, Li, and Tang (2020) obtained nanoparticles (160 nm) from some insoluble okara soy polysaccharides (a by-product of soybean processing) covalently attached to proteins in a glycoprotein matrix (arabinogalactan-proteins and glucomannan-proteins) that could perform as an outstanding Pickering stabiliser for HIPEs. The structure of the nanoparticles was stable, and the gels could be formed over their tested pH or ionic strength range. Moreover, these gels exhibited excellent stability during prolonged storage and heating up to temperatures between 50 and 90 °C. These nanoparticles exhibited an interesting potential to behave as Pickering stabilisers for emulsifying HIPES with ability to form HIPE gels. Moreover, using the high-added-value of the soybean by-product in their processing industries is advantageous.

Polysaccharides have also been used as Pickering particles in HIPEs. Zhu, Huan, Bai, et al. (2020) successfully prepared stable O/W Pickering HIPEs stabilised by chitin nanofibrils using a simple two-step strategy. The high stabilisation ability of rod-like chitin nanofibrils originated from the restricted coarsening, droplet breakage, and coalescence upon emulsion formation. This resulted from an irreversible adsorption at the interface at the same time a fibrillar networks is highly interconnected in the continuous phase. Furthermore, the authors proposed a new manufacturing strategy for edible materials combining 3D printing and food-grade Pickering HIPEs. Their results demonstrated that chitin nanofibrils-stabilised HIPEs can fulfil the requirement of clean-labels for foodstuff and green materials.

Wang et al. (2018) showed that avocado oil based HIPEs were formulated and stabilised by citrus nanofibers (CNFs) and tannic acid (TA) by means of shear-induced emulsification method. CNFs/TA complex colloidal nanofibers with enhanced interfacial reactivity can be utilised for preparing stable avocado oil based HIPEs by one-step homogenisation. Forming an antioxidant interface using the interfacial cargo of TA further markedly enhanced the oxidative stability of the emulsions. This study offered valuable information to prepare polyphenol-nanofiber colloidal complexes and their use as antioxidants in food solutions.

Protein-polysaccharide particles formed with plant-based proteins are also remarkable for stabilising HIPEs. Zeng et al. (2017) reported the usage of mono-dispersed gliadin-chitosan hybrid particles as a particulate emulsifier for HIPEs development. The hybrid particles with partial wettability were fabricated at pH 5.0 using an easy antisolvent method. Stable HIPEs with up to an 83% internal phase can be prepared with low particle concentrations (0.5-2%). The hybrid particles were effectively adsorbed and anchored at the O/W interface to exert steric hindrance against coalescence. The protective effect of Pickering HIPEs on curcumin was confirmed and represents a sustainable alternative to convert polyunsaturated liquid oils into viscoelastic soft solids in replacement of hydrogenated oils.

Pickering HIPEs were prepared by Ma et al. (2020) by simply mixing an 15% v/v gliadin nanoparticle aqueous solution with gum Arabic and corn oil (85% v/v). The gum Arabic increased the apparent viscosity, storage modulus, and creaming stability of the HIPEs, resulting in an enhanced resistance to changes in pH, ionic strength, and temperature.

Hao, Peng, and Tang (2020) developed soy protein-based Pickering stabilisers for HIPEs to aid the emulsifying properties of proteins by glycation with carbohydrates. Soy glycinin, considered an important soy storage globulin, showed good performance as a Pickering stabiliser for HIPEs. In addition, its glycation with a soy soluble polysaccharide significantly improved the emulsification performance of the soy glycinin, the gel network formation, and stability against heating or freeze-thawing of the corresponding HIPEs. The HIPEs stabilised by untreated or glycated soy glycinin also presented great coalescence stability over long-term storage.

Vélez-Erazo et al. (2020) structured sunflower oil using pea protein as an emulsifier with various polysaccharides (carrageenan, xanthan gum, gum Arabic, sodium alginate, pectin, gellan gum, locust bean gum, and tara gum) as stabilisers;

O/W emulsions were made with a protein:polysaccharide ratio of 4:1. Pickering HIPEs with the pea protein:xanthan gum and pea protein:tara gum formulations gave a creamy and uniform appearance, with minimal oil loss. This study explains the behaviour and interaction of pea protein with eight different polysaccharides in edible oils structuring and provides interesting insight for use as fat substitutes in food formulations.

Protein-polysaccharide particles containing animal proteins, in this case dairy proteins, showed remarkable results as Pickering stabilisers. Zhu, McClements, Zhou, et al. (2020) investigated the application of whey protein isolate-low methoxyl pectin (WPI-LMP) particles, generated by complex coacervation, as a food-grade particle stabiliser. The coacervation pH greatly influenced the emulsifying ability of the WPI-LMP particles, which could generate an HIPE with an oil fraction up to 79%. However, the emulsification ability of the WPI-LMP coacervates was sensitive to ionic strength and their concentration.

4.1.4. Conclusions

Novel opportunities are emerging for the stabilisation of food emulsions using solid biopolymer nanoparticles and microparticles. Food scientists and the food industry are in search of sustainable, cheap, clean-label, eco-friendly, and effective food-grade particles suitable to stabilise Pickering emulsions.

The primary advantage of solid biopolymer stabilisation is its longevity regarding coalescence, showing no significant structural changes, even as rather coarse droplets develop after several months. This is due to the effective steric structural barrier formed by the adsorbed solid particles. The stable inter-biopolymer electrostatic complexes formed by oppositely charged proteins and polysaccharides can produce and stabilise emulsions effectively. However, they can be influenced by many parameters including salt concentration, pH values, and the protein to polysaccharide ratio. In contrast, covalently crosslinked complexes are more permanent and stronger. These systems usually present great stability towards coalescence and, when the three-dimensional network is formed in the continuous phase, creaming or sedimentation is impaired.

It is well-known that only a few solid particles are suitable for food industries. Good stabilisation of O/W emulsions has been reported when using prolamins in

combination with other water-soluble polymers which, in turn, reduce the hydrophobicity of the prolamin particles. In addition, cellulose-based and chitin derivatives have attracted much attention due to their non-toxicity, biocompatibility, and biodegradability. Furthermore, chitosan and nanocelluloses satisfies the increasing demands for a sustainable and environmentally friendly stabiliser for Pickering emulsions.

Lastly, the interest in the development of gel-like emulsions has been growing due to the unique properties of three-dimensional solid-like behaviour that offer the emulsions a variety of applications in food industries. Pickering HIPEs formulated with the adequate solid particles have a promising potential to achieve long-term stable emulsions.

The current challenge entails translating the knowledge of emulsion stabilisation using solid particles into useful industrial applications. The presence of several possibilities boosts researches in order to select new suitable and clean-label ingredients that can improve existing formulations and explore new applications.

4.1.5. Acknowledgements

4.1.6. References

Ahsan, H. M., Zhang, X., Li, Y., Li, B., & Liu, S. (2019). Surface modification of microcrystalline cellulose: Physicochemical characterization and applications in the Stabilization of Pickering emulsions. International Journal of Biological Macromolecules, 132, 1176–1184.

Altuna, L., Herrera, M. L., & Foresti, M. L. (2018). Synthesis and characterization of octenyl succinic anhydride modified starches for food applications. A review of recent literature. Food Hydrocolloids, 80, 97–110.

Ashaolu, T. J., & Zhao, G. (2020). Fabricating a pickering stabilizer from Okara dietary fibre particulates by conjugating with soy protein isolate via maillard reaction. Foods, 9(2).

Atarian, M., Rajaei, A., Tabatabaei, M., Mohsenifar, A., & Bodaghi, H. (2019). Formulation of Pickering sunflower oil-in-water emulsion stabilized by chitosan-stearic acid nanogel and studying its oxidative stability. Carbohydrate Polymers, 210, 47–55.

Bai, L., Huan, S., Xiang, W., Liu, L., Yang, Y., Nugroho, R. W. N., … Rojas, O. J. (2019). Self-Assembled Networks of Short and Long Chitin Nanoparticles for Oil/Water Interfacial Superstabilization. ACS Sustainable Chemistry and Engineering, 7(7), 6497–6511.

Barkhordari, M. R., & Fathi, M. (2018). Production and characterization of chitin nanocrystals from prawn shell and their application for stabilization of Pickering emulsions. Food Hydrocolloids, 82, 338–345.

Benetti, J. V. M., do Prado Silva, J. T., & Nicoletti, V. R. (2019). SPI microgels applied to Pickering stabilization of O/W emulsions by ultrasound and high-pressure homogenization: rheology and spray drying. Food Research International, 122, 383–391.

Berton-Carabin, C. C., & Schroën, K. (2015). Pickering Emulsions for Food Applications: Background, Trends, and Challenges. Annual Review of Food Science and Technology, 6(1), 263–297.

Binks, B. P. (2002). Particles as surfactants—similarities and differences. Current Opinion in Colloid & Interface Science, 7(1–2), 21–41.

Cameron, N. R., & Sherrington, D. C. (1996). High internal phase emulsions (HIPEs) --- Structure, properties and use in polymer preparation. In Biopolymers Liquid Crystalline Polymers Phase Emulsion (pp. 163–214). Berlin, Heidelberg: Springer Berlin Heidelberg.

Chen, H., Ji, A., Qiu, S., Liu, Y., Zhu, Q., & Yin, L. (2018). Covalent conjugation of bovine serum album and sugar beet pectin through Maillard reaction/laccase catalysis to improve the emulsifying properties. Food Hydrocolloids, 76, 173–183.

Chen, Q. H., Liu, T. X., & Tang, C. H. (2019). Tuning the stability and microstructure of fine Pickering emulsions stabilized by cellulose nanocrystals. Industrial Crops and Products, 141(August).

Chevallier, M., Riaublanc, A., Cauty, C., Hamon, P., Rousseau, F., Thevenot, J., … Croguennec, T. (2019). The repartition of whey protein microgels and caseins between fat droplet surface and the continuous phase governs the heat stability

of emulsions. Colloids and Surfaces A: Physicochemical and Engineering Aspects, 563, 217–225.

Chevallier, M., Riaublanc, A., Lopez, C., Hamon, P., Rousseau, F., Thevenot, J., & Croguennec, T. (2018). Increasing the heat stability of whey protein-rich emulsions by combining the functional role of WPM and caseins. Food Hydrocolloids, 76, 164–172.

Dai, H., Wu, J., Zhang, H., Chen, Y., Ma, L., Huang, H., … Zhang, Y. (2020). Recent advances on cellulose nanocrystals for Pickering emulsions: Development and challenge. Trends in Food Science and Technology, 102(2), 16–29.

Dai, L., Sun, C., Wei, Y., Mao, L., & Gao, Y. (2018). Characterization of Pickering emulsion gels stabilized by zein/gum arabic complex colloidal nanoparticles. Food Hydrocolloids, 74, 239–248.

De Folter, J. W. J., Van Ruijven, M. W. M., & Velikov, K. P. (2012). Oil-in-water Pickering emulsions stabilized by colloidal particles from the water-insoluble protein zein. Soft Matter, 8(25), 6807–6815.

Destribats, M., Rouvet, M., Gehin-Delval, C., Schmitt, C., & Binks, B. P. (2014). Emulsions stabilised by whey protein microgel particles: Towards food-grade Pickering emulsions. Soft Matter, 10(36), 6941–6954.

Dickinson, E. (2010). Food emulsions and foams: Stabilization by particles. Current Opinion in Colloid and Interface Science, 15(1–2), 40–49.

Dickinson, E. (2012). Use of nanoparticles and microparticles in the formation and stabilization of food emulsions. Trends in Food Science and Technology, 24(1), 4–12.

Dickinson, E. (2013). Stabilising emulsion-based colloidal structures with mixed food ingredients. Journal of the Science of Food and Agriculture, 93(4), 710–721.

Dickinson, E. (2015a). Colloids in Food: Ingredients, Structure, and Stability. Annual Review of Food Science and Technology, 6(1), 211–233.

Dickinson, E. (2015b). Microgels - An alternative colloidal ingredient for stabilization of food emulsions. Trends in Food Science and Technology, 43(2), 178–188.

Dickinson, E. (2017). Biopolymer-based particles as stabilizing agents for emulsions and foams. Food Hydrocolloids, 68, 219–231.

Ding, M., Zhang, T., Zhang, H., Tao, N., Wang, X., & Zhong, J. (2019). Effect of preparation factors and storage temperature on fish oil-loaded crosslinked

gelatin nanoparticle pickering emulsions in liquid forms. Food Hydrocolloids, 95, 326–335.

Ding, M., Zhang, T., Zhang, H., Tao, N., Wang, X., & Zhong, J. (2020). Gelatin molecular structures affect behaviors of fish oil-loaded traditional and Pickering emulsions. Food Chemistry, 309.

Donsì, F., Voudouris, P., Veen, S. J., & Velikov, K. P. (2017). Zein-based colloidal particles for encapsulation and delivery of epigallocatechin gallate. Food Hydrocolloids, 63, 508–517.

Du Le, H., Loveday, S. M., Singh, H., & Sarkar, A. (2020). Pickering emulsions stabilised by hydrophobically modified cellulose nanocrystals: Responsiveness to pH and ionic strength. Food Hydrocolloids, 99(May 2019).

Feng, X., Dai, H., Ma, L., Yu, Y., Tang, M., Li, Y., … Zhang, Y. (2019). Food-grade gelatin nanoparticles: Preparation, characterization, and preliminary application for stabilizing pickering emulsions. Foods, 8(10).

Gao, Z. M., Yang, X. Q., Wu, N. N., Wang, L. J., Wang, J. M., Guo, J., & Yin, S. W. (2014). Protein-based pickering emulsion and oil gel prepared by complexes of zein colloidal particles and stearate. Journal of Agricultural and Food Chemistry, 62(12), 2672–2678.

Gong, J., Li, J., Xu, J., Xiang, Z., & Mo, L. (2017). Research on cellulose nanocrystals produced from cellulose sources with various polymorphs. RSC Advances, 7(53), 33486–33493.

Grishkewich, N., Mohammed, N., Tang, J., & Tam, K. C. (2017). Recent advances in the application of cellulose nanocrystals. Current Opinion in Colloid and Interface Science, 29, 32–45.

Hao, Z. Z., Peng, X. Q., & Tang, C. H. (2020). Edible pickering high internal phase emulsions stabilized by soy glycinin: Improvement of emulsification performance and pickering stabilization by glycation with soy polysaccharide. Food Hydrocolloids, 103.

Hirsch, A., Cho, Y.-H., Kim, Y. H. B., & Jones, O. G. (2019). Contributions of protein and milled chitin extracted from domestic cricket powder to emulsion stabilization. Current Research in Food Science, 1, 17–23.

Hu, Y. Q., Yin, S. W., Zhu, J. H., Qi, J. R., Guo, J., Wu, L. Y., … Yang, X. Q. (2016). Fabrication and characterization of novel Pickering emulsions and Pickering

high internal emulsions stabilized by gliadin colloidal particles. Food Hydrocolloids, 61, 300–310.

Jin, W., Zhu, J., Jiang, Y., Shao, P., Li, B., & Huang, Q. (2017). Gelatin-Based Nanocomplex-Stabilized Pickering Emulsions: Regulating Droplet Size and Wettability through Assembly with Glucomannan. Journal of Agricultural and Food Chemistry, 65(7), 1401–1409.

Jones, O. G., & McClements, D. J. (2010a). Biopolymer Nanoparticles from Heat-Treated Electrostatic Protein-Polysaccharide Complexes: Factors Affecting Particle Characteristics. Journal of Food Science, 75(2).

Jones, O. G., & McClements, D. J. (2010b). Functional biopolymer particles: Design, fabrication, and applications. Comprehensive Reviews in Food Science and Food Safety, 9(4), 374–397.

Ju, M., Zhu, G., Huang, G., Shen, X., Zhang, Y., Jiang, L., & Sui, X. (2020). A novel pickering emulsion produced using soy protein-anthocyanin complex nanoparticles. Food Hydrocolloids, 99.

Kaku, Y., Fujisawa, S., Saito, T., & Isogai, A. (2020). Synthesis of Chitin Nanofiber-Coated Polymer Microparticles via Pickering Emulsion. Biomacromolecules.

Kalashnikova, I., Bizot, H., Bertoncini, P., Cathala, B., & Capron, I. (2013). Cellulosic nanorods of various aspect ratios for oil in water Pickering emulsions. Soft Matter, 9(3), 952–959.

Kasaai, M. R. (2018). Zein and zein -based nano-materials for food and nutrition applications: A review. Trends in Food Science and Technology, 79, 184–197.

Khemissi, H., Bassani, H., Aschi, A., Capron, I., Benyahia, L., & Nicolai, T. (2018). Exploiting Complex Formation between Polysaccharides and Protein Microgels to Influence Particle Stabilization of W/W Emulsions. Langmuir, 34(39), 11806–11813.

Li, M. F., He, Z. Y., Li, G. Y., Zeng, Q. Z., Su, D. X., Zhang, J. L., … He, S. (2019). The formation and characterization of antioxidant pickering emulsions: Effect of the interactions between gliadin and chitosan. Food Hydrocolloids, 90, 482–489.

Li, Q., Wang, Y., Wu, Y., He, K., Li, Y., Luo, X., … Liu, S. (2019). Flexible cellulose nanofibrils as novel pickering stabilizers: The emulsifying property and packing behavior. Food Hydrocolloids, 88, 180–189.

Li, S., Zhang, B., Li, C., Fu, X., & Huang, Q. (2020). Pickering emulsion gel stabilized by octenylsuccinate quinoa starch granule as lutein carrier: Role of the gel network. Food Chemistry, 305, 125476.

Li, X. M., Zhu, J., Pan, Y., Meng, R., Zhang, B., & Chen, H. Q. (2019). Fabrication and characterization of pickering emulsions stabilized by octenyl succinic anhydride -modified gliadin nanoparticle. Food Hydrocolloids, 90(September 2018), 19–27.

Li, Xia, Li, J., Gong, J., Kuang, Y., Mo, L., & Song, T. (2018). Cellulose nanocrystals (CNCs) with different crystalline allomorph for oil in water Pickering emulsions. Carbohydrate Polymers, 183, 303–310.

Li, Xiufeng, & de Vries, R. (2018). Interfacial stabilization using complexes of plant proteins and polysaccharides. Current Opinion in Food Science, 21, 51–56.

Liang, H. N., & Tang, C. H. (2014). Pea protein exhibits a novel Pickering stabilization for oil-in-water emulsions at pH 3.0. LWT - Food Science and Technology, 58(2), 463–469.

Liu, F., & Tang, C. H. (2013). Soy protein nanoparticle aggregates as pickering stabilizers for oil-in-water emulsions. Journal of Agricultural and Food Chemistry, 61(37), 8888–8898.

Liu, F., & Tang, C. H. (2014). Emulsifying properties of soy protein nanoparticles: Influence of the protein concentration and/or emulsification process. Journal of Agricultural and Food Chemistry, 62(12), 2644–2654.

Liu, F., & Tang, C. H. (2016a). Soy glycinin as food-grade Pickering stabilizers: Part. I. Structural characteristics, emulsifying properties and adsorption/arrangement at interface. Food Hydrocolloids, 60, 606–619.

Liu, F., & Tang, C. H. (2016b). Soy glycinin as food-grade Pickering stabilizers: Part. II. Improvement of emulsification and interfacial adsorption by electrostatic screening. Food Hydrocolloids, 60, 620–630.

Liu, F., & Tang, C. H. (2016c). Soy glycinin as food-grade Pickering stabilizers: Part. III. Fabrication of gel-like emulsions and their potential as sustained-release delivery systems for β-carotene. Food Hydrocolloids, 56, 434–444.

Liu, X., Huang, Y. Q., Chen, X. W., Deng, Z. Y., & Yang, X. Q. (2019). Whole cereal protein-based Pickering emulsions prepared by zein-gliadin complex particles. Journal of Cereal Science, 87, 46–51.

Liu, X., Liu, Y. Y., Guo, J., Yin, S. W., & Yang, X. Q. (2017). Microfluidization initiated cross-linking of gliadin particles for structured algal oil emulsions. Food Hydrocolloids, 73, 153–161.

Ma, L., Zou, L., McClements, D. J., & Liu, W. (2020). One-step preparation of high internal phase emulsions using natural edible Pickering stabilizers: Gliadin nanoparticles/gum Arabic. Food Hydrocolloids, 100.

Mao, L., Lu, Y., Cui, M., Miao, S., & Gao, Y. (2019). Design of gel structures in water and oil phases for improved delivery of bioactive food ingredients. Critical Reviews in Food Science and Nutrition, 1–16.

Mao, L., Wang, D., Liu, F., & Gao, Y. (2018). Emulsion design for the delivery of β-carotene in complex food systems. Critical Reviews in Food Science and Nutrition, 58(5), 770–784.

Mitbumrung, W., Suphantharika, M., McClements, D. J., & Winuprasith, T. (2019). Encapsulation of Vitamin D3 in Pickering Emulsion Stabilized by Nanofibrillated Mangosteen Cellulose: Effect of Environmental Stresses. Journal of Food Science, 84(11), 3213–3221.

Murray, B. S. (2019). Pickering emulsions for food and drinks. Current Opinion in Food Science, 27, 57–63.

Muxika, A., Etxabide, A., Uranga, J., Guerrero, P., & de la Caba, K. (2017). Chitosan as a bioactive polymer: Processing, properties and applications. International Journal of Biological Macromolecules, 105, 1358–1368.

Nicolai, T., & Durand, D. (2013). Controlled food protein aggregation for new functionality. Current Opinion in Colloid and Interface Science, 18(4), 249–256.

Nsor-Atindana, J., Chen, M., Goff, H. D., Zhong, F., Sharif, H. R., & Li, Y. (2017). Functionality and nutritional aspects of microcrystalline cellulose in food. Carbohydrate Polymers, 172, 159–174.

Rayner, M., Marku, D., Eriksson, M., Sjöö, M., Dejmek, P., & Wahlgren, M. (2014). Biomass-based particles for the formulation of Pickering type emulsions in food and topical applications. Colloids and Surfaces A: Physicochemical and Engineering Aspects, 458(1), 48–62.

Ribeiro, E. F., Borreani, J., Moraga, G., Nicoletti, V. R., Quiles, A., & Hernando, I. (2020). Digestibility and Bioaccessibility of Pickering Emulsions of Roasted Coffee Oil Stabilized by Chitosan and Chitosan-Sodium Tripolyphosphate Nanoparticles. Food Biophysics, (1903).

Ribeiro, E. F., de Barros Alexandrino, T. T., Assis, O. B. G., Junior, A. C., Quiles, A., Hernando, I., & Nicoletti, V. R. (2020). Chitosan and crosslinked chitosan nanoparticles: synthesis, characterization and their role as Pickering emulsifiers. Carbohydrate Polymers, 116878.

Rutkevičius, M., Allred, S., Velev, O. D., & Velikov, K. P. (2018). Stabilization of oil continuous emulsions with colloidal particles from water-insoluble plant proteins. Food Hydrocolloids, 82, 89–95.

Saari, H., Wahlgren, M., Rayner, M., Sjöö, M., & Matos, M. (2019). A comparison of emulsion stability for different OSA-modified waxy maize emulsifiers: Granules, dissolved starch, and non-solvent precipitates. PLoS ONE, 14(2).

Sánchez de la Concha, B. B., Agama-Acevedo, E., Aguirre-Cruz, A., Bello-Pérez, L. A., & Álvarez-Ramírez, J. (2020). OSA Esterification of Amaranth and Maize Starch Nanocrystals and Their Use in "Pickering" Emulsions. Starch/Staerke, 1900271, 1–5.

Sarkar, A., & Dickinson, E. (2020). Sustainable food-grade Pickering emulsions stabilized by plant-based particles. Current Opinion in Colloid and Interface Science, 49, 69–81.

Schmitt, C., Moitzi, C., Bovay, C., Rouvet, M., Bovetto, L., Donato, L., … Stradner, A. (2010). Internal structure and colloidal behaviour of covalent whey protein microgels obtained by heat treatment. Soft Matter, 6, 4876.

Semenova, M. (2017). Protein–polysaccharide associative interactions in the design of tailor-made colloidal particles. Current Opinion in Colloid and Interface Science, 28, 15–21.

Shao, H., Tang, C. Y., Shuai, M. B., Xu, K. Q., Zhou, Y. L., Hu, X., & Qi, J. J. (2015). Improving the Surface Wettability of Parylene C Film by Hyperthermal Hydrogen Induced Cross-Linking Technology. Advanced Materials Research, 1120–1121, 64–67.

Sharkawy, A., Barreiro, M. F., & Rodrigues, A. E. (2019). Preparation of chitosan/gum Arabic nanoparticles and their use as novel stabilizers in oil/water Pickering emulsions. Carbohydrate Polymers, 224.

Shi, W. J., Tang, C. H., Yin, S. W., Yin, Y., Yang, X. Q., Wu, L. Y., & Zhao, Z. G. (2016). Development and characterization of novel chitosan emulsion films via pickering emulsions incorporation approach. Food Hydrocolloids, 52, 253–264.

Song, X., Zheng, F., Ma, F., Kang, H., & Ren, H. (2020). The physical and oxidative stabilities of Pickering emulsion stabilized by starch particle and small molecular surfactant. Food Chemistry, 303.

Stone, A. K., Tanaka, T., & Nickerson, M. T. (2019). Protein quality and physicochemical properties of commercial cricket and mealworm powders. Journal of Food Science and Technology, 56(7), 3355–3363.

Su, J., Guo, Q., Chen, Y., Mao, L., Gao, Y., & Yuan, F. (2020). Utilization of β-lactoglobulin- (−)-Epigallocatechin- 3-gallate(EGCG) composite colloidal nanoparticles as stabilizers for lutein pickering emulsion. Food Hydrocolloids, 98(17), 105293.

Sun, G., Zhao, Q., Liu, S., Li, B., & Li, Y. (2019). Complex of raw chitin nanofibers and zein colloid particles as stabilizer for producing stable pickering emulsions. Food Hydrocolloids, 97(1), 105178.

Sun, Q. (2018). Starch Nanoparticles. Starch in Food: Structure, Function and Applications: Second Edition. Elsevier Ltd.

Tang, C. H. (2019). Nanostructured soy proteins: Fabrication and applications as delivery systems for bioactives (a review). Food Hydrocolloids, 91, 92–116.

Tang, J., Sisler, J., Grishkewich, N., & Tam, K. C. (2017). Functionalization of cellulose nanocrystals for advanced applications. Journal of Colloid and Interface Science, 494, 397–409.

Tavernier, I., Wijaya, W., Van der Meeren, P., Dewettinck, K., & Patel, A. R. (2016). Food-grade particles for emulsion stabilization. Trends in Food Science and Technology, 50, 159–174.

Wang, C., Fu, X., Tang, C. H., Huang, Q., & Zhang, B. (2017). Octenylsuccinate starch spherulites as a stabilizer for Pickering emulsions. Food Chemistry, 227, 298–304.

Wang, J. S., Wang, A. B., Zang, X. P., Tan, L., Ge, Y., Lin, X. E., … Ma, W. H. (2018). Physical and oxidative stability of functional avocado oil high internal phase emulsions collaborative formulated using citrus nanofibers and tannic acid. Food Hydrocolloids, 82, 248–257.

Wang, L. J., Hu, Y. Q., Yin, S. W., Yang, X. Q., Lai, F. R., & Wang, S. Q. (2015). Fabrication and characterization of antioxidant pickering emulsions stabilized by zein/chitosan complex particles (ZCPs). Journal of Agricultural and Food Chemistry, 63(9), 2514–2524.

Wang, P. P., Luo, Z. G., Chun-Chen, Xiong-Fu, & Tamer, T. M. (2020). Effects of octenyl succinic anhydride groups distribution on the storage and shear stability of Pickering emulsions formulated by modified rice starch. Carbohydrate Polymers, 228.

Wang, Y., & Padua, G. W. (2012). Nanoscale characterization of zein self-assembly. Langmuir, 28(5), 2429–2435.

Weissmueller, N. T., Lu, H. D., Hurley, A., & Prud'Homme, R. K. (2016). Nanocarriers from GRAS Zein Proteins to Encapsulate Hydrophobic Actives. Biomacromolecules, 17(11), 3828–3837.

Winuprasith, T., Khomein, P., Mitbumrung, W., Suphantharika, M., Nitithamyong, A., & McClements, D. J. (2018). Encapsulation of vitamin D3 in pickering emulsions stabilized by nanofibrillated mangosteen cellulose: Impact on in vitro digestion and bioaccessibility. Food Hydrocolloids, 83, 153–164.

Wu, B. C., & McClements, D. J. (2015). Modulating the morphology of hydrogel particles by thermal annealing: Mixed biopolymer electrostatic complexes. Journal of Physics D: Applied Physics, 48(43).

Xiao, J., Li, Y., & Huang, Q. (2016). Recent advances on food-grade particles stabilized Pickering emulsions: Fabrication, characterization and research trends. Trends in Food Science and Technology, 55, 48–60.

Xiao, J., Li, Y., Li, J., Gonzalez, A. P., Xia, Q., & Huang, Q. (2015). Structure, morphology, and assembly behavior of kafirin. Journal of Agricultural and Food Chemistry, 63(1), 216–224.

Xiao, J., Lu, X., & Huang, Q. (2017). Double emulsion derived from kafirin nanoparticles stabilized Pickering emulsion: Fabrication, microstructure, stability and in vitro digestion profile. Food Hydrocolloids, 62, 230–238.

Xiao, J., Wang, X., Perez Gonzalez, A. J., & Huang, Q. (2016). Kafirin nanoparticles-stabilized Pickering emulsions: Microstructure and rheological behavior. Food Hydrocolloids, 54, 30–39.

Xu, Y. T., Liu, T. X., & Tang, C. H. (2019). Novel pickering high internal phase emulsion gels stabilized solely by soy β-conglycinin. Food Hydrocolloids, 88, 21–30.

Xu, Y. T., Tang, C. H., & Binks, B. P. (2020). High internal phase emulsions stabilized solely by a globular protein glycated to form soft particles. Food Hydrocolloids, 98.

Xu, Y. T., Tang, C. H., Liu, T. X., & Liu, R. (2018). Ovalbumin as an Outstanding Pickering Nanostabilizer for High Internal Phase Emulsions. Journal of Agricultural and Food Chemistry, 66(33), 8795–8804.

Yang, T., Li, X. T., & Tang, C. H. (2020). Novel edible pickering high-internal-phase-emulsion gels efficiently stabilized by unique polysaccharide-protein hybrid nanoparticles from Okara. Food Hydrocolloids, 98.

Zamani, S., Malchione, N., Selig, M. J., & Abbaspourrad, A. (2018). Formation of shelf stable Pickering high internal phase emulsions (HIPE) through the inclusion of whey protein microgels. Food and Function, 9(2), 982–990.

Zeeb, B., McClements, D. J., & Weiss, J. (2017). Enzyme-Based Strategies for Structuring Foods for Improved Functionality. Annual Review of Food Science and Technology, 8(1), 21–34.

Zeng, T., Wu, Z. ling, Zhu, J. Y., Yin, S. W., Tang, C. H., Wu, L. Y., & Yang, X. Q. (2017). Development of antioxidant Pickering high internal phase emulsions (HIPEs) stabilized by protein/polysaccharide hybrid particles as potential alternative for PHOs. Food Chemistry, 231, 122–130.

Zhang, S., Holmes, M., Ettelaie, R., & Sarkar, A. (2020). Pea protein microgel particles as Pickering stabilisers of oil-in-water emulsions: Responsiveness to pH and ionic strength. Food Hydrocolloids, 102(June 2019), 105583.

Zhang, X., Zhou, J., Chen, J., Li, B., Li, Y., & Liu, S. (2020). Edible foam based on pickering effect of bacterial cellulose nanofibrils and soy protein isolates featuring interfacial network stabilization. Food Hydrocolloids, 100.

Zhang, Y., Chen, Z., Bian, W., Feng, L., Wu, Z., Wang, P., … Wu, T. (2015). Stabilizing oil-in-water emulsions with regenerated chitin nanofibers. Food Chemistry, 183, 115–121.

Zhu, F. (2019). Starch based Pickering emulsions: Fabrication, properties, and applications. Trends in Food Science and Technology, 85, 129–137.

Zhu, Q., Li, Y., Li, S., & Wang, W. (2020). Fabrication and characterization of acid soluble collagen stabilized Pickering emulsions. Food Hydrocolloids, 106.

Zhu, X. F., Zhang, N., Lin, W. F., & Tang, C. H. (2017). Freeze-thaw stability of pickering emulsions stabilized by soy and whey protein particles. Food Hydrocolloids, 69, 173–184.

Zhu, Y. Q., Chen, X., McClements, D. J., Zou, L., & Liu, W. (2018). Pickering-stabilized emulsion gels fabricated from wheat protein nanoparticles: Effect of

pH, NaCl and oil content. Journal of Dispersion Science and Technology, 39(6), 826–835.

Zhu, Ya, Huan, S., Bai, L., Ketola, A., Shi, X., Zhang, X., … Rojas, O. J. (2020). High Internal Phase Oil-in-Water Pickering Emulsions Stabilized by Chitin Nanofibrils: 3D Structuring and Solid Foam. ACS Applied Materials and Interfaces, 12(9), 11240–11251.

Zhu, Yuqing, Chen, X., McClements, D. J., Zou, L., & Liu, W. (2018). pH-, ion- and temperature-dependent emulsion gels: Fabricated by addition of whey protein to gliadin-nanoparticle coated lipid droplets. Food Hydrocolloids, 77, 870–878.

Zhu, Yuqing, McClements, D. J., Zhou, W., Peng, S., Zhou, L., Zou, L., & Liu, W. (2020). Influence of ionic strength and thermal pretreatment on the freeze-thaw stability of Pickering emulsion gels. Food Chemistry, 303.

Zielińska, E., Karaś, M., & Baraniak, B. (2018). Comparison of functional properties of edible insects and protein preparations thereof. LWT - Food Science and Technology, 91(January), 168–174.

Zou, Y., Yang, X., & Scholten, E. (2018). Rheological behavior of emulsion gels stabilized by zein/tannic acid complex particles. Food Hydrocolloids, 77, 363–371.

Table 4.1 Examples of Pickering emulsions stabilized by protein- and polysaccharide-based particles.

	Particle material	Dispersed/continuous phases	Homogenization	Findings	Reference
Polysaccharides	Rice starch	Sunflower oil (50% v/v) / OSA-modified rice starch (1-2 wt%)	High speed homogenizer 11,000 r/min for 2 min	Starch particles and surfactants improved oxidative stability	Song et al. 2020
	Waxy maize and waxy potato starches	Orange oil (5% w/w) / OSA-starch spherulites	High speed + high pressure homogenizer 150,000 rpm for 3 min	Retarded the lipid oxidation rate	Wang et al. 2017
	Quinoa starch; waxy maize; oat starch	MCT (5 wt%) / starch in phosphate buffer (pH 7) (200-3200 mg/g oil)	High-shear mixer 22 000 rpm, for 1-5 min	Systems dominated by small granules at the interface were less affected by emulsification time	Saari et al. 2019
	Bacterial cellulose (BC)	Dodecane (10-50 v%)/ BCNFs suspensions (0.1-0.5 wt%)	High shear blender 10,000 rpm for 2 min	Strong inter-droplet network formation led to a gel-like behavior	Li et al. 2019
	Chitosan	Canola oil (0.2-.0.8 wt%) / ACPs (1.0 wt%) (pH 6.4-7.0)	Homogenized using a rotor/stator 12 000 rpm for 1 min	Generation of interconnected structures and gel formation.	Wang et al. 2020
	Chitin	Corn oil (10% v/v) / Chitin nanocrystals (0.1, 0.5, 1 and 1.5% w/v)	Ultra-sonic homogenizer 2 min with 10-s intervals	Higher stability attributed to lower droplet sizes	Barkhordari & Fathi, 2018
	Rice starch	N-hexan (10-70%) / OSA-modified	High-speed homogenizer 20,000 rpm for 1 min	Emulsion stability affected by	Wang et al. 2020

		rice starch (OS-RS) (0.1-5%)		distribution of OS groups related to the concentration of NaOH	
	Waxy maize starch	MCT (5%; w/w) / OSA-modified starch (200 mg/mL oil) in phosphate buffer (pH 7, 0.2 M NaCl)	Vortexing for 10 s and high-shear mixed at 22,000 rpm	Emulsion droplet size and stability affected by differences in starch particle size and molecular structure	Saari et al. 2019
	Microcrystalline cellulose	Dodecane oil (10%, v/v) / CMCNa modified MCC composites (0.5-2% w/v in water)	Ultra turrax 12000 rpm for 3 min.	Stability attributed to the inter-droplet network formation	Ahsan et al. 2019
	Nanofibrillated cellulose	Soybean oil + Vitamin D3 (10% w/w) / NFC (1% w/w) in buffer solution (10 mM NaH2PO, pH 7.0)	High-shear mixer for 2 min + high-pressure homogenizer at 12,000 psi for 3 cycles	The network of aggregated fibers slowed down lipid digestion	Winuprasith et al. 2018
Proteins	β-lactoglobulin (β-Lg) fibrils	Soy oil 10% (v/v) / β-Lg fibrils in water (1 mg/mL to 25 mg/mL)	High-speed shear 20,000 rpm for 3 min	Excellent stabilizer at pH far from pI (pH5.0)	Gao et al. 2017
	Gliadin + WPI	Corn oil (30-70 wt%)/ aqueous GNP solution (1% w/w)	High-shear mixer 12,000 rpm for 2 min	WPI addition could facilitate emulsion gel formation	Zhu, Chen, McClements, Zou, & Liu, 2018
	Soybean protein isolate (SPI)	Soybean oil (10-30 wt%)/ SPI microgel suspensions	Ultra-turrax 9,000 rpm for 2 min + high pressure or sonication (20 kHz, 400 W)	Stabilization of O/W emulsions with low oil contents	Benetti, Silva & Nicoletti, 2019
	Soybean protein	Soy oil (20% v/v) / SPI-ACN	10,000 rpm for 2 min using	Protective effect on oxidative	Ju et al. 2020

isolate (SPI)	complex dispersion	Ultra-turrax	stability	
Acid-soluble collagen	Algal oil (30% v/v) / collagen solution (0.01 to 1.5 wt%)	Ultrasound 10 min, 400 W	Gel-like structure with an increase in acid-soluble collagen concentration	Zhu et al. 2020
Gelatin nanoparticles	Fish oil (50% v/v) / gelatin nanoparticles solutions (0.2-4.0%)	Ultra turrax 11,500 rpm for 60 s	Creaming stability was dependent on the molecular structure, concentration, and form of the stabilizer	Ding et al. 2020
Zein nanoparticles	Cinnamon essential oil (12.5 % w/w) + vegetal oil (37,5% w/w) / ZN solution	High shear homogenizer 12,000 rpm for 10 min	Effect in replacing 20% butter in cakes and extending the shelf-life	Feng et al. 2020
Pea protein microgel	Sunflower (20 wt%) / PPM dispersion (0.05-1.0 wt%)	Rotor-stator 8,000 rpm for 5 min	Ultra-stable droplets only at 1.0 wt% protein concentration	Zhang et al. 2020
Okara dietary fiber + SPI	Soy oil (1:2 and 1:3) / ODF-SPI conjugates (5% w/v) dispersion	High-speed shear 20,000 rpm for 2 min	Maillard reaction time directly proportional to emulsion stability	Ashaolu & Zhao, 2020
Protein-polysaccharide complexes Chitin nanofibers + zein colloid particles	Soybean oil (20% w/w) / ChNFs-ZCPs complex dispersion	High-speed blending 12,000 rpm for 3 min	Oiling-off in the upper layer was avoided in the presence of ChNFs	Sun et al. 2019
Zein + Gum arabic	MCT (10-70 wt%) / ZGAPs (1% w/v) dispersions	High-speed homogenizer 12,000 rpm for 3 min	Long-term storage stability at oil fraction ≥ 50%	Dai et al. 2018

	SPI + bacterial cellulose	Dodecane oil (20-50% v/v) SPI/TOBC (12.5:1) complexes dispersions	High-speed shear 16,000 rpm for 2 min	Better stability attributed to the increase in the complexes contents	Zhang et al. 2020
	Gliadin + chitosan	Corn oil (50% v/v) / GCNPs dispersion	High-speed dispersive homogenizer 10 kr/min for 2 min	Retarding effects on lipid oxidation in emulsions stabilized by curcumin-loaded particles	Li et al. 2019
	WPI + HPM/kC/Sodium alginate	Soybean oil (60% wt%) / WPI (10 wt %), HMP (2 wt %) or kC (2 wt %) or sodium alginate (2%)	High-speed shear 1,600 rpm for 2 min	Three-dimensional networks obtained by connecting opposite charges	Iqbal et al. 2019
High-internal-phase emulsions (HIPE)	Cellulose nanocrystals (CNCs)	Soy oil (80 wt% / OSA-modified CNCs (0.1 -1.2 wt%)	High-speed shear 11,500 rpm	Stable and gel-like emulsions	Chen et al. 2018
	Whey protein microgel	Corn oil (75% w/w) / WPM (0.5% w/w)	High-speed shear 17,000 rpm	Rigid layer around the oil droplets preventing coalescence	Zamani et al. 2018
	Ovalbumin	Dodecane (10-92% w/w) / OVA dispersion (0,2-3,0 wt%)	High-speed shear 5,000 rpm for 2 min	Strong structural integrity and strong refolding ability	Xu et al. 2018
	Soy β-conglycinin	Dodecane (10-89% wt%) / β-CG solubilized in phosphate buffer (pH 7.0) (0.08–1.0 wt%)	High-speed dispersing 5,000 rpm for 1 min	Stable upon heating and storage (60 days) but very prone to freeze-thawing	Xu, Liu & Tang (2019)
	Bovine serum	Dodecane (60-93% w/w) / gBSA	High-speed dispersing 5,000 rpm for 1 min	Stability corroborated by	Xu, Tang, &

albumin	particle solution		tendency of gBSA to form HIPE gels.	Binks (2020)
Insoluble soybean polysaccharides	Soy oil (0.1–0.9 wt%) / ISP nanoparticles dispersions (0.125-1.5 wt%)	Ultra turrax 13,500 rpm for 60s.	Stability against storage and heating and reversibility of freeze-thawing-destabilization/re-emulsification	Yang, Li, & Tang (2020)
Chitin nanofibrils	Sunflower oil (66-88 wt%) / NCh suspension (0.5 wt%)	High-speed 22,000 rpm for 1 min	NCh forms a dense, connected network at the oil/water interface, preventing oil coalescence	Zhu et al. (2020)
Citrus nanofibers	Avocado oil (75 wt%) / CNFs-TA suspensions	Ultra turrax 23,000 rpm for 3 min	Oxidative stability attributed to antioxidant interfacial shells around avocado oil droplets	Wang et al. (2018)

Octenyl succinic anhydride (OSA), Cellulose nanocrystals (CNCs), Soy protein isolate (SPI), Sodium stearate (SS), β-lactoglobulin (β -Lg) , Bacterial cellulose nanofibrils (BCNFs), Aggregated chitosan particles (ACPs), Sodium carboxymethyl cellulose (CMCNa) , Microcrystalline cellulose (MCC), Nanofibrillated cellulose (NFC), Anthocyanins (ACN), Chitin nanofibers + zein colloid particles (ChNFs-ZCPs), Okara dietary fiber + Soy protein isolate (ODF-SPI), Medium-chain triglyceride (MCT), Zein and Gum Arabic complex colloidal nanoparticles (ZGAPs), 2, 2, 6, 6-tetramethylpiperidine-1-oxyl radical (TEMPO), TEMPO-oxidized bacterial cellulose (TOBC), Whey protein isolate (WPI), High methoxyl pectin (HMP), κ-carrageenan (kC), Ovalbumin (OVA), Whey protein microgel (WPM), Soy β-conglycinin (β-CG), Bovine serum albumin (BSA), glycated BSA (gBSA), Insoluble soybean polysaccharides (ISP) , Chitin nanofibrils (NCh), Citrus nanofibers (CNFs), Tannic acid (TA), Complex colloidal nanofibers (CNFs-TA).

4.2. CHAPTER 2

In vitro digestion of roasted coffee oil emulsions

Digestibility and bioaccessibility of Pickering emulsions of roasted coffee oil stabilized by chitosan and chitosan-sodium tripolyphosphate nanoparticles

Elisa Franco Ribeiro [1,2], Jennifer Borreani [2], Gemma Moraga [2], Vânia Regina Nicoletti [1], Amparo Quiles [2], Isabel Hernando [2]

[1] Food Engineering and Technology Department, São Paulo State University (Unesp), Institute of Biosciences, Humanities and Exact Sciences (Ibilce), Campus São José do Rio Preto, Cristóvão Colombo Street 2265, São José do Rio Preto, São Paulo State, 15054-000, Brazil.

[2] Grupo de Microestructura y Quimica de Alimentos, Departamento de Tecnología de Alimentos, Universitat Politècnica de València (UPV), Camino de Vera, s/n, Valencia, 46071, Spain.

Abstract: Due to the valuable lipid fraction composition present in roasted coffee oil, it has become important to develop methods that modify its structure, such as emulsion-based encapsulation systems, favoring its use in food industry. Pickering emulsions have appeared as a potential alternative to protect oil droplets stabilized by solid particles rather than the use of surfactants. This work investigated the ability of chitosan (CS) nanoparticles produced by deprotonation and by ionic gelation to stabilize emulsions with different lipid phase content as an alternative to encapsulate roasted coffee oil. An in vitro digestion model consisting of mouth, gastric and intestinal phases was used to characterize the rate and extent of lipid phase digestion, emulsion microstructure, and bioaccessibility of total phenolic compounds. All emulsions presented some structural changes attributed to flocculation and coalescence throughout simulated gastrointestinal digestion. Better droplet stabilization using the deprotonation method was achieved when lower oil content was used, leading to higher bioaccessibility of total phenolic compounds.

Keywords: Encapsulation, phenolic compounds, microstructure, delivery systems, functional foods.

4.2.1. Introduction

Coffee oil has been considered a promising material in food, pharmaceutical and cosmetic industries (Oliveira, 2011; Calligaris, 2009; Wagemaker, 2011), being an important value-added byproduct. The lipid fraction of coffee beans varies considerably between C. arabica and C. canephora species and consists of approximately 75% of triacylglicerols (Speer, 2006). The free fatty acid fraction is composed mainly of unsaturated acids, such as linoleic and oleic acids, which account for 43% - 54% and 7% - 14% of total fatty acids, respectively (Farah, 2012). The components present in the unsaponifiable fraction, such as tocopherols, diterpenes, sterols, and other minor components, have been reported to have antioxidant, antimicrobial and anticarcinogenic activities (Raba, 2015; Cárdenas, 2015; Hatzold, 2012), besides conferring emollient properties and protection against UV radiation (Grollier and Plessis, 1988; Wagemaker, 2015). In addition, the aromatic compounds found in coffee beans are mostly liposoluble substances capable of being extracted together with the lipid fraction of the roasted coffee beans (Sarrazin et al., 2000). Anesei et al. (2000) observed that the roasting process does not affect the oxidation level of coffee oil, attributing the oxidative stability to the presence of polyphenols and to Maillard reaction products. Moreover, studying the physicochemical properties of roasted coffee oil (RCO), Calligaris et al. (2009) detected more than 30 volatile compounds, which has aroused great interest in RCO as a flavoring for food industry.

Emulsions used as potential systems for encapsulation have showed to offer protection against chemical degradation, increasing bioavailability and possibility of controlled release of several microingredients (Qian, 2012; Aldelmann, 2012). The production of emulsified systems stabilized by colloidal solid particles instead of surfactants has been evidenced by the pioneering works of Ramsden (1903) and Pickering (1907). Since then, there has been a growing interest for their use in food, pharmaceutical, and cosmetic applications mainly due to the potential adverse effects of conventional surfactants. It would be interesting to evaluate the physicochemical and structural properties of Pickering emulsions of RCO in order to expand its possible applications in the food industry.

The main requisite of solid particles to stabilize emulsions is their partially wetting property by oil and water, since in Pickering emulsions the particles do not

need to be amphiphilic as in conventional emulsions (Dickinson, 2010; Berton-Carabin; Schroen, 2015). On the other hand, production of such particles requires specific techniques. Chemical modifications of chitosan (CS) are important to give it the desired physicochemical properties, such as hydrophilicity, and hence to provide some affinity for the oil-water interface. One way of modification is by changing the pH: due to the presence of free amine and hydroxyl groups in its structure, chitosan has a pH-responsive behavior. The amines are protonated at low pH, leading to solubility in water, whereas at high pH they become deprotonated by losing their charges and therefore become insoluble (Liu, 2012). Moreover, aggregates are formed at pH > pKa (6.5) resulting in an increase of hydrophobicity and then in higher affinity for oil. Another alternative for modifying CS refers to using an ionic crosslinking agent. Polyanions such as sodium tripolyphosphate (TPP) can interact by ionic gelation with positively charged amino groups of CS. Therefore, CS-TPP nanoparticles are formed through electrostatic interaction (Shah, 2016b).

In the present work, the effectiveness of CS nanoparticles produced by two different methods to stabilize emulsions of RCO was evaluated by investigating the changes that occur in the emulsion structure, as well as in the droplet size of emulsions during in vitro digestion. Furthermore, the encapsulation efficiency of RCO was evaluated based on the bioaccessibility of its bioactive compounds.

4.2.2. Materials and Methods

4.2.2.1. Materials

Low molecular weight chitosan powder (CAS: 9012-76-4; degree of deacetylation: 77%) was purchased from Sigma-Aldrich. Sodium tripolyphosphate (TPP) was purchased from LS Chemicals. Glacial acetic acid, sodium hydroxide and chloride acid were purchased from Panreac AppliChem. Roasted coffee oil was kindly supplied by Cia. Iguaçu de Café Solúvel (Brazil).

4.2.2.2. Preparation of chitosan nanoparticles

Chitosan nanoparticles (CS) were produced by deprotonation of the amino groups on the D-glucosamine units, according to the methodology proposed by Mwangi et al. 2016b) with some modifications. Initially a 1% (v/v) acetic acid solution was prepared with deionized water. The biopolymer was added to the stirred acetic

acid solution resulting in a 0.9 g of chitosan/100 g solution. For complete dissolution of chitosan, the solution remained under magnetic stirring for 24 h at room temperature. Nanoparticles were formed after changing the pH value from 3.5 to 6.7 with sodium hydroxide (NaOH) 6M. The 0.9% (w/w) CS dispersion was characterized through dynamic light scattering by Malvern Zetasizer Nano ZS (Malvern Instruments, Malvern, U.K.) and presented mean particle size of 474.6 nm and zeta potential of 0.0086 mV.

4.2.2.3 Preparation of Pickering emulsions

The aqueous phase of the emulsions consisted of a CS dispersion with fixed chitosan concentration of 0.9 g/100 g dispersion. The oil was added to the CS dispersion reaching the proportions of 33 g oil/100 g emulsion and 50 g oil/100 g emulsion. These formulations were selected based on a preliminary investigation on the effects of chitosan and oil fractions on the emulsion stability (unpublished data). In brief, for the emulsions designated as CS_33 (Figure 4.2.1a) and CS_50 (Figure 4.2.1c), 33 g and 50 g of RCO/100 g emulsion, respectively, were slowly added to the CS dispersion (pH 6.7) under constant stirring at 12,000 rpm using an Ultraturrax homogenizer (IKA-Ultraturrax T18, Germany) until complete homogenization. After oil addition, the emulsions continued under stirring for 5 min. The emulsions designated as CS-TPP_33 (Figure 4.2.1b) and CS-TPP_50 (Figure 4.2.1d) were prepared following the methodology proposed by Xiao et al. (2016) with some modifications. For these emulsions the oil was added to the stirring chitosan solution at the original pH (~3,5). After oil addition, the TPP solution (0.36 g/100 g water) was added to the emulsions in order to obtain a final aqueous phase with fixed CS:TPP ratio of 5:1 (w/w), remaining under stirring for 5 min more. In this step, the intermolecular crosslinking is induced between the positive charges of chitosan and the negative ones of TPP. The final concentration of chitosan was the same for crosslinked and non-crosslinked emulsions. All emulsions with their respective nomenclature and composition are presented in Table 4.2.1.
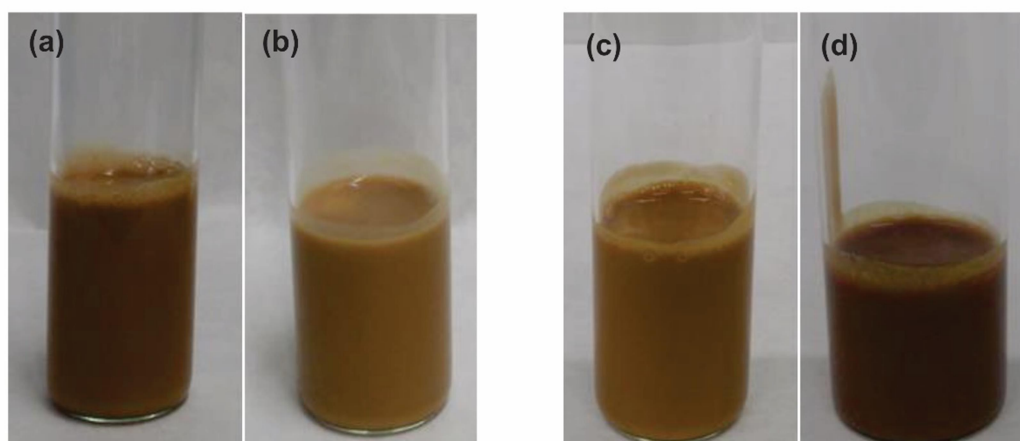
Figure 4.2.1 Visual aspect of the emulsions prepared with (a) chitosan nanoparticles and 33 g of oil /100 g of emulsion; (b) chitosan-tripolyphosphate nanoparticles and 33 g of oil / 100 of emulsion; (c) chitosan nanoparticles and 50 g of oil /100 g of emulsion; (d) chitosan-tripolyphosphate nanoparticles and 50 g of oil / 100 of emulsion.

Table 4.2.1 Nomenclature and composition of emulsions.

Emulsion	Roasted coffee oil (g/100 g emulsion)	Chitosan (g/100 g emulsion)	TPP* (g/100 g emulsion)	Water (g/100 g emulsion)
CS_33	33	0.6	-	66.4
CS-TPP_33	33	0.6	0.12	66.28
CS_50	50	0.45	-	49.55
CS-TPP_50	50	0.45	0.09	49.46

*Sodium tripolyphosphate

4.2.2.4 Rheological measurements

Measurements of the rheological behavior of fresh emulsions were performed on a rotational rheometer (Kinexus, Malvern, Worcestershire, UK) using parallel-plate geometry (diameter: 35 mm, gap: 1 mm) and monitored by the rSpace software interface. Flow behavior was evaluated from shear stress versus shear rate curves built along a linearly increasing shear rate range of 1 to 200 s-1 (300 s) followed by a reverse ramp in the same shear rate and time values. The measurements were made

for each emulsion in triplicate and the temperature was kept at 25°C for 5 min before beginning all experiments.

The Herschel-Bulkley model (Equation 1) was fitted to the flow curves and the resulting parameters were used to calculate the apparent viscosity at a fixed shear rate (Equation 2). The fixed shear rate used to mimic gastrointestinal conditions was estimated according to Equation (3) (Steffe, 1996) considering the parameters used in the in vitro digestion model.

$$\sigma = \sigma_0 + k\dot{\gamma}^n \tag{1}$$

$$\eta = \frac{\sigma_0}{\dot{\gamma}} + k\dot{\gamma}^{(n-1)} \tag{2}$$

$$\dot{\gamma} = \frac{2\pi N D_a}{(D_v - D_a)} \tag{3}$$

In the above equations σ is the shear stress (Pa), $\dot{\gamma}$ is the shear rate (s^{-1}), σ_0 is the yield stress (Pa), k is the consistency index (Pa•s^n), n is the flow index behavior (dimensionless), η is the apparent viscosity (Pa•s), N is the rotational speed (12.66 rps) of the stirrer, Dv is the vessel diameter (0.068 m), and Da is the impeller diameter (0.02 m). The rheological parameters were determined by non-linear curve fitting using OriginPro 8 software.

4.2.2.5 In vitro digestion model

The in vitro model of the gastrointestinal tract consisting of mouth, gastric and small intestinal phases was used to simulate the biological fate of the ingested samples. To simulate oral digestion, the methodology proposed by Morell et al. (2004) was used. Simulated Salive Fluid (SSF) was composed of sodium bicarbonate (NaHCO$_3$, 5.208 g/L), potassium phosphate dibasic trihydrate (K$_2$HPO$_4$•3•H$_2$O, 1.369 g/L), sodium chloride (NaCl, 0.877 g/L), potassium chloride (KCl, 0.477 g/L), calcium chloride (CaCl$_2$,0.34 g/L), α-amylase type VI-B from porcine pancreas (Sigma, A3176)(8.70 g/L), mucin from porcine stomach type II (PGM) (Sigma, M2378) (2.16 g/L) and the pH was adjusted to 7. The SSF was added to the emulsion in a final ratio of 1:1 (v/w) and mixed for 5 s. In accordance to Sanz et al. (2007), the "bolus" sample from the mouth phase was mixed in a 0.05 L-capacity vessel (diameter of 0.068 m) with 10 mL of pre-incubated (37°C for 5 min) Simulated

Gastric Fluid (SGF) composed of sodium chloride (NaCl, 3.10 g/L), calcium chloride (CaCl2, 0.11 g/L), potassium chloride (KCl, 1.1 g/L), sodium carbonate (Na$_2$CO$_3$, 0.60 g/L) with continuous stirring at 760 rpm with a 0.02 m-width turbine propeller. The solution was adjusted to pH 2 and added to 0.10 mg of pepsin (Sigma, P7125) under continuous stirring at 37°C for 1 h. For Simulated Intestinal Fluid (SIF) based on models proposed by Li et al. (2011), an electrolyte solution composed by calcium chloride (CaCl$_2$, 32.2 mg/mL) and sodium chloride (NaCl, 254.2 mg/mL) in phosphate buffer solution was prepared and the pH was adjusted to 7. Furthermore, the phosphate buffer was used to prepare the bile (58 mg/mL) and lipase solutions. Lipase (Sigma, L3126) solution was prepared depending on the amount of oil used in each emulsion, reaching enzyme-substrate ratio of 1:2.5 (w/w). Then, to simulated intestinal digestion, 5 mL of bile extract (Sigma, B8631) solution and 1 mL of electrolyte mixture were added and the pH value was increased to pH 7.0 with sodium hydroxide (NaOH) 1 M. After this step, time was assumed as t0, followed by addition of 3 mL of fresh lipase suspension and the pH-stat method was started maintaining 37°C for two additional hours.

4.2.2.6 Confocal laser scanning microscopy (CLSM)

Samples of fresh emulsions and those obtained after each one of the digestion phases were analyzed by a Nikon C1 confocal microscope unit fitted on a Nikon Eclipse E800 V-PS100E microscope (Nikon, Tokyo, Japan). Nile Red (Fluka, Sigma-Aldrich, Missouri, USA) solubilized in polyethylene glycol at 0.01 g/100 g and Fluorescein isothiocyanate (FITC) (Electronic Microscopy Sciences, Hatfield, USA) in ethanol (0.05 g/100 g) were used to stain the fat and polysaccharides, respectively. He-Ne (543 nm) and Ar (488 nm) lasers were used as the light source for the excitation of fluorescent dyes. Ten microliters of the sample were placed on a glass slide and observed at 40X-objective 15 min after diffusion of the dyes into the sample. Images with a 1024x1024 pixel resolution were acquired using digital image processing software (EZ-C1 v.3.40, Nikon, Tokyo, Japan).

4.2.2.7 Emulsion droplet sizes

The particle size distributions were analyzed by laser diffraction (Mastersizer S, Malvern Instruments Ltd., U.K.). The refractive indexes of water and oil were 1.33 and 1.47, respectively. Measurements were carried out in the fresh emulsions as well

as in the digested emulsions at t0 (the moment when there are structural modifications in the emulsion at intestinal phase with the addition of bile salts and electrolytes and the emulsion is susceptible to the enzyme action). The average size of the emulsion droplets was expressed as the volume-surface mean diameter (D3,2).

4.2.2.8 Free fatty acids release

Fat digestion was determined using pH-stat titration (Mettler-Toledo DL50, Greinfensee, Switzerland) by monitoring the pH of the digestion solution during two hours as described by Li and McClements (2010). The volume of added NaOH solution (0.5 M) was recorded and the amount of free fatty acids released by lipolysis of the initial triacylglycerols was calculated from the titration curves as the percentage of free fatty acid released. The measurements were carried out in triplicate.

In accordance to the mathematical model developed by Li and McClements (2010), it was possible to find the rate and the extent of digestion, following Equation (4):

$$\phi = \phi_{max}\left(1 - \left(1 + \frac{3kMt}{2d_0\rho_0}\right)^{-2}\right) \qquad (4)$$

in which "ϕ" is the percentage of the digestible free fatty acids released, M is the molecular weight of the triglyceride oil (~0.841 kg.mol-1), d_0 is the initial droplet mean diameter (m) and ρ_0 is the density of the oil (~935.9 kg.m-3). Both parameters, rate (k) and extent (ϕ_{max}) of digestion were determined by fitting this equation to the experimental data using OriginPro 8 software.

4.2.2.9 Bioaccessibility of total phenolic compounds

In order to evaluate the bioaccessibility of the total phenolic compounds (TPC) in the emulsions containing RCO, TPC was determined in the RCO and in the different phases from in vitro digestion. The bioaccessibility was determined using the method described by Qian et al (2012). The micelle fraction is considered to present the soluble compounds that are available to be transferred to the human blood during digestion. It was obtained by centrifuging the intestinal raw digesta at 8,000 rpm during 30 min (Centrifuge 5804 R., Hamburg, Germany). Centrifugation resulted in a three-phase system, from which the micelle phase was taken from the middle transparent layer. For TPC determination, ethanolic extracts were obtained by

stirring the micelle phase with absolute ethanol (10 mg/mL) for 10 s in a vortex and centrifuging (Centrifuge 5415 R., Hamburg, Germany) at 10,000 rpm for 10 min at 4°C. This procedure was repeated and then the top layers were mixed. Analysis of TPC followed the methodology proposed by Arnal and Del Río (2004) and the concentration was determined by a previously prepared calibration curve. The content of TPC was expressed as milligram equivalent of gallic acid per gram of oil. Bioaccessibility of the samples was calculated according to Equation 5:

$$\text{Bioaccessibility }(\%) = \frac{\text{TPC}_{\text{Micellar}}}{\text{TPC}_{\text{Oil}}} \, x \, 100 \tag{5}$$

4.2.2.10 Statistical analysis

Analysis of variance (ANOVA) was performed on the data using the STATISTICA software, version 10.0 (StatSoft Inc, Tulsa, EUA). The least significant differences between the averages were calculated by the Fisher test with a 95% confidence interval to compare the test averages.

4.2.3. Results and discussion

4.2.3.1. Rheology of fresh emulsions

The average apparent viscosities of the emulsions obtained from triplicate determinations of flow curves were plotted along ascending and descending shear rate ramps, showing the typical thixotropic behavior (Figure 4.2.2). The Herschel-Bulkley model was well fitted to all the flow curves with correlation coefficients (R^2) higher than 0.99. Table 4.2.2 presents the fitting parameters and the apparent viscosities for the different emulsions at shear rate of 33 s^{-1} (η_{33}). This value corresponds to the calculated shear rate (Equation 3) in the gastrointestinal digestion model used in this study and it is within the range 10 – 100 s^{-1} reported by Steffe (1996) for chewing and swallowing, as well as it is close to the physiological shear rate range (1 – 10 s^{-1}) considered by Lentle et al. (2007).
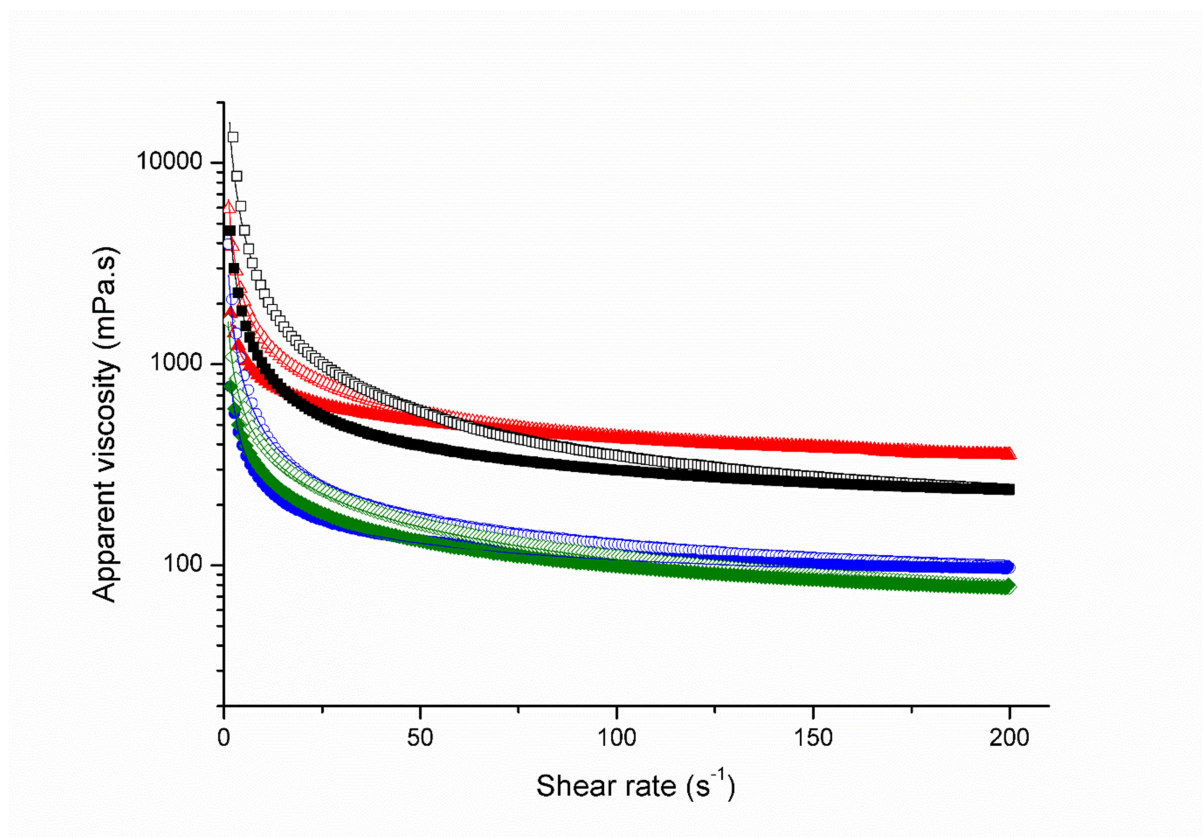
Figure 4.2.2 Apparent viscosity of the emulsions as a function of ascending (open symbols) and descending (closed symbols) shear rate ramps: CS_33 (○,●), CS-TPP_33 (◇,◆), CS_50 (□,■), CS-TPP_50 (△,▲)

Table 4.2.2 Yield stress (σ_0), consistency index (k), flow behavior index (n) and apparent viscosity at 33 s^{-1} (η_{33}) of emulsions according to the fitted Herschel-Bulkley model.

	σ_0 (Pa)	k (Pa s^n)	n	η_{33} (Pa s)	R^2
Ascending shear rate ramp					
CS_33	3.1 ± 1.4 [c,d]	0.26 ± 0.16 [c]	0.80 ± 0.08 [b,c]	0.21 ± 0.02 [d]	0.9974
CS-TPP_33	0.7 ± 0.4 [e]	1.0 ± 0.3 [b]	0.50 ± 0.02 [d]	0.20 ± 0.05 [d]	0.9996
CS_50	22.23 ± 0.18 [a]	0.15 ± 0.06 [c]	0.96 ± 0.12 [a]	0.81 ± 0.01 [a]	0.9994
CS-TPP_50	6.7 ± 1.4 [b]	1.08 ± 0.12 [b]	0.77 ± 0.01 [b,c]	0.68 ± 0.04 [ab]	0.9989
Descending shear rate ramp					
CS_33	1.1 ± 0.3 [d,e]	0.20 ± 0.04 [c]	0.84 ± 0.03 [b]	0.15 ± 0.03 [d]	0.9998
CS-TPP_33	0.9 ± 0.3 [e]	0.40 ± 0.12 [c]	0.68 ± 0.02 [d]	0.15 ± 0.04 [d]	0.9995
CS_50	5 ± 3 [b,c]	0.5 ± 0.2 [c]	0.81 ± 0.02 [b,c]	0.37 ± 0.17 [c]	0.9999
CS-TPP_50	0.62 ± 1.14 [e]	1.45 ± 0.04 [a]	0.73 ± 0.02 [c,d]	0.58 ± 0.03 [b]	0.9998

Mean values ± standard deviations. Values with different letters within the same column are significantly different ($p < 0.05$) according to the LSD multiple range test.

As it was expected, emulsions with higher amount of oil, showed higher values of yield stress and viscosity. The yield stress values for ascending shear rate curves varied from 0.66 to 22.23 Pa among the emulsions, whereas for descending shear rate curves the values ranged between 0.62 and 5 Pa. Concerning the flow index (n), all emulsions presented n < 1 that characterizes shear-thinning behavior, agreeing to the concave up flow curves shown in Figure 4.2.2. For both oil contents, the presence of TPP seemed to influence both the initial resistance required to flow and the flow behavior, since TPP provided a reduction in σ_0 values, as well as a decrease in the flow index, indicating more accentuated shear-thinning behavior. This could be related to changes in the microstructure of the emulsions. Xiao et al. (2016) also reported shear-thinning behaviour for emulsions stabilized by chitosan/TPP, which may be caused by structural reorganization and/or orientation of the dispersed oil droplets during flow. These authors also attributed the yield stress to the need of breaking flocs formed when the emulsions are at rest, which is in agreement with the lower yield stress values predicted by the Herschel-Bulkley model fitted to the descending shear rate ramp, i.e. measured after a certain shearing time. The higher yield stress observed in emulsions containing higher oil fraction could be related to the observation made by Zeeb et al. (2013), who stated that at high oil droplet concentrations and low or intermediate stabilizing protein concentrations, droplet–droplet networks are formed.

The values of apparent viscosity, η_{33}, demonstrate that the effect of TPP varied depending on the oil content in the emulsion. Emulsions with higher oil content showed the highest apparent viscosities and the greatest time-dependence (thixotropy). When analyzing results of the ascending shear rate ramp, the comparison between emulsions with higher oil content (CS_50 versus CS-TPP_50) showed that the addition of TPP caused a decrease in η_{33}. On the other hand, an opposite behavior was detected from data collected along the descending shear rate ramp, showing that the presence of TPP imparted a lower thixotropy to emulsions with 50% oil fraction, which is evidenced when comparing the descending and ascending flow curves (Figure 4.2.2) and the values of η_{33} (Table 4.2.1). Such differences were not so pronounced ($p > 0.05$) when comparing the emulsions with lower oil content (CS-TPP_33 versus CS_33). In the lower oil content condition, the amount of CS nanoparticles in the emulsions was probably enough to cover the total

oil droplet surfaces, resulting in higher resistance against the shearing process and in lower thixotropy.

4.2.3.2. Microstructure analysis of emulsions during simulated digestion

The microstructure of the emulsions with different oil fractions, with and without crosslinking, in each phase of digestion can be observed in the images obtained by confocal laser scanning microscopy presented in Figure 4.2.3. The fat is stained red and the aqueous phase is stained green. The fresh emulsions prepared with 33 g of oil/100 g presented various droplet sizes, although some free oil can be observed when chitosan was crosslinked with TPP. In CS_50 emulsion defined droplets were formed, but when the emulsions were produced with TPP part of the oil appeared dispersed and apparently not encapsulated. An incomplete emulsification is observed in both emulsions prepared with TPP, which could be related to interactions between CS and TPP that would be affecting the emulsifying ability of chitosan.

During *in vitro* digestion all the emulsions presented some structural changes. Both oral and gastric phase influenced on the droplet size revealing coalescence phenomenon; this phenomenon was less noticeable for CS_50 emulsion. The conditions in gastric phase influenced the fat droplet structures providing a restructuring effect, mainly in CS-TPP_50 emulsion, which is evidenced by the appearance of small and large round globules. The moment before lipase addition to the simulated digestion was considered "time 0" (t_0). This phase is considered important because it corresponds to the moment at which the action of the enzyme will occur and it allows obtaining information on the enzyme performance in the emulsions. At this moment, the globules had their structures already changed by interactions not only with molecules in the oral and gastric phase, but also with bile salts and electrolytes, in such a way that they are exposed to lipase access. During the intestinal phase there was a decrease of fat content probably due to the lipase action in all the emulsions. As reported by Li et al. (2011), changes in the surface area of lipid droplets may occur by digestion of molecules adsorbed to the droplet interface in the stomach or small intestine, affecting the rate and extent of lipid digestion by altering the ability of lipase to adsorb to the surfaces through competitive adsorption.
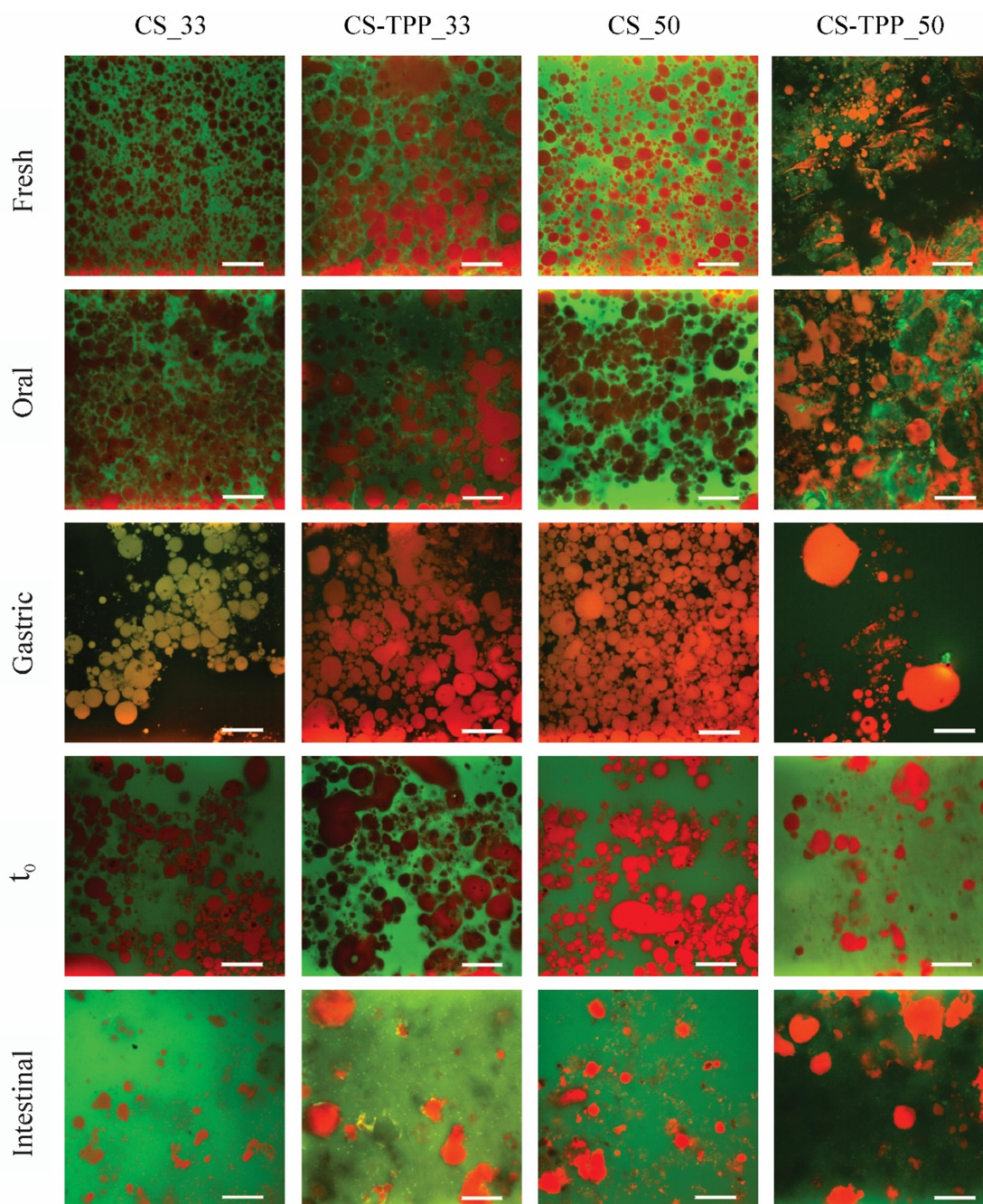
Figure 4.2.3 Confocal laser scanning micrographs of emulsions stabilized by chitosan and chitosan-TPP before (fresh) and during the digestion phases. The scale bars measure 60 μm

4.2.3.3. Particle size distribution in the emulsions

The droplet size distribution of different emulsions showed that initially they had almost monomodal distribution, except for CS-TPP_33 (Figure 4.2.4a). This trend was also observed at the moment before enzyme addition (t_0) (Figure 4.2.4b),

suggesting that these droplets were unstable and could be undergoing aggregation in that emulsion.
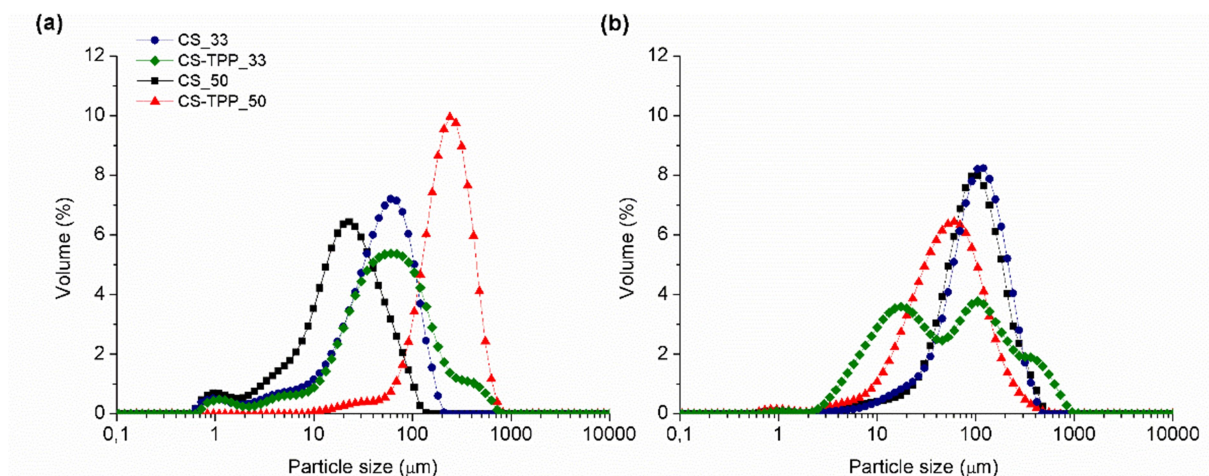
Figure 4.2.4 Particle size distribution in the emulsions before digestion (a) and at t_0 (b)

Moreover, the emulsions that were not submitted to crosslinking with TPP exhibited an increase in mean particle size at t_0 comparing to the average droplet size in fresh emulsions. Based on D3,2, the average droplet diameter of emulsions with 33 g oil/100 g emulsion and 50 g oil/100 g emulsion increased from 13.6 µm to 57.8 µm and from 8.7 µm to 45.9 µm, respectively. An increase in the mean particle diameter after exposure of the emulsions to the simulated small intestinal fluids has been previously reported. Two factors can be responsible for the physical stability reduction of the emulsions during digestion, leading to a decrease in their stability against coalescence: i) displacement of non-ionic surfactant molecules originally adsorbed to the lipid droplet surfaces by active species, such as phospholipids, bile salts, and lipase, altering the composition, structure, and properties of the interfacial layer surrounding the lipid droplets; ii) conversion of emulsified triacylglycerols to free fatty acids and monoacylglycerols by lipases, resulting in a change in the internal composition, structure, and properties of lipid droplets (Qian, 2012; Shah, 2016b) .

On the other hand, this phenomenon was not observed for CS-TPP emulsions. Emulsions with higher amount of oil presented a decrease in the average droplet size, from 148.5 µm in fresh emulsions to 24.3 µm at t_0. This may be related to the microstructure observed by confocal microscopy. In the freshly prepared emulsions with this formulation, the oil was not completely encapsulated, with the

presence of free oil as a dispersed phase, which might have resulted in size measurements of oil droplets that were uncoated by chitosan particles. Nevertheless, changes during digestion steps may have enhanced emulsification, leading to the decrease in the oil droplet sizes after digestion.

4.2.3.4 Free fatty acids released

The amount of free fatty acids released (FFAs) in the intestinal phase was evaluated in the four emulsions during in vitro digestion. Through the volume of NaOH used to maintain the pH at 7 in the digestion, it was possible to calculate the percentage of FFAs released, shown in Figure 4.2.5. The rate and extent of lipid digestion were calculated in order to evaluate the influence of CS nanoparticles used to protect the oil (Table 4.2.3).
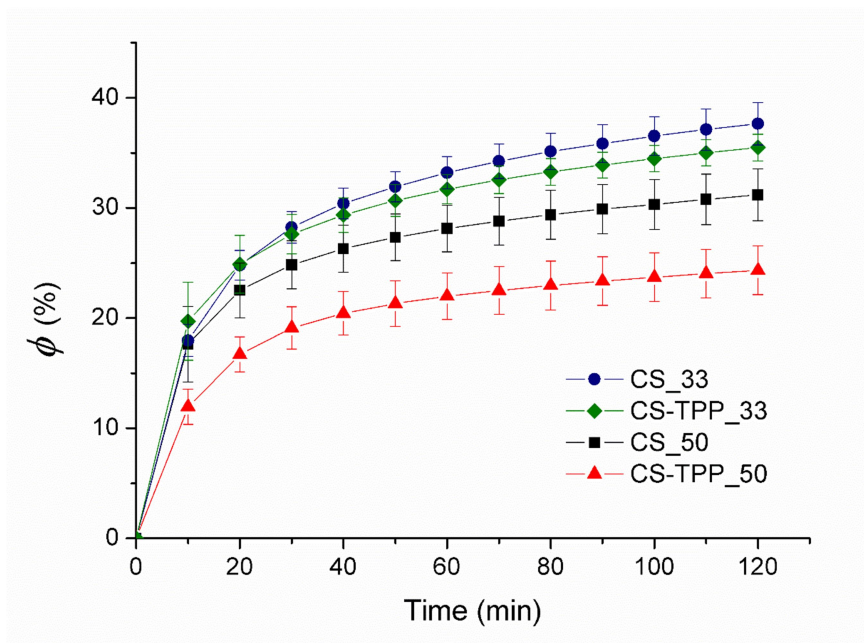
Figure 4.2.5 Fatty acids released (ϕ) versus time in emulsions during in vitro digestion. The error bars represent standard deviations.

The CS_33, CS-TPP_33 and CS_50 emulsions presented similar behavior, without significant differences ($p > 0.05$), at the first 10 minutes of the digestion, with faster FFAs release than in CS-TPP_50 emulsion. At the end of the simulated digestion there were significant differences ($p < 0.05$) in the proportion of free fatty acids released between the emulsions produced with different amount of oil as can be observed in Table 4.2.3.

Table 4.2.3 Parameters describing the digestion rate (k) and digestion extent (ϕ_{max}) of emulsions.

Emulsion	k (μmol s^{-1} m^{-2})	ϕ_{max}(%)	R^2
CS_33	47.9 ± 6.9 [a,b]	37.9 ± 1.8 [a]	0.9886
CS-TPP_33	51.5 ± 13.5 [a,b]	34.9 ± 0.3 [a]	0.9785
CS_50	71.8 ± 25.5 [a]	30.6 ± 2.4 [b]	0.9617
CS-TPP_50	29.3 ± 2.5 [b]	24.6 ± 2.1 [c]	0.9926

Mean values ± standard deviations. Values with different letters within the same column are significantly different ($p < 0.05$) according to the LSD multiple range test.

The presence of TPP influenced the digestibility of emulsion with higher oil content, leading to a 20% reduction in the FFAs release. As it can be observed in the CLSM micrographs (Figure 4.2.4), emulsion CS-TPP_50 presented free oil, representing a non-structured dispersed system and, therefore, of harder access for lipase. In addition, emulsions with lower oil content showed no significant difference, probably due to the more defined and coated oil droplets by chitosan. Several studies have reported the influence of droplet size on the rate and extent of lipid digestion. They evidenced the enhancement of lipid digestion for emulsions with reduced droplet sizes (Li & McClements, 2010; Li et al., 2011; Sarkar, Ye, & Singh, 2016; Salvia-Trujillo et al., 2017).

Winuprasith et al. (2018) related that higher digestion rate and extent of WPI-stabilized emulsions were provided by the greater surface area available for lipase action due to presence of smaller droplets in the initial phase, as well as to presence of few droplet aggregates in the gastric phase. In part, this is in agreement with the results obtained in the present work for fresh emulsions. Initially, emulsions that presented the smallest droplet sizes presented higher digestion rate and extent. On the other hand, according to McClements (2018), it is important take into account the droplet sizes present in the small intestine where the lipase will actually perform. Thus, particle sizes measured at t_0 in the current study did not showed the same trend than that found for fresh emulsions. In agreement with our results, a number of studies showed no correlation between FFAs and surface area of emulsions, suggesting that structural characteristics may be important factors contributing to the rate and extent of lipid digestion (Ahmed, 2012; Bellesi, 2016). The rheology of the different emulsions could also be related to the results obtained for free fatty acids

release, as it is known that an increase in the viscosity may influence mixing of the sample with digestive components, which could limit the ability of lipase to reach the surface of lipid droplets.

4.2.3.5 Bioaccessibility of total phenolic compounds

The influence of emulsion formulation on bioaccessibility of TPC during in vitro digestion was determined by the ratio between TPC solubilized in the micelle phase and TPC content in the oil, according to equation (5) (Table 4.2.4). Although the emulsification process did not alter the phenolic content in the oil, changes were observed in the intestinal phase at which there were significant differences ($p < 0.05$) between emulsions and the pure oil. The emulsions that presented lower amounts of TPC in the intestinal phase (CS_50 and CS-TPP_50), also followed the same tendency in the micelle fraction. Accordingly, in these emulsions the bioaccessibility was lower than in CS_33 and CS-TPP_33. As a result, there were fewer solubilized phenolic compounds in the pure coffee oil than in the emulsions, revealing great efficiency in the retention of these compounds by the emulsified oil through the digestion.

Concerning bioaccessibility, there were no significant differences between the emulsions with or without TPP for the same oil content, even though the use of TPP had an influence on droplet sizes, rheology, and FFAs release in the emulsions containing 50 g oil/g emulsion. On the other hand, the oil content significantly affected the bioaccessibility of TPC. Emulsions formulated with lower amount of oil provided higher bioaccessibility, in agreement with the results of FFAs released.

According to Ahmed et al. (2012) curcumin bioaccessibility showed to be dependent on the lipid carrier concentration in emulsion-based delivery systems. High lipid content can lead to a non-digested fraction of lipid phase, in which part of the curcumin could not be released from oil droplets into the micelle phase, contributing to decreased bioaccessibility. In the current study, the bioaccessibility of phenolic compounds reached 53.7% and 62.8% for emulsions with lower lipid content and decreased to 47.2% and 45.5% when increasing lipid content. Due to the lower amount of FFAs released, some of the phenolic compounds might remain entrapped within the non-digested oil droplets, thus preventing their solubilization into micelles and leading to low bioaccessibility (Qian, 2012; Shah, 2016b). On the other hand, higher bioaccessibility may be related to high extent of lipid digestion that

provided large amount of micelle phase capable of solubilizing phenolic compounds. In addition, viscosity may also have influenced on the bioaccessibility of bioactive compounds. In the present study, high viscosities presented by emulsions with high lipid content provide low digestibility, and consequently low bioaccessibility due to poor solubilization into micelle phase as reported above. It is suggested that higher apparent viscosity may have an effect on the movement of molecules such as lipase toward droplet surface, which hinders lipid digestion (Winuprasith, 2018).

Table 4.2.4 Total phenolic compounds (mg GAE/g oil) of emulsions at the different digestion phases and bioaccessibility.

Digestion phase	CS_33	CS-TPP_33	CS_50	CS-TPP_50	Oil
Fresh emulsion	16.9 ± 2.6 [a]	13.7 ± 1.5 [a]	13.3 ± 2.7 [a]	14.7 ± 2.8 [a]	*17.2 ± 2.1 [a]
Intestinal phase	45.4 ± 5.4 [a]	42.7 ± 6.4 [a]	28.9 ± 4.2 [b]	30.0 ± 5.1 [b]	18.2 ± 1.2 [c]
Micelle fraction	9.3 ± 0.4 [ab]	10.8 ± 1.7 [a]	8.1 ± 0.7 [b]	7.8 ± 0.9 [b]	5.8 ± 0.1 [c]
Bioaccessibility (%)	53.7 ± 2.4 [ab]	62.8 ± 9.9 [a]	47.2 ± 4.1 [b]	45.5 ± 5.6 [b]	33.6 ± 0.6 [c]

Mean values ± standard deviations. Values with different letters within the same line are significantly different ($p < 0.05$) according to the LSD multiple range test.

GAE: Gallic acid equivalents

*This value corresponds to the total phenolic compounds in the roasted coffee oil.

4.2.4. Conclusions

Pickering emulsions with different contents of roasted coffee oil stabilized by chitosan (CS) nanoparticles or chitosan-tripolyphosphate (CS-TPP) nanoparticles presented different rheological behavior, oil droplet size distributions in fresh emulsions, as well as different microstructure, lipid digestibility and bioaccessibility along in vitro digestion. The presence of TPP decreased the emulsifying ability of chitosan under the conditions investigated in the present study. CS-TPP stabilized emulsions presented partially free and non-encapsulated oil, thus decreasing its digestibility. Nevertheless, digestive conditions seemed to produce a partial structuring of the systems, which was observed at the microstructural level. In samples with higher oil content and TPP-CS nanoparticles, the restructuring effect of digestion was not enough to counterbalance the high proportion of non-encapsulated oil. In fact, lipid digestibility in these emulsions was low. The high viscosity of these samples may also have influenced the low lipid digestibility. The bioaccessibility of

phenolic compounds showed to be related to the lipid phase concentration and consequently to free fatty acids released throughout the gastrointestinal tract. In addition, CS nanoparticles themselves showed to be able of adsorbing onto oil droplet surfaces, providing efficiency in encapsulating and protecting bioactive compounds during lipid digestion. In general, the process of encapsulation of roasted coffee oil, both with chitosan or with chitosan and TPP, favored the bioaccessibility of phenolic compounds when compared to free oil.

4.2.5. Acknowledgment

4.2.6. References

Adelmann, H., Binks, B. P., Mezzenga, R. (2012). Oil powders and gels from particle-stabilized emulsions. Langmuir, 28(3), p. 1694-1697.

Anesei, M., de Pilli, T., Massini, R., Lerici, C. R. (2000). Oxidative stability of the lipid fraction in roasted fraction in roasted coffee. Italian Journal of Food Science, 12(4), p. 457-462.

Arnal, L. and Del Rìo, M. (2004). Effect of cold storage and removal astringency on quality of persimmon fruit (Diospyros kaki, L.) cv. Rojo Brillante. Food Science and Technology International, 10(3), p. 179-185.

Bellesi, F. A., Martinez, M. J., Pizones Ruiz-Henestrosa, V. M., & Pilosof, A. M. R. (2016). Comparative behavior of protein or polysaccharide stabilized emulsion under in vitro gastrointestinal conditions. Food Hydrocolloids, 52, p. 47–56.

Berton-Carabin, C. C.; Schroën, K. (2015). Pickering emulsions for food applications: background, trends, and challenges. Annual review of food science and technology, 6, p. 263-297.

Calligaris, S., Munari, M., Arrighetti, G., Barba, L. (2009). Insights into the physicochemical properties of coffee oil. European Journal of Lipid science and Technology, 111(12), p.1270-1277.

Cárdenas, C.; Quesada, A. R., Medina, M. Á. (2015). Kahweol, a coffee diterpene with anti- inflammatory properties. In: PREEDY, V.R. (Ed.). Coffee in Health and Disease Prevention, 1 Ed. UK: London, p. 627-632.

Dickinson, E. (2010). Food emulsions and foams: Stabilization by particles. Current Opinion in Colloid & Interface Science, 15(1–2), p. 40-49.

Farah, A. (2012). Coffee: Emerging health effects and disease prevention. In: Y. -F. Chu (Ed.). Coffee Constituents. New York: John Wiley & Sons, Ltd, p. 21-58.

Hatzold, T. (2012). Coffee: Emerging health effects and disease prevention. In: Y. -F. Chu (Ed.). Introduction. New York: John Wiley & Sons, Ltd, p. 1-20.

Hu, M., Li, Y., Decker, E., Xiao, H. and McClements, D. (2010). Influence of tripolyphosphate cross-linking on the physical stability and lipase digestibility of chitosan-coated lipid droplets. Journal of Agricultural and Food Chemistry, 58(2), p. 1283-1289.

Lentle, R., Janssen, P. M., Asvarujanon, P., Chambers, P., Stafford, K., and Hemar, Y. (2007). High definition mapping of circular and longitudinal motility in the terminal ileum of the brushtail possum Trichosurus vulpecula with watery and viscous perfusates. Journal of Comparative Physiology B, 177, p. 543–556.

Li, Y., Hu, M. and McClements, D. (2011). Factors affecting lipase digestibility of emulsified lipids using an in vitro digestion model: Proposal for a standardised pH-stat method. Food Chemistry, 126(2), p. 498-505.

Li, Y., & McClements, D. J. (2010). New mathematical model for interpreting ph-stat digestion profiles: Impact of lipid droplet characteristics on in vitro digestibility. Journal of Agricultural and Food Chemistry, 58(13), p. 8085–8092.

Liu, H., Wang, G., Zou, S., Wei, Z., Tong, Z. (2012). Simple, reversible emulsion system switched by pH on the basis of chitosan without any hydrophobic modification. Langmuir, 28, p. 11017−11024.

McClements, D. J. (2018). Enhanced delivery of lipophilic bioactives using emulsions: a review of major factors affecting vitamin, nutraceutical, and lipid bioaccessibility. Food & Function, 9, p. 22–41.

McClements, D. J., Li, Y. (2010). Review of in vitro digestion models for rapid screening of emulsion-based systems. Food & Function, 1, p. 32-59.

Morell, P., Fiszman, S., Varela, P. and Hernando, I. (2014). Hydrocolloids for enhancing satiety: Relating oral digestion to rheology, structure and sensory perception. Food Hydrocolloids, 41, p. 343-353.

Muzzarelli, R. A. A.; Orlandini, F.; Pacetti, D.; Boselli, E.; Frega, N. G.; Tosi, G.; Muzzarelli, C. Chitosan taurocholate capacity to bind lipids and to undergo enzymatic hydrolysis: An in vitro model. Carbohydrate Polymers, 66(3), 363–371.

Mwangi, W. M., Ho, K. W., Ooi, C. W., Tey, B. T.,Chan, E. (2016a). Facile method for forming ionically cross-linked chitosan microcapsules from Pickering emulsion templates. Food Hydrocolloids, 55, p. 26-33

Mwangi, W. M., Ho, K. W., Tey, B. T., Chan, E. S. (2016b). Effects of environmental factors on the physical stability of pickering emulsions stabilized by chitosan particles. Food Hydrocolloids, 60, p. 543-550.

Oliveira, A. F., Cruz, P. M., Eberlin, M. N., Cabral, F. A. (2005). Brazilan roasted coffee oil obtained by mechanical expelling: compositional analysis by CG-MS. Ciência e Tecnologia de Alimentos, 25(4), p. 677-682.

Pickering, S. U. (1907). Emulsions. Journal of the Chemical Society, 91, p. 2001–2021.

Qian, C., Decker, E., Xiao, H. and McClements, D. (2012). Nanoemulsion delivery systems: Influence of carrier oil on β-carotene bioaccessibility. Food Chemistry, 135(3), p. 1440-1447.

Raba, D. N., Poiana, M. A., Borozan, A. B., Stef, M., Radu, F. and Popa, M. V. (2015). Investigation on crude and high-temperature heated coffee oil by ATR-FTIR spectroscopy along with antioxidant and antimicrobial properties. PLOS ONE, 10(9), p.1-20.

Ramadan, M. F., Kroh, L. W., Morsel, J. T. (2003). Radical Scavenging Activity of Black Cumin (Nigella sativa L.), Coriander (Coriandrum sativum L.), and Niger (Guizotia abyssinica Cass.) Crude Seed Oils and Oil Fractions. Journal of Agricultural and Food Chemistry, 51, p. 6961-6969.

Ramsden, W. (1903). Separation of solids in the surface-layers of solutions and 'suspensions' (observations on surface-membranes, bubbles, emulsions, and mechanical coagulation). –Preliminary account. Proceedings of the Royal Society of London, 72, p. 156–64.

Rodríguez, M. S., Albertengo, L. E. (2005). Interaction between chitosan and oil under stomach and duodenal digestive chemical conditions. Bioscience, Biothecnology, and Biochemistry, 69(11), p. 2057-2062.

Salvia-Trujillo, L., Verkempinck, S. H. E., Sun, L., Van Loey, A. M., Grauwet, T., & Hendrickx, M. E. (2017). Lipid digestion, micelle formation and carotenoidbioaccessibility kinetics: Influence of emulsion droplet size. Food Chemistry, 229, 653–662.

Sanz, T., Handschin, S., Nuessli, J. and Conde-Petit, B. (2007). Effect of thickening agent and fat in custard microstructure upon in vitro enzymatic digestion. Food Science and Technology International, 13(5), p. 381-388.

Sarkar, A., Ye, A., & Singh, H. (2016). On the role of bile salts in the digestion of emulsified lipids. Food Hydrocolloids, 60, p. 77–84.

Sarrazin, C., Le Quéré, J.L., Gretsch, C., Liardon, R. (2000). Representativeness of coffee aroma extracts: a comparison of different extraction methods. Food Chemistry, 70, p. 99-106.

Shah, B., Li, Y., Jin, W., An, Y., He, L., Li, Z., Xu, W. and Li, B. (2016a). Preparation and optimization of Pickering emulsion stabilized by chitosan-tripolyphosphate nanoparticles for curcumin encapsulation. Food Hydrocolloids, 52, p. 369-377.

Shah, B., Zhang, C., Li, Y. and Li, B. (2016b). Bioaccessibility and antioxidant activity of curcumin after encapsulated by nano and Pickering emulsion based on chitosan-tripolyphosphate nanoparticles. Food Research International, 89, p. 399-407.

Speer, K., Kölling-Speer, I. (2006). The lipid fraction of the coffee bean. Brazilian Journal of Plant Physiology, 18, p. 201-216.

Steffe, J. F. (1996). Rheological methods in food process engineering (2ed). Freeman Press, East Lansing.

Wagemaker, T. A. L., Carvalho, C. R. L., Maia, N. B., Baggio, S., R., Filho, O. G. (2011). Sun protection factor, content and composition of lipid fraction of green coffee beans. Industrial Crops and Products, 33(2), p. 469-473.

Xiao, Z., Wang, E., Zhu, G., Zhou, R., Niu, Y. (2016). Preparation, characterization and rheological behavior of chitosan nanocapsule emulsion encapsulated tuberose fragrance. Polish Journal of chemical Technology, 18(2), p. 1-8.

Zeeb et al. (2013). Transglutaminase-induced crosslinking of sodium caseinate stabilized oil droplets in oil-in-water emulsions. Food Research International, 54 p. 1712–1721.

4.3. CHAPTER 3

Chitosan nanoparticles and their role in stabilizing emulsion

Chitosan and crosslinked chitosan nanoparticles: Synthesis, characterization and their role as Pickering emulsions

Elisa Franco Ribeiro [a,b], Taís Téo de Barros Alexandrino [c,d], Odilio Benedito Garrido Assis [d], Américo Cruz Junior [e], Amparo Quiles [b], Isabel Hernando [b], Vânia Regina Nicoletti [a]

[a] **São Paulo State University (Unesp), Institute of Bioscience, Humanities and Exact Sciences (Ibilce)**, Campus São José do Rio Preto, SP, 15054-000, Brazil

[b] **Food Microstructure and Chemistry Research Group, Universitat Politècnica de València (UPV)**, 46022, Valencia, Spain

[c] **Federal University of São Carlos**, Campus São Carlos (UFSCar), 13565-905, São Carlos, SP Brazil

[d] **National Nanotechnology Laboratory for Agriculture, LNNA, Embrapa Instrumentação**, 13561-206, São Carlos, SP, Brazil

[e] **Federal University of Santa Catarina (UFSC)**, 88040-900, Florianópolis, SC, Brazil.

Abstract: Chitosan has been modified in order to produce nanoparticles with promising characteristics in diverse food applications, e.g. Pickering emulsions. Chitosan deprotonation and ionic crosslinking with tripolyphosphate were assessed in this work. Chitosan nanoparticles produced by these two methods were characterized according to surface charge, particle size distribution, chemical structure, wettability and microstructure imaging. The nanoparticles' performance in the formation of oil-in-water Pickering emulsions was studied by physicochemical and rheological assays. Chitosan nanoparticles produced by amino deprotonation were larger and resulted in emulsions with larger oil droplets, with rheological behavior of the emulsions being greatly affected by increasing concentration of chitosan, which formed a network structure in the continuous phase. On the contrary, the tripolyphosphate-crosslinked chitosan nanoparticles were smaller and produced emulsions with smaller droplets, which remained less viscous even when chitosan concentration was increased and showed evidences of Pickering stabilization when analyzed by microscopy techniques.

4.3.1. Introduction

Micro and nanoparticles play an important role in the most emerging applications, particularly in innovative methods for improving or developing new food systems. These structures present specific characteristics that can be used to enhancing not only the shelf life but also the flavor, nutritional and textural aspects of food products (Ye et al., 2017).

Organic materials have been intensively explored due to their nontoxicity and biodegradability, besides their versatility in comparison to the inorganic ones (Hatton, Miiller & Silva, 2008). Chitosan, for example, is a polysaccharide consisting of alternating units of (1→4) N-acetyl glucosamine and glucosamine obtained from the partial deacetylation of chitin. After some adequate modifications in its structure, it has been reported to be an efficient raw material for producing nanoparticles with technological benefits (Divya & Jisha, 2018; Hasheminejad, Khodaiyan & Safari, 2019; Liang et al., 2017).

Micro and nanoparticles of chitosan can be produced by different ways, although deprotonation and ionic crosslinking are advantageous techniques considering the low complexity and the needless of high shear forces application or addition of harsh organic solvents (Sailaja, Amareshwar & Chakravarty, 2011). In deprotonation method, particles are formed by self-assembly when the charges of cationic CS are neutralized by anionic agents, e.g. sodium hydroxide, under agitation. On the other hand, ionic crosslinking promotes the electrostatic interaction between the amine groups of chitosan with the negative charge group of polyanions, as tripolyphosphate (TPP), also under agitation. Each of these methods generates nanoparticles with distinct characteristics such as surface charges, particle size, structure and ability to bond to specific compounds (Ali, Rajendran & Joshi, 2011; Rampino, Borgogna, Blasi, Bellich & Cesàro, 2013). The distinct properties of the resulting particles, from both methods, may define the ideal use for specific applications.

Recent trends have reported the use of food-grade nanoparticles in the stabilization of Pickering emulsions (Xiao et al., 2016). In these oil-in-water emulsions, the oil droplets are stabilized by the presence of surrounding solid particles that reduces the interfacial tension. According to Xiao et al. (2016), for an effective stabilization of Pickering emulsions, the solid particles should be partially

wetted by both continuous and dispersed phase, preserve the proper wettability and have to be smaller in size than the oil droplets. Many studies have reported the use of deprotonated chitosan or crosslinked chitosan for stabilizing food systems containing lipids or lipophilic compounds, including curcumin (Shah et al., 2016a; Shah, Zhang, Li & Li, et al., 2016b), tocotrienol (Mwangi, Ho, Ooi, Tey & Chan, 2016), corn oil (Wang & Heuzey, 2016), palm oil (Ho et al., 2016), and others. Nevertheless, there is little data about the performance of chitosan nanoparticles in the structure of Pickering emulsions composed by added-value oils.

Roasted coffee oil is a byproduct extracted from roasted coffee beans. It is a valuable source of oleic and linoleic acid (~45%) (Hurtado-Benavides, Dorado, Sánchez-Camargo, 2016), volatile compounds that confers interesting flavor (Oliveira et al., 2005) and bioactive compounds. A previous investigation has showed the efficacy of using chitosan nanoparticles in controlling the release and improving bioaccessibility of bioactive compounds in Pickering emulsions containing roasted coffee oil (Ribeiro et al., 2020).

The present study aimed at synthetizing and characterizing chitosan nanoparticles produced by deprotonation and ionic crosslinking. Their performance on structuring oil-in-water Pickering emulsions is discussed on the basis of physicochemical parameters, microstructure and rheological behavior of the emulsions.

Hypotheses

Chitosan nanoparticles produced by different methods stabilize oil droplets in oil-in-water emulsions by different mechanisms.

4.3.2 Materials and Methods

4.3.2.1 Materials

Low molecular weight chitosan powder (N°CAS: 9012-76-4; degree of deacetylation: 77%) was purchased from Sigma-Aldrich. Sodium tripolyphosphate (TPP) was purchased from LS Chemicals. Glacial acetic acid, sodium hydroxide and chloride acid were purchased from Dinâmica (Indaiatuba, Brazil). Roasted coffee oil was kindly supplied by Cia. Iguaçu de Café Solúvel (Cornélio Procópio, Brazil).

Analytical grade chemicals and ultrapure water with 18.2 MΩ cm resistivity were used in all the experiments.

4.3.2.2 Synthesis of chitosan and chitosan-TPP nanoparticles

Chitosan nanoparticles were obtained by two methods: (i) deprotonation of the amino groups on the D-glucosamine units, and (ii) by adding sodium tripolyphosphate (TPP) as a crosslinking agent to induce intermolecular bonding between the positive charges of chitosan amino groups and the negative phosphates in TPP structure. Initially, the chitosan powder was added to aqueous acetic acid solution at 1%, under magnetic stirring for 24 h at room temperature for complete dissolution. For amino deprotonation, chitosan solutions at concentrations of 0.9 g/100 g and 1.5 g/100 g were prepared and the particles were generated after increasing the pH value from 3.5 to 6.7 with NaOH 6M. The nanoparticles resulting from this procedure were designated as 0.9CN and 1.5CN. For the ionic crosslinking method the TPP aqueous solution at pH 8 was drop-wise added to stirring chitosan solution at its initial pH (3.5), attaining final chitosan concentrations of 0.9 g/100 g and 1.5 g/100 g of solution, and pH values of 4.34 and 5.16, respectively, resulting in CS:TPP mass ratio of 3:1. The resulting nanoparticles were designated as 0.9CN-TPP and 1.5CN-TPP respectively.

4.3.2.3 Characterization of chitosan nanoparticles
4.3.2.3.1 Zeta (ζ) potential and particle size measurements

The zeta potential and size distribution of the chitosan nanoparticles were determined using a particle Zetasizer analyzer (Nano-ZS, Malvern Instruments, UK) and the samples were previously diluted in the ratio 1:100 for a reliable data (Tosi et al., 2020). The surface charge of the particles was measured at 25 ºC by laser Doppler microelectrophoresis technique, whereas the size distribution was obtained by dynamic light scattering (DLS) at the same temperature. The refractive index of dispersant medium required by the equipment to provide adequate measurements was obtained by an electronic refractometer resulting in the value of 1.330. Polydispersity index (PDI) was automatically displayed from cumulants' analysis by the internal Zetasizer software for all of the range of particles analyzed. Each experiment was performed in triplicate.

4.3.2.3.2 Fourier transform infrared (FT-IR) spectroscopy

In order to evaluate the changes in chemical structure of chitosan nanoparticles, pure chitosan powder, TPP, and the different chitosan nanoparticles were analyzed in a FT-IR spectrometer (Vertex 70, Bruker, Germany) equipped with smart iTR diamond Attenuated Total Reflectance (ATR) sampling accessory (Nicolet iS10, Thermo Scientific, USA). The chitosan nanoparticles were freeze dried (L101, Liobrás, Brazil) before FT-IR analysis. The spectra were obtained by performing 32 scans at a wavenumber resolution of 4 cm^{-1} at room temperature.

4.3.2.3.3 Contact angle measurement

The contact angle measurements of chitosan nanoparticles were performed by the sessile drop method according to Ho et al. (2016), using an optical contact angle measuring device (CAM101, KSV Instruments, Finland) equipped with image analysis software (CAM 2008). Briefly, chitosan nanoparticle suspensions were cast onto the surface of glass slides and left to dry into a desiccator at room temperature. This procedure was successively carried out until resulting in a uniform surface entirely covered by nanoparticles. A 0.2 mL drop of water was deposited on the surface of the resulting film. The static contact angle of the sessile drop of water was then determined automatically by fitting Young-Laplace equation around the imaged droplets. Three chitosan films were prepared for each sample and the measurements were performed with five droplets at different locations on each of the three films.

4.3.2.4 Preparation of Pickering emulsions

The emulsions prepared with crosslinked and non-crosslinked chitosan nanoparticles, containing 10% (w/w) of roasted coffee oil, were produced by adding the oil to the nanoparticle suspension under homogenization (Ultra-Turrax T25, IKA, Germany) at 12,000 rpm. After oil addition, the samples continued under mixing for 5 min more. All the emulsions were prepared in triplicate and stored at room temperature for 24 hours to be analyzed.

4.3.2.5 Characterization of Pickering emulsions

4.3.2.5.1 Emulsion droplet size analysis

The droplet size and shape of emulsions was analyzed by optical microscope (Olympus, CX31) with a 40x magnification objective coupled with a digital camera

(Olympus, SC30). In order to give significant results, the average droplet size was calculated from 300 droplets using the image processing software ImageJ 1.52. The median size (D_{50}) of the cumulative frequency distribution as well as the values of Sauter diameter ($D_{3,2}$) were assumed as the most representative particle size, as some samples showed non-symmetric distributions (Walstra, 2003; Lu et al., 2019). In addition, the width of particle size distribution (span) was calculated according to Equation (1):

$$Span = \frac{D_{90} - D_{10}}{D_{50}} \qquad (1)$$

in which D_{10} is defined as the diameter at which 10% of the particles lies below this value. Similarly, D_{50} and D_{90} correspond to the diameters at which 50% and 90% of the cumulative volumes of the distribution have smaller particle sizes than that value, respectively.

4.3.2.5.2 Confocal Laser Scanning Microscopy (CLSM)

Samples of emulsions were analyzed under a Leica TCS SP5 confocal microscope (Leica Microsystems, Mannheim, Germany) according to methodology described by Ribeiro et al. (2020). In this method, Nile Red dye (Fluka, Sigma-Aldrich, Missouri, USA) was solubilized in liquid polyethylene glycol (PEG 400) at 0.01 g/100 g and Fluorescein isothiocyanate (FITC) (Electronic Microscopy Sciences, Hatfield, USA) in ethanol at 0.05 g/100 g. The dyes were used to stain the lipid and biopolymer fraction, respectively, by diffusing 10 µL of each dye into the samples placed on the glass slide, which were then left at rest for 15 min before image acquisition. He-Ne (543 nm) and Ar (488 nm) lasers were used as the light source for exciting the fluorescent dyes. Images were then acquired using 40X-objective lens digital with 1024×1024-pixel resolution.

4.3.2.5.3 Transmission electron microscopy

Transmission electron microscopy (TEM) was performed according to Schröder, Sprakel, Schröen, Spaen & Berton-Carabin (2018) procedure for emulsions prepared with chitosan nanoparticles. Diluted samples with water were deposited onto copper grids covered with carbon film (200 mesh) and a standard

filter paper was used to absorb the excess solvent. Images were acquired on a JEOL JEM1011 transmission electron microscope (Peabody, USA) operating at 80 kV.

4.3.2.5.4 Rheological properties

The rheological behavior of the emulsions was studied under steady and oscillatory shear. Measurements were carried out in an AR-2000EX rheometer (TA Instruments, Delaware, USA) using serrated parallel-plate geometry with gap of 300 μm. Steady shear flow ramps were performed in a range of shear rate from 0.001 to 100 s^{-1} and the resulting apparent viscosity was acquired for each point. The Cross (Equation 2) and Carreau (Equation 3) models were fitted to the experimental data (Rao, 2014):

$$\eta_{app} = \eta_\infty + \frac{\eta_0 - \eta_\infty}{\left[1 + \left(\dfrac{\dot{\gamma}}{\dot{\gamma}_c} \right)^m \right]} \tag{2}$$

$$\eta_{app} = \eta_\infty + \frac{\eta_0 - \eta_\infty}{\left[1 + \left(\dfrac{\dot{\gamma}}{\dot{\gamma}_c} \right)^2 \right]^N} \tag{3}$$

In which is the apparent viscosity (Pa•s), $\dot{\gamma}$ is the shear rate (s^{-1}), is the apparent viscosity at infinite shear rate (Pa•s), η_0 is the apparent viscosity at zero shear rate (Pa•s), m and N are dimensionless exponents and $\dot{\gamma}_c$ is the critical shear rate (s^{-1}) which marks the end of the Newtonian plateau and/or the beginning of the shear-thinning region.

For the oscillatory shear assays, samples were evaluated in order to obtain the storage (G') and loss (G'') modulus from the mechanical spectra. Measurements were taken in the frequency range of 0.01 to 10 Hz, and all the assays were performed in the linear viscoelastic region experimentally determined in triplicate by performing strain sweeps at different frequencies (0.01% strain). A power law model was used to fit the experimental data as given by Equations (4) and (5):

$$G = k' \omega^{n'} \tag{4}$$

$$G' = k'' \omega^{n''} \tag{5}$$

In which k', k'', n' and n'' are fitting parameters that provide information about the viscoelastic nature of the emulsions (Albano, Franco & Telis, 2014). The accuracy of the fitting procedures was evaluated based on the adjusted determination coefficient (R^2_{adj}) and root-mean-square error (RMSE).

4.3.2.6 Statistical Analysis

Analysis of variance (ANOVA) was performed on the data using the STATISTICA software (StatSoft Inc., Tulsa, EUA). The least significant differences between the averages were calculated by the Fisher test with a 95% confidence interval.

4.3.3 Results and discussion

4.3.3.1 Characterization of the chitosan nanoparticles
4.3.3.1.1 Zeta potential and polydispersity index
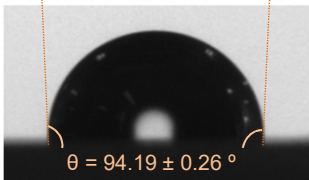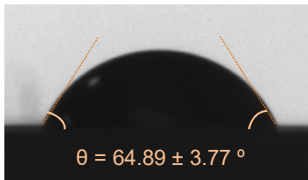
Zeta potential and polydispersity index (PDI) were analyzed for the chitosan nanoparticles produced by the two different methods described in item 2.2, using the two previously established chitosan concentrations in solution (0.9 g/100 g and 1.5 g/100 g). Means and standard deviations are presented in Table 4.3.1. Stability of particle suspensions is dependent on the surface charge of the suspended particles, being favored when electrostatic repulsion occurs at higher modulus of zeta potential (Qi, Xu, Jiang, Hu & Zou, 2004). In all of the cases studied in this work, the nanoparticles presented positively charged surface. The resulting values indicated that the particles produced in this study were similar to those reported in literature (Ali et al., 2011; Pereira, Silva, Oliveira, Oliveira & Fraceto, 2017). Nanoparticles synthetized with TPP resulted in zeta potential slightly higher than measured for nanoparticles obtained by deprotonation, showing that TPP nanoparticles tend to be more stable in suspension.

The differences in the zeta potential could be attributed to the mode of chitosan rearranging in the presence of TPP or sodium hydroxide, neutralizing more or less amino groups. Kašpar, Jakubec & Štěpánek (2013) found that transition between stability and agglomeration occurred around +17 mV for CN-TPP, giving insights about the stability of suspension in the present work. As indicated by zeta potential values, more stable dispersions were obtained by using TPP as crosslinking

agent, which resulted in an increase in the surface charge of the particles, assuring a greater repulsion between them.

Table 4.3.1 Zeta potential, predominant medium size, polydispersity index and contact angle of CN and CN-TPP particles.

Sample	Zeta potential (mV)	Predominant médium size (nm)	Polydispersity index (PDI)	Contact angle
0.9CN	16.1 ± 0.7 [b]	538.5 ± 234.8 [b]	0.944 ± 0.048 [a]	θ = 94.19 ± 0.26 °
1.5CN	18.3 ± 0.4 [b]	938.5 ± 332.6 [a]	0.912 ± 0.050 [a]	
0.9CN-TPP	24.1 ± 1.8 [a]	331.3 ± 269.6 [b]	0.551 ± 0.033 [b]	θ = 64.89 ± 3.77 °
1.5CN-TPP	22 ± 1.8 [a]	413.2 ± 124.7 [b]	0.478 ± 0.091 [b]	

Mean values ± standard deviations. Values with different letters within the same column are significantly different ($p < 0.05$) according to the LSD multiple range test at 95% of confidence.

The calculated polydispersity indexes (Table 4.3.1), also confirm the positive effect of crosslinking in providing better stability to the particle suspensions. For the samples with higher zeta potential, the PDI resulted in lower values, indicating a comparatively narrower particle size distribution in these systems. It is worth to stress that numerically, the higher the polydispersity index the higher will be the non-uniformity and the range of particle size distribution (ordinarily PDI values greater than 0.7 are interpreted as resultant from a wide distribution of sizes and the presence of great agglomerates) (Danaei et al., 2018).

4.3.3.1.2 Particle size distribution

Particle size analysis revealed non-symmetric large distributions for all samples with distinct sizes (Figure 4.3.1). In each group the distribution features are similar to a bimodal disperse profile pointing out to the formation of great agglomerates, mainly for syntheses with lower concentration of chitosan. Concerning nanoparticles obtained by deprotonation, when reacting 0.9 g of chitosan/100 g, the predominant particle size was found to be around 538 nm compared to 331 nm when processed via TPP ionic crosslinking. The second peak is attributed to aggregate

formation with average dimensions in the range of 4800 to 5500 nm found for both samples, mainly for 0.9CN particles, which are in reasonable agreement to zeta potential and polydispersity index predictions (Table 4.3.1). It is expected that when the amino groups of chitosan are deprotonate, hydrophobic interactions take place and the polymer will collapse in a curl state, configuring nanoparticles with irregular dimensions. Nevertheless, in the particles that resulted from molecular linkages between the chitosan protonated amino groups and the TPP phosphates, the short-range attractions between opposite charges lead to a strong tendency for the chitosan (a linear polymer) to wrap around the TPP molecules. In such condition the system is prone to shrinkage, generating particles of smaller sizes. The closer the balance between charges, the greater will be the expected shrinkage. This phenomenon is predicted by the colloid-polymer mixtures model (Wilk et al., 2010).
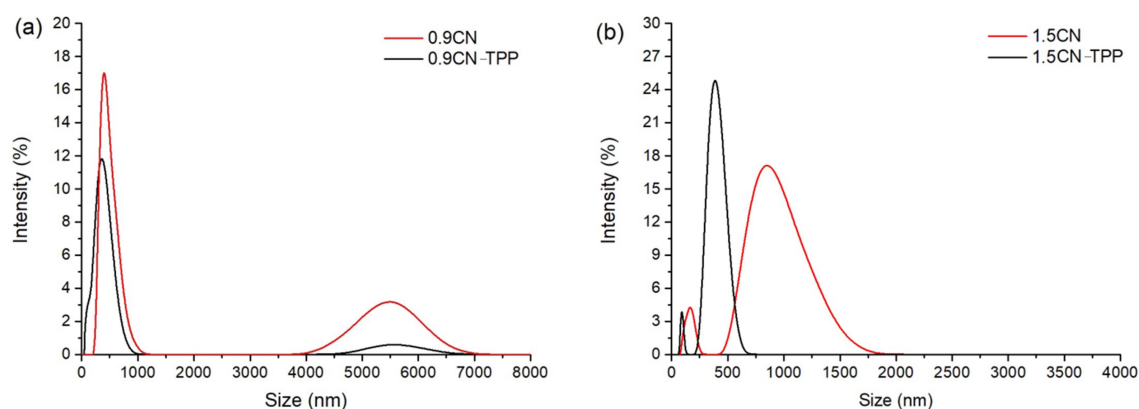
Figure 4.3.1 Chitosan particle size distributions prepared with chitosan concentrations of (a) 0.9 g/100 g and (b) 1.5 g/100 g, by deprotonation (CN) and ionic crosslinking (CN-TPP).

The effect of increasing chitosan concentration, from 0.9 to 1.5 g, directly reflected in the particle dimensions as observed in Figure 4.3.1b. Except for the second peak observed for 0.9CN treatments in the range of 4800 to 5500 nm, higher concentration of chitosan in the synthesis resulted in larger nanoparticles, as already reported in several studies (Vaezifar et al., 2013; Rázga, Vnuková, Némethová, Mazancová & Lacík 2016; Sreekumar, Goycoolea, Moerschbacher & Rivera-Rodriguez, 2018). The predominant sizes for 1.5CN particles lay in 938 nm for deprotonation process and in 413 nm for ionic gelation. Small fractions of particles, smaller than 260 nm in size, were recorded in both suspensions. From the analytical

data, it is evident that ionic crosslinking, when compared to deprotonation process, yields more stable particles, as inferred by higher zeta potential values, lower polydispersity indexes and narrower particle size distributions.

4.3.3.1.3 Fourier transform infrared (FT-IR) spectroscopy

FT-IR spectroscopy was used to investigate the appearance and/or breakdown of bonds in the nanoparticle molecular structure as a consequence of the production method. Figure 4.3.2 shows the spectra of infra-red absorbance in the whole range of scanned wavelength. The TPP spectrum is characterized by three main regions with peaks centered around 1143 cm^{-1} attributed to stretching vibrations of P=O groups; at 896 and 469 cm^{-1} related, respectively, to P-O and P-O-P vibrations (Antoniou et al., 2015). The pure chitosan presents typical polysaccharide spectrum with the following main peaks: a broad band at 3348-3284 cm^{-1} corresponding to stretching vibrations of the –NH and –OH groups; absorption peaks at 1419 cm^{-1} associated to –CH$_2$ stretching; methyl C–H symmetrical bending at 1373 cm^{-1}; primary and secondary OH in-plane bending vibration at 1317 and 1261 cm^{-1}, respectively; vibrations bands at 1643 cm^{-1} and 1566 cm^{-1} indicated the presence of secondary amide (C=O) and secondary amino group (NH bending), respectively; 1064 cm^{-1} and 1027 cm-1 for primary amine CN stretching and 891 cm^{-1} for pyranose ring (Mohan, 2004; Mwangi et al. 2016).
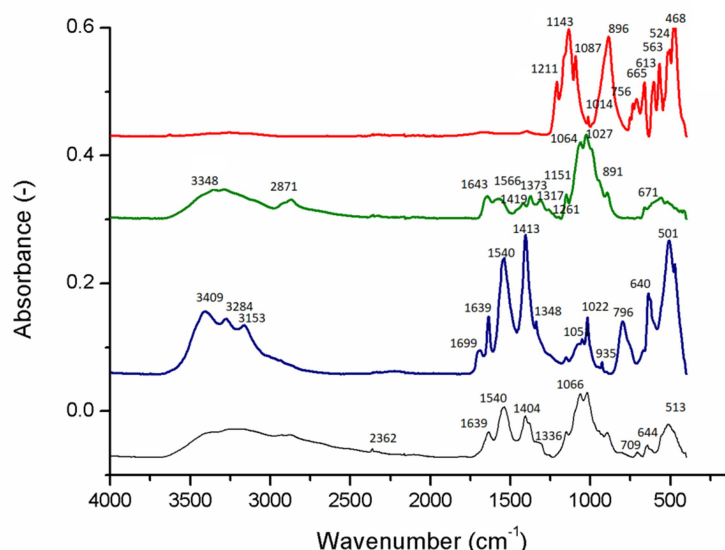
Figure 4.3.2 FT-IR spectra of sodium tripolyphosphate powder (TPP) (⎯), pure chitosan powder (⎯), chitosan nanoparticle at pH 6.7 (CN) (⎯) and chitosan-sodium tripolyphosphate nanoparticle (CN-TPP) (⎯) at CS:TPP mass ratio of 3:1.

For chitosan nanoparticles, both method of production influenced the final chemical structure. The dissolution of chitosan in acid solution creates positively charged amino groups (NH^{3+}) susceptible to ionic interactions with negatively charged molecules. In this way, when increasing the pH of chitosan solution new absorption bands appeared at 3409 - 3153 cm^{-1} corresponding to –NH stretching. In addition, the appearance of peaks at 1699 cm^{-1}, 1348 cm-1 and 1051 cm^{-1} suggests the binding of hydroxyl ions to NH^{3+}, leading to chitosan self-aggregation. On the other hand, the interaction between phosphate ions of TPP and chitosan in solution is evidenced by the displacement of the peaks of chitosan amide I from 1643 cm^{-1} to 1639 cm^{-1} and amide II from 1027 cm^{-1} to 1022 cm^{-1} in the crosslinked particles, due to the interaction between the TPP anionic phosphoric groups and chitosan cationic amine groups (Luo, Zhang, Cheng & Wang, 2010).

4.3.3.1.4 Contact angle

The differences in the affinity of the nanoparticles to water were evaluated through the water contact angle formed over dried films constituted by the nanoparticles. Table 4.3.1 present images of water droplets as recorded on the surfaces of the particles deposited on glass slides, along with correspondent values and standard deviations.

The water affinity of various particles has been studied with the aim of evaluating their behavior at the oil-water interface in emulsions (Ho et al., 2016; Linke & Drusch, 2018; Haider, Majeed, Williams, Safdar & Zhang, 2017). Generally, contact angle below 65° indicates a hydrophilic surface while values above 65° define a hydrophobic behavior (Vogler, 1998). In this way, the wetting tendency is larger as the contact angle becomes smaller.

In the present study, the nanoparticles produced by deprotonation exhibited a more hydrophobic behavior, considering that the measured contact angles were greater than those obtained for CN-TPP. The hydrophobicity response of chitosan nanoparticles is related to nonpolar acetyl units associated to the reduction of charges along the polymer backbone. In acid aqueous solutions the chitosan molecular structure presents cationic amines ($-NH^{3+}$) as outlined in Figure 4.3.3 The deprotonation of these amino groups occurs when the solvent changes towards an alkaline pH, leading to the formation of $-NH_2$ in pH above the chitosan pKa (~ 6.5) (Ho et al. 2016). The deprotonation of $-NH^{3+}$ groups favors the self-aggregation of

chitosan molecules by intermolecular attraction between the acetyl units (N-acetyl-D-Glucosamine), conferring to the formed particles a hydrophobic feature.
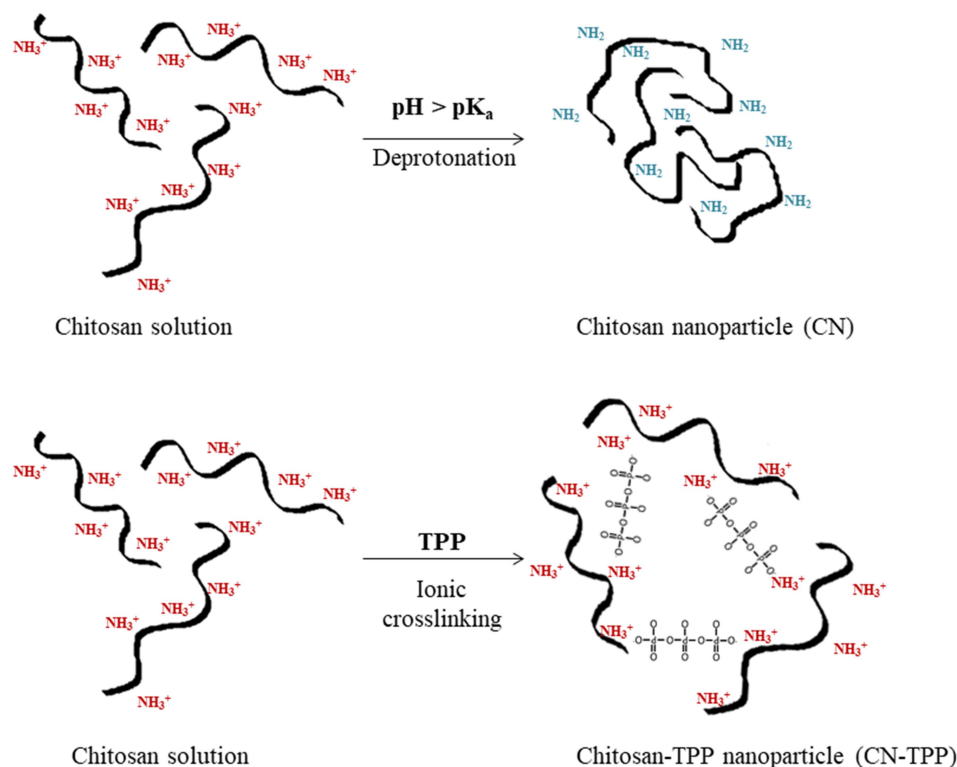
Figure 4.3.3 Deprotonation of amino groups of chitosan and ionic crosslinking between chitosan and TPP.

It is also noteworthy to emphasize that the higher mobility of the hydroxyl ions that binds to the amine group weakens the intermolecular electrostatic repulsions and reduces considerably the stiffness of the chitosan chains (Kaloti & Bohidar, 2010), thus making the chitosan chain more flexible.

The use of TPP for ionic crosslinking resulted in particles with lower contact angle, probably due to the presence of residual non-bonded NH^{3+} groups in the chitosan chain. As already commented, by adding TPP to the acid solution of chitosan, the positive amino groups of chitosan structure bonded the negative phosphate groups of sodium tripolyphosphate. Nevertheless, not all the amino groups were neutralized by TPP as a consequence of the polymer configuration and steric hindrances. In fact, the remaining NH^{3+} groups resulted in more soluble complexes, as schematized in Figure 4.3.3 This is in close agreement with zeta

potential results, confirming that crosslinked chitosan nanoparticles are more positively charged than deprotonated samples.

4.3.3.2 Characterization of Pickering emulsions
4.3.3.2.1 Analysis of emulsion microstructure

Microscopic images of emulsions are presented in Figure 4.3.4. The optical microscopy images show more spherical droplets of emulsions obtained when CN-TPP was used, for both chitosan concentrations. Likewise, the crosslinked nanoparticles provided smaller oil droplets and smaller span than CN nanoparticles (Table 4.3.2), what is probably related to the smallest particle sizes produced by TPP crosslinking. Moreover, as mentioned in section 3.3.1 and showed in Table 4.3.2, the higher zeta potential may be correlated to the greater stability of suspensions, contributing to the higher homogeneity in oil droplet sizes, which is clearly visible in the optical micrographs.

Table 4.3.2 Droplet size (determined by optical microscopy) and electrical charge (zeta potential) of emulsions.

Emulsions	D(50) (µm)	D(3,2) (µm)	Span	Zeta potential (mV)
0.9CN	3.748	7.478	1.407	5.6 ± 0.3 [b]
0.9CN-TPP	2.712	3.690	1.037	13.1 ± 1.2 [a]
1.5CN	3.139	11.536	2.006	7.5 ± 1.9 [b]
1.5CN-TPP	3.092	4.921	1.169	6.3 ± 0.9 [b]

Mean values ± standard deviations. Values with different letters within the same column are significantly different ($p < 0.05$) according to the LSD multiple range test at 95% of confidence.

In order to investigate the distribution of chitosan nanoparticles around oil droplets, the microstructure of the emulsion produced with crosslinked and non-crosslinked chitosan in the lower polymer concentration (0.9 g /100 g) was analyzed by confocal microscopy.

In this analysis, chitosan was marked by shades of green. The micrographs showed that chitosan nanoparticles are adsorbed at the interface, stabilizing the oil droplets by the Pickering mechanism. Confocal images showed that the nanoparticles produced by deprotonation can adsorb onto the oil droplet surface; nevertheless, as the CN particles have lower zeta potential than CN-TPP (Table 4.3.1), the oil droplets stabilized by CN particles can not only share particles in

common, but also interact among each other due to the lower repulsion forces. These phenomena resulted in the spreading of chitosan in the continuous phase, developing an interconnected network able to stabilize the emulsion droplets. On the other hand, ionic crosslinking provided the formation of individual particles that arranged themselves to concentrate over the droplet surfaces. Because crosslinked nanoparticles had higher zeta potential, the repulsion force maintains the oil droplets away from each other – hindering the network formed by CN.
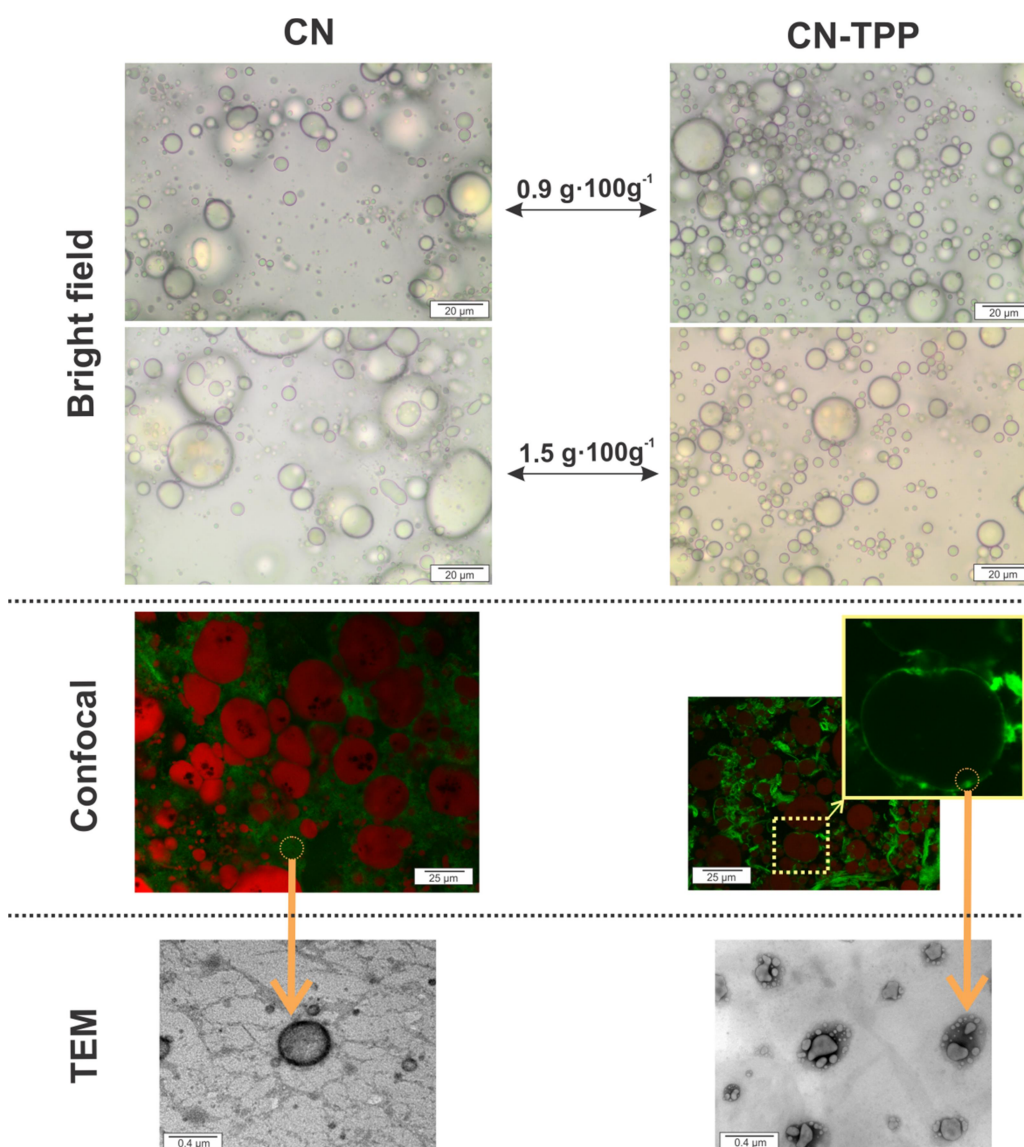
Figure 4.3.4 Microscopic images of emulsions produced by deprotonated (CN) and ionic crosslinked (CN-TPP) chitosan nanoparticles. Confocal microscopy and TEM images were obtained for emulsions formulated with the lowest concentration of chitosan (0.9 g /100 g).

Details on the morphology of chitosan nanoparticles of emulsions formulated with 0.9 g chitosan/100 g can be observed by TEM images included in Figure 4.3.4. Nanoparticles produced by only changing the pH of aqueous phase (09CN) showed more rounded shape compared with crosslinked nanoparticles (09CN-TPP), as well as had different sizes, which is in agreement to results of particle size distribution. In addition, the image suggests the formation of a chitosan network in the continuous phase (indicated by arrows) with free polymer chains contributing to support the particles in suspension and providing oil droplets stabilization. Although different conformations appeared for TPP-crosslinked nanoparticles, more homogeneous size distribution was obtained as described in section 4.3.3.1.2. Similar images of chitosan-tripolyphosphate nanoparticles were acquired by Rampino et al. (2013). These authors reported an aggregation of particles when anionic groups of TPP started interacting with few cationic groups of chitosan, leading to chain folding. Furthermore, a rearrangement of chains might have occurred due to the presence of partially neutralized positive charges of chitosan in the primary aggregates and the size stability of particles could be reached as a function of time. In accordance to the authors, this phenomenon produced more compact particles caused by the fusion of single smaller particles into one entity, what was possible due to the aqueous environment still present during TEM analysis as the air-dried samples were not completely desiccated. Thus, a rearrangement was favored with time leading to a Gaussian distribution curve (Rampino et al., 2013).

4.3.3.2.2 Rheological behavior of the emulsions

4.3.3.2.2.1 Steady shear assays

Flow behavior of the four emulsions was assessed by plotting the apparent viscosity as function of shear rate (Figure 4.3.5). The graphs showed that all of the emulsions presented a Newtonian plateau at very low shear rates, in which apparent viscosity is practically constant. As the shear rate increased, the shear-thinning behavior became evident by the decreasing values of apparent viscosity starting at a critical shear rate. Taking into account that this behavior is commonly represented by the Cross and Carreau model, non-linear regressions were performed and the corresponding fitting parameters are shown in Table 4.3.3.

Although both of the models could be fitted to the experimental data with good accuracy (R^2_{adj} >0.900), the Carreau model was able to better represent the flow behavior with higher R^2_{adj} and lower RMSE (Table 4.3.3). In fact, the Carreau model has been chosen to represent the flow behavior of oil-in-water emulsions (Román, Martínez & Gomez, 2015; Graça, Raimundo & Souza, 2016; Espert, Salvador, San & Hernández, 2020). Nevertheless, the experimental data did not cover the region that concerns the apparent viscosity at infinite shear rate (η_∞) for the studied samples. This parameter was then supposed to be found at higher shear rates, with its values tending to be lower than the apparent viscosity observed at the maximum shear rate assessed.

The emulsions formulated with 1.5CN and 0.9CN-TPP showed the higher apparent viscosity at zero shear rate (η_0). The   values tend to increase with decreasing water content (or increasing stabilizer concentration), which is in agreement with literature (Román et al., 2015) and with the observations for emulsions produced with deprotonated chitosan. On the other hand, emulsions prepared with TPP-crosslinked chitosan tended to follow an opposite trend.
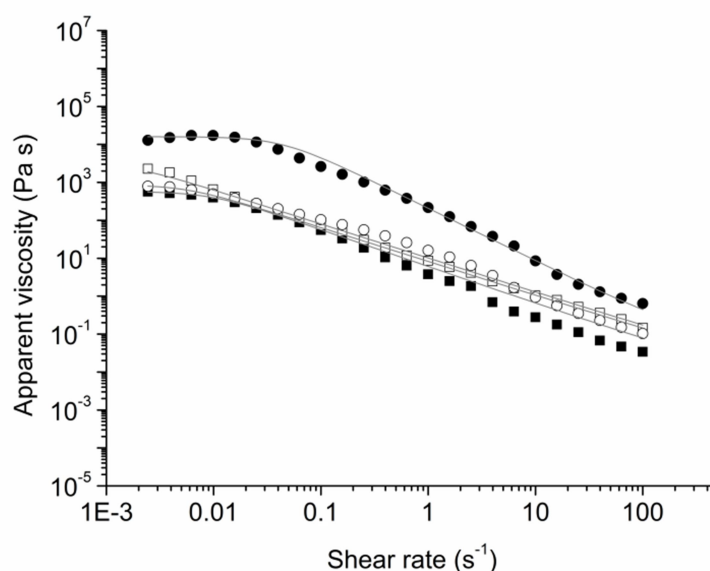
Figure 4.3.5. Experimental data of apparent viscosity versus shear rate for the emulsions 0.9CN (■), 1.5CN (●), 0.9CN-TPP (□) and 1.5CN-TPP (O) fitted to the Carreau model (——).

Table 4.3.3. Fitting parameters of the Cross and Carreau models to experimental data of emulsion's apparent viscosity.

Model	Fitting parameter	Emulsion			
		0.9CN	1.5CN	0.9CN-TPP	1.5CN-TPP
Cross	η_0	951.19 ± 915.23 [b]	15444.60 ± 11257.2 [a]	4467.49 ± 2253.95 [ab]	1078.45 ± 743.57 [b]
	η_∞	<0.01	<0.08	<0.01	<0.01
	$\dot{\gamma}_c$	0.0249 ± 0.0224 [ab]	0.0469 ± 0.0007 [a]	0.0021 ± 0.0014 [b]	0.0094 ± 0.0016 [b]
	m	1.2809 ± 0.2975 [a]	1.3984 ± 0.02793 [a]	0.9775 ± 0.07064 [a]	0.9937 ± 0.1267 [a]
	R^2_{adj}	>0.9620	>0.9528	>0.9003	>0.9971
	$RMSE$	<32.65	<678.63	<219.18	<18.56
Carreau	η_0	730.54 ± 555.88 [b]	16180.10 ± 11835.20 [a]	4723.39 ± 1386.70 [ab]	815.25 ± 481.20 [b]
	η_∞	<0.01	<0.08	<0.01	<0.01
	$\dot{\gamma}_c$	0.0157 ± 0.0118 [ab]	0.0288 ± 0.0015 [a]	0.0009 ± 0.0011 [b]	0.0075 ± 0.0015 [b]
	N	0.5919 ± 0.1713 [a]	0.6432 ± 0.0276 [a]	0.4716 ± 0.0238 [a]	0.4819 ± 0.0561 [a]
	R^2_{adj}	>0.9916	0.9686	0.9374	0.9948
	$RMSE$	<25.25	<552.81	<173.68	<26.57

Mean values ± standard deviations. Values with different letters within the same line are significantly different ($p < 0.05$) according to the LSD multiple range test at 95% of confidence.

This difference can be attributed to the fact that deprotonated chitosan nanoparticles produced emulsions by forming a network in the dispersed phase, capable to adsorb and to entrap the oil (Figure 4.3.4) as discussed in section 4.3.3.2.1 In contrast, CN-TPP nanoparticles adsorbed onto the oil droplet interface to produce dispersed and stabilized oil droplets. Thus, increasing the concentration of deprotonated particles seemed to reinforce the CN network. The lower zeta potential found for these particles leads them to interact among each other by adsorption in multilayers (Sharma, Kumar, Chon & Sangwai, 2014). It makes more difficult the molecular movement by setting up physical barriers against the flow (Maskan & Göğüş, 2000). Regarding CN-TPP, the presence of more particles in the suspension was able to efficiently encapsulate the oil (Table 4.3.2) without significantly increasing the viscosity of the continuous phase. As the oil content (and thus the dispersed phase volume) was the same for all the emulsions, the apparent viscosities of the 1.5CN-TPP emulsion was of the same order of the 0.9CN-TPP one, as shown in Figure 4.3.5. It agrees with the fact that CN-TPP are not dispersed into the continuous phase as CN, but adhered to separate droplets. In other words, in the studied conditions, the rheological parameters of the CN-TPP emulsions are more governed by the continuous phase than by the dispersed phase (oil + adsorbed particles).

In addition to the differences in η_0, both emulsions prepared with deprotonated chitosan nanoparticles had higher critical shear rate ($\dot{\gamma}_c$). These samples were able to maintain relatively constant the apparent viscosities in larger regions of low shear rate than emulsions produced with TPP-crosslinked chitosan, which showed lower viscosity and shorter Newtonian plateau. The network formed in emulsions prepared with CN plays an important role on increasing the values of critical shear rate. At low shear rate, this tridimensional structure resists to the shearing process as it was a solid – with this resistance tending to higher values when the network is strengthened by increasing particle concentration. Because the emulsions formulated with crosslinked chitosan behave more as a suspension, the dispersed phase reorganized at lower shear rates to flow more easily. Once the shear rate was increased and the Newtonian plateau was overcome, the emulsions entered in the power law region commonly reported in literature (Rao, 2014). They showed similar degree of shear-thinning behavior, as indicated by the close N values, characterizing the decreasing viscosity with increasing shear rate. Shear-thinning behavior of emulsions is usually associated to the collapse of part of the droplets and of droplet aggregates, in addition to the alignment of biopolymer molecules present in the continuous phase during shearing (Niknam, Ghanbarzadeh, Ayaseh, Rezagholi, 2018). This phenomenon has a more significant effect in 0.9CN and 1.5CN emulsions than in those prepared with CN-TPP nanoparticles, as already discussed in section 4.3.3.1.2 thus, confirming the previously rheological observations.

4.3.3.2.2.2 Oscillatory shear assays

The emulsion structure was also evaluated by dynamical analysis through measurements of storage (*G'*) and loss (*G''*) modulus under low strain amplitude. All of the mechanical spectra showed that *G'* > *G''* without crossing-over (Figure 4.3.6), indicating that the emulsions tended to storage energy instead of losing it when the strain was applied over the frequency range. A similar viscoelastic behavior was observed for chitosan-based emulsion in a previous work (Alison et al., 2016). The fitting procedure of the power law equation to the experimental data of *G'* and *G''* against frequency provides important information about the emulsion behavior. Table

4.3.4 shows the corresponding fitting parameters, which were able to fit the experimental data with good accuracy.
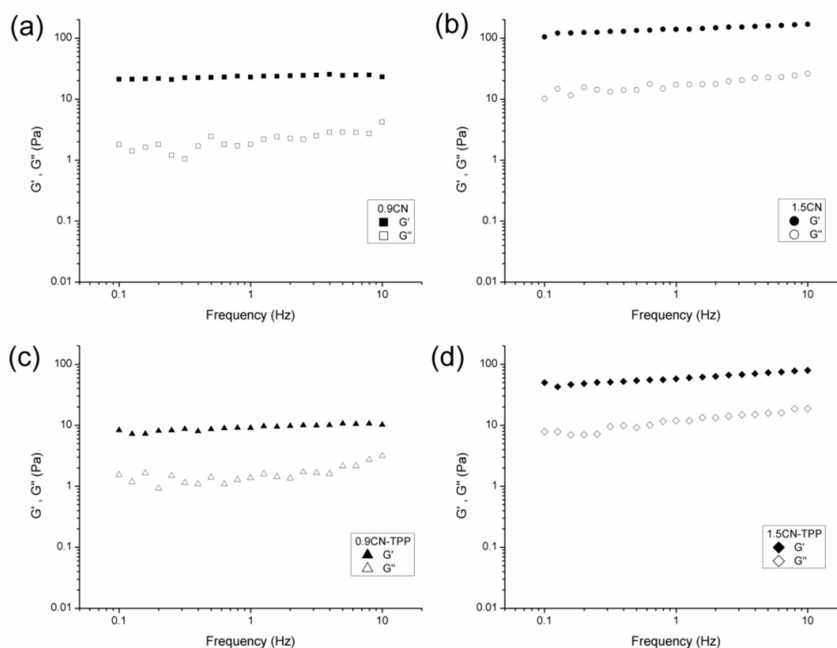
Figure 4.3.6 Storage (closed symbols) and loss (open symbols) modulus for the emulsions prepared with (a) 0.9CN, (b) 1.5CN, (c) 0.9CN-TPP and (d) 1.5CN-TPP.

The fitted mechanical spectra showed that emulsions prepared with deprotonated chitosan behaved as true gel, as the values of *G'* are more constant over the frequency range when compared to the CN-TPP stabilized emulsions at the same particle concentration (n'CN < n'CN-TPP) (Steffe, 1996). According to Zhang et al. (2019), this is a result of a good dispersion of the nanoparticles throughout the medium, which confers a solid-like behavior to the system. In spite of this difference, all of the emulsions had their shear flow dominated by elastic deformation because *n'* values were lower than 1 (Chen et al., 2017).

This means that their structure is subjected to a breakdown at higher shear values, which is in accordance to the larger Newtonian plateau zone observed in steady shear assays. The emulsions formulated with CN-TPP presented mechanical spectra with a slightly higher dependency on frequency, which is characteristic of weak gels. They are supposed to flow under high shear in opposition to the structure breakdown observed for true gels.

Table 4.3.4 Fitting parameters of the Power-Law equation to experimental data of storage (G') and loss (G'') modulus.

Fitting parameters	Emulsions			
	0.9CN	1.5CN	0.9CN-TPP	1.5CN-TPP
k'	24.40 ± 5.27 [b]	115.22 ± 34.36 [a]	7.45 ± 0.94 [b]	44.24 ± 9.33 [b]
n'	0.05 ± 0.02 [c]	0.08 ± 0.01 [bc]	0.11 ± 0.02 [ab]	0.13 ± 0.01 [a]
R^2_{adj}	>0.7950	>0.9202	>0.7407	>0.9598
$RMSE$	<0.8366	<6.2731	<0.8655	<1.9055
k''	0.98 ± 0.19 [b]	9.12 ± 1.75 [a]	1.04 ± 0.34 [b]	6.95 ± 1.69 [a]
n''	0.28 ± 0.05 [a]	0.19 ± 0.02 [a]	0.18 ± 0.08 [a]	0.22 ± 0.01 [a]
R^2_{adj}	>0.4630	>0.8486	>0.5901	>0.9098
$RMSE$	<0.5090	<1.6669	<0.3500	<0.9287

Mean values ± standard deviations. Values with different letters within the same line are significantly different ($p < 0.05$) according to the LSD multiple range test at 95% of confidence.

Although there were no significant differences, increasing the concentration of nanoparticles tended to produce emulsions with slightly higher n' values. The higher the particle concentration the higher is the probability of structural reorganization by the increased interparticle interactions. Regarding the intercepts *k'*, higher capacity for storing energy in the emulsions with deprotonated nanoparticles at higher nanoparticles concentration was observed. In addition, the clustered complex with deprotonated nanoparticles seemed to absorb more deformation energy than the dispersed system with CN-TPP (of lower *k'* compared to CN), and this observation becomes significant when the structure is reinforced by increasing the particle concentration. In close agreement with the steady state results, even though there was an increase in *k'* at higher CN-TPP particle concentration, the way these particles adsorb onto the oil droplet surface did not significant affect the dispersant properties and the overall gel strength. However, it is important to highlight that these observations apply for the range of particle concentration studied. The appearance of significant differences between the rheological parameters may mark a limit value at which the oil droplet surface is saturated with CN-TPP and the surplus particles remain dispersed within the continuous phase. The reduction in the osmotic pressure as a consequence of increasing particle concentration in the dispersant may lead them to cluster and to lose flowability (Lu et al., 2019; Sharma, Kumar, Chong & Sangwai, 2014) – which was, in fact, observed for deprotonated chitosan nanoparticles at all concentrations.

The dependency of the loss modulus on the frequency seemed to be not affected by different emulsion formulations ($0.1676 < n'' < 0.2155$). In contrast, k'' was higher for the emulsions with higher concentration of nanoparticles and also higher in emulsion elaborated with deprotonated nanoparticles. This means that these emulsions loss energy more easily in these conditions, which could be attributed to the disruption of the CN network and particle segregation. Moreover, a higher concentration of particles implies that they interact more intensively among each other and lose more energy by frictional forces along shearing than diluted systems.

In summary, the rheological results confirm that CN nanoparticles were able to emulsify roasted coffee oil by forming a tridimensional network in the continuous phase that entrapped the free oil into its structure. It was possible because of the low electrostatic repulsions which allows them to come close to each other to create the observed viscoelastic true gels. These nanoparticles can interact to build an elastic gel network that supports higher stress application (Alison et al., 2016), but its structure is lost when a critical shear is applied. On the other hand, CN-TPP nanoparticles produce the emulsions by adsorbing on the surface of oil droplets. This different mechanism might be related to the repulsion effects (higher zeta potential) of CN-TPP nanoparticles that keep oil droplets away from each other, contributing allowing for the dispersion of the stabilized oil droplet into the continuous phase and conferring to the emulsions a fluid-like behavior that resembles a suspension (Yuan et al., 2017; Hu, Marway, Kasem, Pelton & Cranston 2016).

4.3.4. Conclusions

Nanoparticles of deprotonated and crosslinked chitosan were produced with promising characteristics for stabilizing oil droplets and be tailored for specific purposes. Both type of chitosan nanoparticles presented high zeta potential and partial wettability by water, with bimodal particle size distribution and different structural conformation. Analysis through FT-IR evidenced the creation of new bonds along the chitosan chain according to the production method used, providing distinct properties to the polymer in different states of aggregation. The emulsions formulated with TPP-crosslinked nanoparticles present no gravitational separation during 24 hours, in spite of the lower viscosity observed even when chitosan concentration was increased from 0.9 to 1.5 g/100 g, which showed that this type or particles may serve

as Pickering stabilizers to produce fluid emulsions suitable for processes subjected to high shear rates. On the other hand, the rheological behavior of emulsions prepared with deprotonated chitosan nanoparticles was more susceptible to increasing chitosan concentration, and they might be investigated in future works regarding their potential to be used as high-internal phase systems thanks to their ability to entrapping oil into a more viscous network formed in the continuous phase at higher chitosan concentrations. Although the current study focused on the performance of different chitosan nanoparticles in oil droplet formation and on the behavior of nanoparticle-based emulsions, investigation on the long-term stability of the emulsions is recommended, as the further application of these systems depends on the required shelf life and should be defined case-by-case.

4.3.5. Acknowledgments

4.3.6. References

Albano, K. M., Franco, C. M. L., & Telis, V. R. N. (2014). Rheological behavior of Peruvian carrot starch gels as affected by temperature and concentration. Food Hydrocolloids, 40, 30-43.

Ali, S. W., Rajendran, S., & Joshi, M. (2011). Synthesis and characterization of chitosan and silver loaded chitosan nanoparticles for bioactive polyester. Carbohydrate Polymers, 83(2), 438-446.

Alison, L., Rühs, P. A., Tervoort, E., Teleki, A., Zanini, M., Isa, L., & Studart, A. R. (2016). Pickering and Network Stabilization of Biocompatible Emulsions Using Chitosan-Modified Silica Nanoparticles. Langmuir, 32(50), 13446-13457.

Antoniou, J., Liu, F., Majeed, H. Qi, J., Yokoyama, W., & Zhong, F. (2015). Physicochemical and morphological properties of size-controlled chitosan–tripolyphosphate nanoparticles. Colloids and Surfaces A: Physicochemical and Engineering Aspects, 465, 137-146.

Chen, K., Chen, M. C., Feng, Y. H., Yu, G. B., Zhang, L. & Li, J. C. (2017). Application and rheology of anisotropic particle stabilized emulsions: Effects of

particle hydrophobicity and fractal structure. Colloids and Surfaces A, 524, p. 8-16.

Danaei, M., Dehghankhold, M., Ataei, S., Davarani, F.H., Javanmard, R., Dokhani, A., Khorasani, S., & Mozafari M. R. (2018). Impact of Particle Size and Polydispersity Index on the Clinical Applications of Lipidic Nanocarrier Systems. Pharmaceutics, 10(57), 1-17.

Divya, K., & Jisha, M.S. (2018). Chitosan nanoparticles preparation and applications. Environmental Chemistry Letters, 16(1), 101-112.

Espert, M., Salvador, A., Sanz, T., & Hernández, M. J. (2020). Cellulose ether emulsions as fat source in cocoa creams: Thermorheological properties (flow and viscoelasticity). LWT – Food Science and Technology, 117, 108640.

Graça, C., Raymundo, A., & Sousa, I. (2016). Rheology changes in oil-in-water emulsions stabilized by a complex system of animal and vegetable proteins induced by thermal processing. LWT – Food Science and Technology, 74, 263-270.

Haider, J., Majeed, H., Williams, P. A., Safdar, W., & Zhang, F. (2017). Formation of chitosan nanoparticles to encapsulate krill oil (Euphausia superba) for application as a dietary supplement. Food Hydrocolloids, 63, 27-34.

Hasheminejad, N., Khodaiyan, F., & Safari, M. (2019). Improving the antifungal activity of clove essential oil encapsulated by chitosan nanoparticles. Food Chemistry, 275, 113-122.

Hatton, R. A., Miller, A. J., & Silva, S. R. P. (2008). Carbon nanotubes: a multi-functional material for organic optoelectronics. Journal of Materials Chemistry, 18(11), 1183-1192.

Ho, K. W., Ooi, C. W., Mwangi, W. W., Leong, W. F., Tey,, B. T. & Chan, E.-S. (2016). Comparison of self-aggregated chitosan particles prepared with and without ultrasonication pretreatment as Pickering emulsifier. Food Hydrocolloids, 52, 827-837.

Hu, Z., Marway, H. S., Kasem, H., Pelton, R., & Cranston, E. D. (2016). Dried and Redispersible Cellulose Nanocrystal Pickering Emulsions. ACS Macro Letters, 5(2), 185-189.

Hurtado-Benavides, A., Dorado A, D., & Sánchez-Camargo, A.d.P. (2016). Study of the fatty acid profile and the aroma composition of oil obtained from roasted

Colombian coffee beans by supercritical fluid extraction. The Journal of Supercritical Fluids, 113, 44-52.

Kaloti, M., & Bohidar, H. B. (2010). Kinetics of coacervation transition versus nanoparticle formation in chitosan–sodium tripolyphosphate solutions. Colloids and Surfaces B: Biointerfaces, 81, 165-173.

Kašpar, O., Jakubec, M., & Štěpánek, F. (2013). Characterization of spray dried chitosan-TPP microparticles formed by two- and three-fluid nozzles. Powder Technology, 240, 31-40.

Liang, J., Yan, H., Wang, X., Zhou, Y., Gao, X., Puligundla, P., & Wan, X. (2017). Encapsulation of epigallocatechin gallate in zein/chitosan nanoparticles for controlled applications in food systems. Food Chemistry, 231, 19-24.

Linke, C., & Drusch, S. (2018). Pickering emulsions in foods - opportunities and limitations. Critical Reviews in Food Science and Nutrition, 58(12), 1971-1985.

Lu, Y., Qian, X., Xia, W., Zhang, W., Huang, J., & Wu, D. (2019). Rheology of the sesame oil-in-water emulsions stabilized by cellulose nanofibers. Food Hydrocolloids, 94, p. 114-127.

Luo, Y., Zhang, B., Cheng, W-H., & Wang, Q. (2010). Preparation, characterization and evaluation of selenite-loaded chitosan/TPP nanoparticles with or without zein coating. Carbohydrate Polymers, 82(3), 942-951.

Maskan, M. & Göğüş, F. (2000). Effect of sugar on the rheological properties of sunflower oil–water emulsions. Journal of Food Engineering, 43(3), 173-177.

Mohan, J. (2004). Infrared Spectroscopy Organic Spectroscopy: In: Principles and Applications (pp. 8-117). Harrow, U.K: Alpha Science International Ltd.

Mwangi, W. W., Ho, K.-W., Ooi, C.-W., Tey, B.-T., & Chan, E.-S. (2016). Facile method for forming ionically cross-linked chitosan microcapsules from Pickering emulsion templates. Food Hydrocolloids, 55, 26-33.

Niknam, R., Ghanbarzadeh, B., Ayaseh, A., & Rezagholi, F. (2018). The effects of Plantago major seed gum on steady and dynamic oscillatory shear rheology of sunflower oil□in□water emulsions. Journal of Texture Studies, 49(5), 536-547.

Oliveira, A. L., Cruz, P. M., Eberlin, M. N., & Cabral, F. A. (2005). Brazilian roasted coffee oil obtained by mechanical expelling: compositional analysis by GC-MS. Food Science and Technology (Campinas), 25, 677-682.

Pereira, A. E. S., Sila, P., M., Oliveira, J., L., Oliveira, H., C., & Fraceto, L., F. (2017). Chitosan nanoparticles as carrier systems for the plant growth hormone gibberellic acid. Colloids and Surfaces B: Biointerfaces, 150, 141-152.

Qi, L., Xu, Z., Jiang, X., Hu, C., & Zou, X. (2004). Preparation and antibacterial activity of chitosan nanoparticles. Carbohydrate Research, 339, 2693-2700.

Rampino, A., Borgogna, M., Blasi, P., Bellich, B., & Cesàro, A. (2013). Chitosan nanoparticles: Preparation, size evolution and stability. International Journal of Pharmaceutics, 455(1), 219-228.

Rao, M. A. (2014). Flow and Functional Models for Rheological Properties of Fluid Foods. In: Rheology of Fluid, Semisolid, and Solid Foods. (pp. 27-58) Food Engineering Series. Springer, Boston, MA.

Rázga, F., Vnuková, D., Némethová, V., Mazancová, P., & Lacík, I. (2016). Preparation of chitosan-TPP sub-micron particles: Critical evaluation and derived recommendations. Carbohydrate Polymers, 151, 488-499.

Ribeiro, E. F., Borreani, J., Ballesteros, G. M., Nicoletti, V. R., Quiles, A., & Hernando, I. (2019). Digestibility and bioaccessibility of Pickering emulsions of roasted coffee oil stabilized by chitosan and chitosan-sodium tripolyphospate nanoparticles. Food Biophysics. 1-12.

Román, L., Martínez, M. M., & Gómez, M. (2015). Assessing of the potential of extruded flour paste as fat replacer in O/W emulsion: A rheological and microstructural study. Food Research International, 74, 72-79.

Sailaja, A.K., Amareshwar, P., & Chakravarty, P. (2011). Different techniques used for the preparation of nanoparticles using natural polymers and their application. International Journal of Pharmacy and Pharmaceutical Sciences, 3(2), 45-50.

Shah, B.R., Li, Y., Jin, W., An, Y., He, L., Li, Z., Xu, W., & Li, B. (2016a). Preparation and optimization of Pickering emulsion stabilized by chitosan-tripolyphosphate nanoparticles for curcumin encapsulation. Food Hydrocolloids, 52, 369-377.

Shah, B.R., Zhang, C., Li, Y., & Li, B. (2016b). Bioaccessibility and antioxidant activity of curcumin after encapsulated by nano and Pickering emulsion based on chitosan-tripolyphosphate nanoparticles. Food Research International, 89, 399-407.

Sharma, T., Kumar, G. S., Chon, B. H., & Sangwai, J. S. (2014). Viscosity of the oil-in-water Pickering emulsion stabilized by surfactant-polymer and nanoparticle-surfactant-polymer system. Korea-Austraila Rheology Journal, 26(4), 377-

387.Schröder, A., Sprakel, J., Schröen, K., Spaen, J. N., & Berton-Carabin, C., C. (2018). Coalescence stability of Pickering emulsions produced with lipid particles: A microfluidic study. Journal of Food Engineering, 234, 63-72.

Sreekumar, S., Goycoolea, F.M., Moerschbacher. B.M., & Rivera-Rodriguez, G.R. (2018). Parameters influencing the size of chitosan-TPP nano- and microparticles. Scientific Reports. 8(1), 4695.

Steffe, J. F. (1996). Rheological methods in food process engineering.(2nd ed.). East Lansing-USA: Freeman Press, (Chapter 1).

Tosi, M. M., Ramos, A. P., Esposto, B. S. & Jafari, S. M. (2020). Dynamic light scattering (DLS) of nanoencapsulated food ingredients. In: Characterization of Nanoencapsulated Food Ingredients (pp. 191-211). Gorgan, Iran: Academic Press.

Vaezifar, S., Razavi S., Golozar, M.A., Karbasi, S., Morshed, M., & Kamali, M. (2013). Effects of Some Parameters on Particle Size Distribution of Chitosan Nanoparticles Prepared by Ionic Gelation Method. Journal of Cluster Science, 24(3), 891-903.

Vogler, E. A. (1998). Structure and reactivity of water at biomaterial surfaces. Advances in Colloid and Interface Science, 74(1-3), 60-117.

Walstra, P. (2003). Physical chemistry of foods. New York, USA: Marcel Decker, (Chapter 13).

Wang, X.-Y., & Heuzey, M.-C. (2016). Chitosan-Based Conventional and Pickering Emulsions with Long-Term Stability. Langmuir, 32(4), 929-936.

Wilk, A., Huißmann, S., Stiakakis, E., Kohlbrecher, J., Vlassopoulos, D., Likos C. N., Meier, G., Dhont, J. K. G., Petekidis, G. & Vavrin, R. (2010). Osmotic shrinkage in star/linear polymer mixtures. European Physical Journal E. 32, 127-134.

Xiao, J., Li, Y., & Huang, Q. (2016). Recent advances on food-grade particles stabilized Pickering emulsions: Fabrication, characterization and research trends. Trends in Food Science & Technology, 55, 48-60.

Ye, F., Miao, M., Lu, K., Jiang, B., Li, X., & Cui, S.W. (2017). Structure and physicochemical properties for modified starch-based nanoparticle from different maize varieties. Food Hydrocolloids, 67, 37-44.

Yuan, D. B., Hu, Y. Q., Zeng, T., Yin, S. W., Tang, C. H., & Yang, X. Q. (2017). Development of stable Pickering emulsions/oil powders and Pickering HIPEs

stabilized by gliadin/chitosan complex particles. Food and Function, 8, 2220-2230.

Zhang, Y., Cui, L., Xu, H., Feng, X., Wang, B. Pukánszky, B., Mao, Z., & Sui, X. (2019). Poly(lactic acid)/cellulose nanocrystal composites via the Pickering emulsion approach: Rheological, thermal and mechanical properties. International Journal of Biological Macromolecules, 137, 197-204.

4.4. CHAPTER 4

Roasted coffee oil microcapsules

Microcapsules of chitosan-based Pickering emulsions containing roasted coffee oil: effect of the drying method and wall material on the physical properties and digestibility

---

Elisa Franco Ribeiro [a,b], Tiago Carregari Polachini [a], Izabela Dutra Alvim [c], Amparo Quiles [b], Isabel Hernando [b], Vania Regina Nicoletti [a]

[a] **São Paulo State University (Unesp), Institute of Bioscience, Humanities and Exact Sciences (Ibilce),** Campus São José do Rio Preto, SP, 15054-000, Brazil

[b] **Food Microstructure and Chemistry Research Group, Universitat Politècnica de València (UPV),** 46022, Valencia, Spain

[c] **Cereal and Chocolate Technology Center, Food Technology Institute (ITAL),** Campinas, São Paulo, 13070-178, Brazil

*Corresponding author: elisa.franco@unesp.br

Abstract: Microcapsules from well-defined emulsion templates has been shown to be an interesting alternative to encapsulate lipids. Thus, this work aimed at producing microcapsules by freeze-drying (FD) and spray-drying (SD) Pickering emulsions of roasted coffee oil (RCO) formulated with self-aggregated or tripolyphosphate-crosslinked chitosan nanoparticles. Physical properties, encapsulation parameters and bioaccessibility of bioactive compounds were investigated as affected by the nanoparticle synthesis and drying technique. All of the samples showed suitable moisture content (2.60% – 3.88%), water activity (0.18 – 2.1) and solubility (63.8% - 87.9%). Self-aggregated chitosan improved oil retention in spray- and freeze-dried samples (>83%) and increased the encapsulation efficiency of FD to values close of SD. Spray-drying produced microcapsules with spherical shapes and smaller size (~11 µm) than FD (~250 µm), which had irregular morphology. Although freeze-drying had lower impact in the bioactive compounds, spray-drying promoted better protection to bioactive compounds during in vitro digestion. Moreover, spray-dried microcapsules with self-aggregated chitosan showed higher bioaccessibility to phenolic compounds and antioxidant activity.

Keywords: roasted coffee oil, crosslinking, spray-drying, freeze-drying, antioxidant activity, phenolic content, digestion.

4.4.1. Introduction

The stabilization of oil-in-water emulsions by the Pickering method has been strongly encouraged as an alternative to replace the conventional surfactants by natural compounds, as biopolymers. These macromolecules may be converted into colloidal particles that can adsorb onto the oil/water interface, thus forming a robust monolayer that prevents droplet coalescence and stabilizes the emulsions due to the high energy level required to remove them from the interface (Yan et al., 2017). With the aim of optimizing the performance of biopolymers as Pickering emulsifiers, physical and/or chemical modifications must be carried out to make them suitable for a given application.

Chitosan, in particular, is a chitin-derived polysaccharide with high biocompatibility and biodegradability that can behave as an agent of controlled delivery of bioactive compounds during encapsulation (Carlan, Estevinho, & Rocha, 2017). This polysaccharide presents high solubility in acid medium due to the protonation phenomena. However, as the electrostatic charges of chitosan are neutralized, it becomes more hydrophobic, with a specific conformational structure that is desirable for food purposes (Baek, Wahid-Pedro, Kim, Kim, & Tam, 2019). Among the many methods for chitosan modification, the self-aggregation and crosslinking technique are widely reported in literature – including for Pickering emulsification (Costa, Gomes, & Cunha, 2018; Mwangi, Ho, Ooi, Tey, & Chan, 2016; Ribeiro, Barros-Alexandrino, et al., 2020). Self-aggregation is performed by deprotonating chitosan molecules in the presence of an alkaline agent, causing the molecules to self-assemble into solid micro- or nanoparticles (Ho et al., 2016). Crosslinking is an alternative method to produce chitosan nanoparticles that consists of adding a crosslinking agent, e.g. sodium tripolyphosphate (TPP), which results in the ionic gelation of chitosan chains through the interaction between the negative charges of the polyanion and the positive charges of the primary amino groups present in chitosan molecules (Shah et al., 2016).

Despite these two methods of chitosan modification create solid colloidal particles with affinity by both polar (water) and non-polar (lipid) compounds, the resulting physicochemical properties of each type of chitosan nanoparticle influence their behavior as Pickering emulsifiers, mainly because of differences in particle size distribution, zeta potential, contact angle, and microstructure. Therefore, these

particles act differently as barriers against the lipid access by environmental factors (Ribeiro, Borreani, et al., 2020).

Emulsions play an important role on preserving lipid compounds (Araiza-Calahorra, Akhtar, & Sarkar, 2018), but their handling and shelf-life are impaired as a consequence of their high water content. Thus, converting emulsions into powdered formulations by water removal is an attractive possibility for preserving food compounds and reducing costs related to storage and transportation. Freeze-drying (FD) and spray-drying (SD) are some of the most used methods for encapsulating materials of interest in a dried food matrix. The first is highlighted by operating at low temperatures, below the freezing point, to proceed to water sublimation – thus preventing undesirable thermal effects (Ezhilarasi, Indrani, Jena, & Anandharamakrishnan, 2013). The latter consists of a simple method that continuously atomizes the emulsion to be quickly dried in contact with a hot air flow (Gharsallaoui, Roudaut, Chambin, Voilley, & Saurel, 2007).

The mechanisms involved in drying and encapsulation give rise to dried microcapsules with distinct physical properties that should be specifically addressed (Karthik & Anandharamakrishnan, 2013). When produced from well-defined Pickering emulsion templates, these microcapsules can be easily used as ingredients in food formulations, but the composition and microstructure of the encapsulating matrix differently affects the delivery of bioactive compounds into the gastrointestinal tract (Mwangi et al., 2016). In particular, studies about the bioaccessibility have been successfully carried out in order to evaluate the release of antioxidants and phenolic compounds from the lipid core during simulated in vitro digestion (Burgos-Díaz, Opazo-Navarrete, Soto-Añual, Leal-Calderón, & Bustamante, 2020; Jara-Palacios, Gonçalves, Hernanz, Heredia, & Romano, 2018).

In the present study, roasted coffee oil (RCO) was considered as the lipid phase to be encapsulated. RCO is a byproduct of the coffee processing industry and presents high contents of unsaturated fatty acids and antioxidant compounds (Hurtado-Benavides, Dorado A, & Sánchez-Camargo, 2016; Ribeiro, Borreani, et al., 2020). Pickering emulsions stabilized by self-aggregated or crosslinked chitosan nanoparticles were used as templates for producing microcapsules by freeze-drying or spray-drying techniques. The effects of the matrix and the drying method on the physical properties of the resulting microcapsules, encapsulation parameters, microstructure and bioaccessibility of the bioactive compounds were reported.

4.4.2 Materials and Methods

4.4.2.1 Material

The following ingredients were used in the production of the roasted coffee oil microcapsules: low molecular weight chitosan powder (degree of deacetylation: 77%) purchased from Sigma-Aldrich (San Luis, USA); roasted coffee oil (RCO) kindly supplied by Cia. Iguaçu de Café Solúvel (Cornélio Procópio, Brazil); maltodextrin DE 10 purchased from Get do Brasil (São João da Boa Vista, Brazil); sodium tripolyphosphate (TPP) purchased from LS Chemicals (Ribeirão Preto, Brazil); glacial acetic acid and sodium hydroxide purchased from Dinâmica (Indaiatuba, Brazil). Analytical grade chemicals and ultrapure water with 18.2 MΩ cm resistivity were used in all the experiments.

4.4.2.2 Synthesis of self-aggregated chitosan and crosslinked chitosan nanoparticles

Chitosan nanoparticles were obtained by two methods as described by Ribeiro et al. (2020): self-aggregated chitosan nanoparticles were produced by deprotonation of the amino groups on the D-glucosamine units, whereas crosslinked chitosan nanoparticles were obtained by adding sodium tripolyphosphate (TPP) as a crosslinking agent. Initially, the biopolymer was added to an acetic acid solution 1% and left under magnetic stirring for 24 h at room temperature until complete dissolution. For the amino deprotonation method, nanoparticles were obtained by dripping NaOH 6 M in order to increase the pH of the solution from 3.5 to 6.7. For the crosslinking method, a TPP aqueous solution was added to the initial chitosan solution in a proportion to result in the mass ratio of 3:1 (CS:TPP). Both methods aimed at obtaining a final concentration of chitosan nanoparticles of 0.9 g/100 g suspension.

4.4.2.3 Preparation of roasted coffee oil Pickering emulsions

RCO was added to the obtained suspensions of self-aggregated or crosslinked chitosan nanoparticles to produce emulsions with 10% (w/w) of lipid phase. The oil was added to the nanoparticle suspensions under homogenization (Ultra-Turrax T25, IKA, Germany) at 12,000 rpm. After oil addition, the samples were kept under mixing for 5 min more. Both the emulsions were prepared in triplicate.

4.4.2.4 Production of roasted coffee oil microcapsules

RCO microcapsules obtained by the different drying methods were produced using the previously prepared emulsions added with maltodextrin DE 10 (35 g/100 g in the emulsion) as a carrier agent. Maltodextrin dispersion into the emulsions was performed using an Ultra-Turrax stirrer at 12,000 rpm for 5 min. As a control system (MO), maltodextrin and RCO were dispersed under the same conditions but using ultrapure water without chitosan nanoparticles. Maltodextrin-added emulsions containing self-aggregated chitosan were denominated CMO, whereas those with crosslinked chitosan were designated CTMO. After preparation, the control system and the maltodextrin-added emulsions were subjected to freeze-drying (FD) or spray-drying (SD).

4.4.2.5 Freeze drying (FD)

For freeze-drying, the emulsions were initially frozen at –40º C in an ultra-freezer for 24 h, followed by drying in a freeze-dryer (model L-101, Liotop, Brazil) for 48 h at an approximated pressure of 200 µmHg. After freeze-drying, samples were finely grinded using the mortar and stored into metallized bags in a desiccator at room temperature. This procedure originated the freeze-dried microcapsules MO-FD (control), CMO-FD and CTMO-FD.

4.4.2.6 Spray-drying (SD)

For the spray-drying process, both emulsions and the control system were dried in a bench-scale spray-dryer (B-290, Büchi, Switzerland) using double-fluid spray nozzle (orifice diameter = 0.7 mm). The equipment was fed through a peristaltic pump and, after preliminary assays, the defined drying conditions were: feed flow rate of 2 mL/min, atomization air rate of 742 L/h, inlet air temperature 160 °C, and aspiration rate of 35 m3/h. The spray-dried samples were designated as MO-SD (control) and CMO-SD (formulated with self-aggregation chitosan), and were stored into metallized bags in a desiccator at room temperature. Spray-dried microcapsules obtained from the emulsion containing TPP-crosslinked nanoparticles, which would have been designated as CTMO-SD, could not be produced: because the TPP-chitosan nanoparticles present a more rigid structure (Ribeiro, Barros-Alexandrino, et al., 2020), their presence in CTMO emulsions caused the nozzle feeding orifice to clog as the sample was pumped.

4.4.2.7 Characterization of roasted coffee oil microcapsules

4.4.2.7.1 Moisture content and water activity (aw) of microcapsules

The moisture content of microcapsules was determined gravimetrically by drying 1.5 g of samples in a vacuum oven (Marconi, MA 030) at 70 °C until constant weight (AOAC, 1990). Water activity was determined using an AquaL 4TEV water activity meter (Decagon Devices, Inc., Pullman, USA). The measurements were carried out at 25 °C.

4.4.2.7.2 Solubility

Microcapsules samples (1 g) were dispersed in 25 mL of water and kept under magnetic stirring for 5 min. The solution was centrifuged at 3000□g for 10 min. The supernatant (20 mL) was transferred to previously weighed Petri dishes and oven dried at 105 °C for 5 h. The solubility (%) was calculated as the weight difference (Cano-Chauca, Stringheta, Ramos, & Cal-Vidal, 2005).

4.4.2.7.3 Particle size distribution

Particle size distribution was measured by laser diffraction (L950, Horiba instruments, Inc., Japan). The mean particle diameter, expressed as the volume mean diameter $D[4,3]$, and the width of particle size distribution (*Span*), were calculated according to Equations (1) and (2), respectively:

$$D[4,3] = \frac{\sum n_i d_i^4}{\sum n_i d_i^3}$$

(1)

$$Span = \frac{D_{90} - D_{10}}{D_{50}}$$

(2)

in which n_i is the number of particles with d_i diameter. D_{10} is defined as the diameter at which 10% of the particles lies below this value. Similarly, D_{50} and D_{90} correspond to the diameters at which 50% and 90% of the cumulative volumes of the distribution have smaller particle sizes than that value, respectively.

4.4.2.7.4 Oil retention

RCO retention (%) in the microcapsules was determined using a Multiskan Go Spectrophotometer (Thermo Fisher Scientific, Vantaa, Finland) following the methodology proposed by Freiberger et al. (2015) with some modifications. The microcapsules (0.5 g) were dissolved in acetic acid solution 1% (5 mL) under stirring for 10 min. Chitosan was precipitated by adding ethanol (5 mL), then the solution was filtered through a 0.45 µm nylon filter and the absorbance was read at 296 nm. As a blank, used for absorbance readings, a suspension of microcapsules produced without RCO was subjected to the same treatment. A calibration curve was previously obtained for calculating RCO concentration. The oil retention was obtained using Equation (3).

$$\text{Retention}\left(\%\right) = 100 \times \frac{C_t}{C_0}$$

(3)

in which C_t is the total oil content in the microcapsules (g) and C_0 is the theoretical oil content (g) expected in the powder, based on the emulsion formulation in dry basis.

4.4.2.7.5 Encapsulation efficiency

The ration between the amount of oil entrapped inside the microcapsules and the oil content in the particle surface is considered as the encapsulation efficiency, given by Equation (4):

$$\text{Encapsulation efficiency}\left(\%\right) = 100 \times \frac{(C_t - C_s)}{C_t}$$

(4)

in which the total oil (C_t) was obtained as described in section 4.4.2.7.4 and the surface oil (C_s) was extracted following the methodology proposed by Silva, Vieira & Hubinger (2014) with modifications. Hexane (5 mL) was added to 0.5 g of microcapsules and shaken for 2 min at room temperature. The dispersion was filtered through a 0.45 µm nylon filter and the powder on the filter was rinsed three times with 5 mL of hexane. The absorbance reading was carried out in a Multiskan Go Spectrophotometer at 296 nm using pure hexane as blank. The RCO concentration

was determined with a previously obtained calibration curve of oil dissolved in hexane.

4.4.2.7.6 Drying yield (%)

The drying yield (%) corresponding to each drying method was determined as the ratio between the total solids recovered and the mass of solids present in the dried emulsions.

4.4.2.7.7 Microstructure

Spray-dried and freeze-dried samples were analyzed according to their microstructure by scanning electron microscopy. Samples were coated with platinum and observed by a field emission scanning electron microscope (FESEM) (Ultra55 FESEM model; Zeiss, Oberkochen, Germany). Each sample was analyzed in duplicate.

4.4.2.7.8 Total Phenolic Content

The total phenolic content (TPC) was determined in triplicate using the Folin-Ciocalteu assay (Singleton & Rossi, 1965). Ethanolic extracts were obtained by stirring the samples with absolute ethanol (10 mg/mL) for 10 s in a vortex and centrifuging (Centrifuge 5415 R., Hamburg, Germany) at 14,500 rpm for 20 min at 4 °C. This procedure was repeated three times and, then, the top layers were mixed to proceed to the Folin-Ciocalteu method (Ribeiro, Borreani, et al., 2020). The resulting absorbance of the samples was measured at 725 nm and the concentration could be determined by a previously prepared calibration curve. The content of TPC was expressed as milligram equivalent of gallic acid per 100 g of microcapsules.

4.4.2.7.9 Antioxidant capacity

The ethanolic extracts were subjected to the analysis of antioxidant capacity by the DPPH (2,2-diphenyl-1-picrylhydrazyl) radical scavenging method (Brand-Williams, Cuvelier, & Berset, 1995). Approximately 100 µL of diluted samples were mixed with 2.9 mL of the DPPH solution in amber tubes. After 1 h of reaction, the absorbance was read at 515 nm in a spectrophotometer (model UV mini-1240, Shimadzu, Chiyoda-ku, Japan). Results were expressed as milligram equivalent of Trolox per 100 g of microcapsules by using a standard curve of Trolox solutions.

In addition, antioxidant activity was evaluated by ferric reducing antioxidant power (FRAP) method (Benzie & Strain, 1996). In this procedure, 90 µL of the ethanolic extract were mixed with 270 µL of distilled water and 2.7 mL of the FRAP reagent (750 mL of acetate buffer 0.3 M, 75 mL of TPTZ 10 mM solution and 75 mL of 20 mM ferric chloride). The mixture was homogenized and immersed into a water bath at 37 ºC for 30 min. The absorbance of the samples was measured at 595 nm in a spectrophotometer (model UV mini-1240, Shimadzu, Chiyoda-ku, Japan). Results were expressed as milligram equivalent of Trolox per 100 g of microcapsules by using a standard curve of Trolox solutions.

4.4.2.8 In vitro digestion
4.4.2.8.1 In vitro digestion model

A simulated in vitro digestion, following the model described by Eriksen et al. (2017), Gómez-Mascaraque et al. (2017), and Minekus et al. (2014), was performed to evaluate the effects of chitosan nanoparticle synthesis and drying methods in the bioaccessibility of the phenolic and antioxidant compounds present in the microcapsules. The digestion process was carried out in a reaction station (Carousel 6 Plus commercial house) with controlled temperature of 37ºC and stirring at 150 rpm. During digestion the samples were kept in the dark and nitrogen atmosphere in both the gastric and intestinal phases. Solutions of simulated salivary fluid (SSF), simulated gastric fluid (SGF) and simulated intestinal fluid (SIF) were prepared according to the compositions described by Minekus et al. (2014). Firstly, for the oral stage, 4 mL of SFF + α-amylase (75 U/mL in the digestion mixture) previously adjusted to pH 7, 19 µL of $CaCl_2$ and 0.981 mL of distilled water were added to 5 g of sample. This mixture was maintained under simulated oral digestion for 2 min and, then, the obtained digested sample was added into the digestion flask in the reaction station to proceed the further steps. Secondly, for the gastric phase, 16 mL of SGF + pepsin (2000 U/mL in the digestion mix) and 8 µL of $CaCl_2$ were added. The pH was adjusted between 2.5 and 3.5 using 1 M HCl, and the volume was completed to 20 mL with distilled water. The mixture was incubated at 37 °C for 1 h under shaking and in the absence of oxygen. Finally, for intestinal digestion, the pH was adjusted between 6.5 and 7.5 using 1 M HCl or 1 M NaOH. Then 8 mL of SIF + pancreatin (16.25 mg/mL), 45 µL of CaCl2, 8 mL of SIF + bile (37.8 mg/mL) and 8 mL of SIF + lipase (2000 U/mL) were added. Once the pH was readjusted, the necessary volume

of distilled water was added for a total volume of 30 mL. The mixture was incubated at 37 ºC for 2 h under shaking, absence of oxygen and darkness. At the end of the digestion, the resulting mixture was centrifuged at 14,500 rpm for 20 min at 4 °C (Centrifuge 5804 R., Hamburg, Germany) and filtered using a vacuum pump and Whatman n. 4 filter paper, 20-25 µm pore size, yielding a two-phase system. The supernatant, considered to present the soluble compounds that are available to be transferred to the human blood, was designed as IN fraction and it was used for calculating the bioacessibility of total phenolic compounds and antioxidant capacity.

4.4.2.8.2 Bioaccessibility

The effect of the microcapsules' matrix and the drying method on the digestion was evaluated with basis on the phenolic content of roasted coffee oil and its antioxidant capacity. These values were used to determine the bioaccessibility index as suggested by Schulz et al. (2017) with some modifications.

The bioaccessibility index is defined as the proportion of the total phenolic content or antioxidant capacity present in the intestinal phase that could become available for absorption into the systemic circulation. It was calculated according to Equation (5):

$$\text{Bioaccessibility index (\%)} = \frac{IN}{ND} \times 100$$

$$(5)$$

in which *IN* is the content of the compound released in the simulated digestion and *ND* is the content of the compound in the non-digested sample. Bioaccessibility index was also calculated for the values of antioxidant activity obtained by DPPH and FRAP method.

4.4.2.9 Statistical Analysis

Analysis of variance (ANOVA) was performed on the experimental data using the STATISTICA software (StatSoft Inc., Tulsa, EUA). The presence of significant differences between the averages was evaluated by the Fisher test with 95% of confidence.

4.4.3 Results and discussion

4.4.3.1 Moisture content, aw and solubility

Physicochemical properties of the microcapsules are closely connected to the food processing as well as to the constituting matrix. Parameters such as moisture content can affect the flow characteristic of bulk powders whereas water activity is related to the free water available for various chemical and biological reactions to occur.

All of the microcapsules presented close moisture contents (from 2.60 to 2.88% wet basis) (Table 4.4.1), which is considered to be suitable for preventing lipid oxidation with microbiological safety (Rahman & Labuza, 2007; Vishnu et al., 2017). Spray-dried microcapsules presented slightly lower moisture content, probably related to the higher surface area of the atomized droplets available for water removal than in freeze-dried samples (Karthik & Anandharamakrishnan, 2013).

On the other hand, slightly higher water activity was observed for spray-dried samples. The presence of self-aggregated chitosan caused the water activity of the microcapsules to increase even though the moisture content decreased in comparison to the MO-SD sample. Self-aggregated chitosan increased the hydrophobicity of the microcapsules' matrix, and the reduced polar interactions between water molecules and the material lead to a decrease in the moisture content. Nevertheless, because the water molecules are not strongly bound to the matrix, it makes the water activity to slightly increase. Even though, the a_w is still found to be within a safety range (<0.3) for microbial development and core preservation (Klinkesorn, Sophanodora, Chinachoti, Decker, & McClements, 2006; Rahman & Labuza, 2007). The incorporation of crosslinked chitosan into the food matrix contributes to a certain degree of hydrophilicity due to the free amino groups that are not bound to TPP (Ribeiro, Barros-Alexandrino, et al., 2020). In addition to the decrease in the moisture content when compared to the MO-FD sample, the matrix constituted of crosslinked chitosan binds better the existing water molecules and decrease the amount of available water molecules for reactions. This behavior is observed not only in MO-FD sample (with higher moisture content) but also in the CMO-FD sample with similar moisture content.

The solubility of the microcapsules in water (Table 4.4.1) is an important parameter related to the easiness of applying the material as a food ingredient. The

aforementioned parameters - water content and water activity - reflect directly in the solubility of the microcapsules. The more hydrophilic wall matrices resulted in microcapsules with higher water solubility. Additionally, spray-drying produced more soluble microcapsules than freeze-drying, probably because of the smallest particle sizes resulting from this process, as discussed in Section 4.4.3.2.

It is important to highlight that control samples constituted exclusively of maltodextrin presented good solubility for both drying methods, but they do not have the desirable interfacial properties to ensure high microencapsulation efficiency as attained by applying the chitosan nanoparticles (Gharsallaoui et al., 2007).

Table 4.4.1 Physicochemical properties of RCO microcapsules produced from chitosan-based Pickering emulsions by different nanoparticle synthesis and drying methods.

Sample	Moisture content (%)	Water activity	Solubility in water (%)
MO-FD	3.88 ± 0.08 [a]	0.1865 ± 0.009 [c]	71.63 ± 6.56 [bc]
CMO-FD	3.58 ± 0.07 [b]	0.2001 ± 0.004 [b]	63.86 ± 6.32 [c]
CTMO-FD	3.52 ± 0.06 [b]	0.1679 ± 0.003 [d]	78.81 ± 6.04 [ab]
MO-SD	3.38 ± 0.03 [c]	0.1956 ± 0.002 [b]	87.90 ± 10.55 [a]
CMO-SD	2.60 ± 0.03 [d]	0.2102 ± 0.003 [a]	70.20 ± 7.21 [bc]

CMO-FD = freeze-dried microcapsules of RCO with self-aggregated chitosan and maltodextrin. CTMO-FD = freeze-dried microcapsules of RCO with TPP-crosslinked chitosan and maltodextrin. MO-FD = freeze-dried microcapsules of RCO with maltodextrin. CMO-SD = spray-dried microcapsules of RCO with self-aggregated chitosan and maltodextrin. MO-SD = spray-dried microcapsules of RCO with maltodextrin. Data are expressed as means values ± standard deviation. Values with different letters within the same column are significantly different ($p < 0.05$) according to the LSD (Fisher) multiple range test.

4.4.3.2 Particle size distribution

Particle size was measured as a volume-weighted mean diameter (D[4,3]) and the values are shown in Table 4.4.2. As expected, spray-drying resulted in much smaller particles than freeze-drying as a result of the atomization of small emulsion droplets followed by hot air drying. In addition, the absence of significant differences among the spray-dried samples meant that self-aggregated chitosan nanoparticle improved encapsulation without causing significant changes in the particles size of

microcapsules, as well as possible texture defects when incorporated to food products.

Regarding the freeze-dried samples, they resulted in quite similar particle sizes with higher polydispersity (higher Span values) than those obtained by spray-drying, as they were milled into smaller and heterogeneous particles, similarly as found by Šturm et al. (2019) for freeze-dried propolis. Slightly higher values were noticed for the control sample, which is probably related to an impaired encapsulation by the exclusive use of maltodextrin as carrier agent. The addition of chitosan nanoparticles play the role of creating a better interfacial film that prevents the resulting microcapsules to agglomerate (Li et al., 2018).

Table 4.4.2 Particle size measurements of RCO microcapsules produced from chitosan-based Pickering emulsions by different drying methods.

Sample	D[4,3] (µm)	Span
MO-FD	276.21 ± 48.18 [a]	3.004 ± 0.183 [b]
CMO-FD	244.45 ± 41.39 [b]	2.942 ± 0.198 [b]
CTMO-FD	231.91 ± 24.80 [b]	3.371 ± 0.342 [a]
MO-SD	10.73 ± 0.22 [c]	1.305 ± 0.006 [d]
CMO-SD	12.83 ± 0.20 [c]	1.698 ± 0.016 [c]

CMO-FD = freeze-dried microcapsules of RCO with self-aggregated chitosan and maltodextrin. CTMO-FD = freeze-dried microcapsules of RCO with crosslinked chitosan and maltodextrin. MO-FD = freeze-dried microcapsules of RCO without chitosan. CMO-SD = spray-dried microcapsules of RCO with self-aggregated chitosan and maltodextrin. MO-SD = spray-dried microcapsules of RCO without chitosan. Data are expressed as means values ± standard deviation. Values with different letters within the same column are significantly different (p < 0.05) according to the LSD (Fisher) multiple range test.

Figure 4.4.1 presented the particle size distribution for the studied samples. In these graphs, higher particle size and polydispersity with a single large peak could be observed for samples obtained by FD. SD produced microcapsules with smaller size but MO-SD sample showed two peaks in contrast to the single peak observed for CMO-SD. Although the presence of two peaks could be interesting for packing and transport purposes (Silva et al., 2014), the oil retention should be carefully analyzed to ensure the microcapsules could encapsulate the lipid phase adequately.
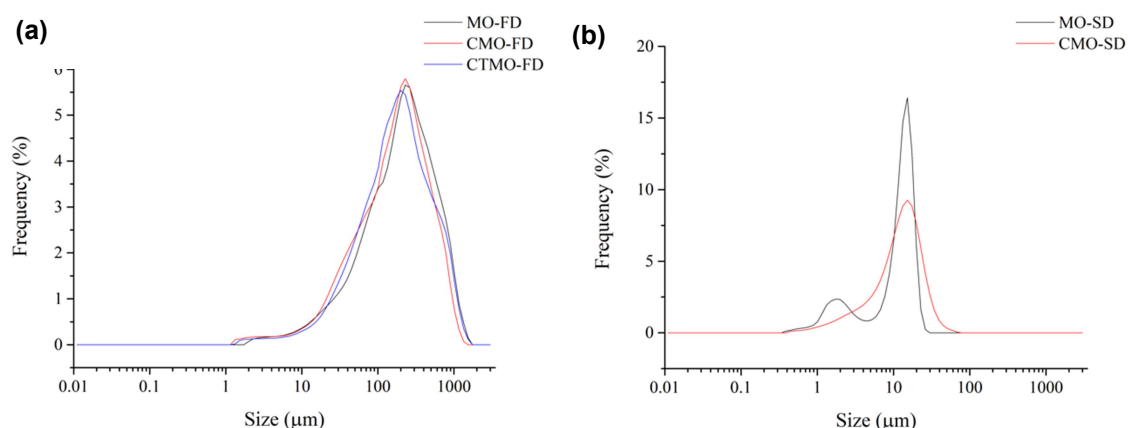
Figure 4.4.1 Particle size distribution of RCO microcapsules produced from chitosan-based Pickering emulsions by (a) freeze-drying (FD) and (b) spray-drying (SD). CMO: self-aggregated chitosan and maltodextrin; CTMO: crosslinked chitosan and maltodextrin; MO: only maltodextrin.

4.4.3.3 Encapsulation parameters

The encapsulation parameters give a picture about the efficiency of a process or a product to enclosure the material of interest. Thus, drying yield was firstly determined to assess the amount of powdered emulsion that could be obtained from fresh emulsions (Table 4.4.3). As expected, FD reached the highest values – very close to 100% – as seen as the whole content of emulsion is freeze-dried without evidences of solids being carried by vacuum. On the other hand, SD yielded lower amounts of powdered material because a low-dense fraction can be aspired by the cyclone while a denser fraction can stay incompletely dried in the atomizing chamber. In the present study, no evidence of incomplete drying was observed; therefore, the low observed yield was mainly attributed to the production of fine particles. The low drying yield was more pronounced in the MO-SD samples, being a consequence of the low bulk density of the fine particles, which in turn is supposed to be a consequence of the lower amount of oil entrapped in the encapsulation matrix, as it was expected in the case of using pure maltodextrin as wall material.

The presence of self-aggregate chitosan in the matrix of spray-dried microcapsules contributed to the material hydrophobicity and its capacity for binding oil (Ribeiro, Barros-Alexandrino, et al., 2020). The loss of a certain amount of oil during encapsulation processes is inevitable. It is important to determine the oil

content retained in the samples since it can be affected by several factors, e. g wall material, solid content, temperature and humidity. As a result of the ability for binding the oil, it induces the higher oil retention and encapsulation efficiency observed in Table 4.4.3. In fact, this observation is in close agreement with the particle size measurements (Figure 4.4.1). As a consequence of the higher oil retention capacity, wall material binds better the oil to create microcapsules with higher oil-loading and resulting in higher drying yield in comparison to MO-SD.

Regarding FD, a great part of the lipid phase was retained in the microparticles (76-95%). However, slightly lower oil retention was observed for the control samples (with only maltodextrin). Together with the slightly higher standard deviation, it can be a result of the lower stabilization capacity of the emulsions composed exclusively by oil and maltrodextrin, which originated less homogeneous microcapsules with the observed lower encapsulation efficiency when compared to the CMO-FD and CTMO-FD. Because the crosslinked chitosan has a higher hydrophilicity than self-aggregated chitosan (Ribeiro, Barros-Alexandrino, et al., 2020), it can enhance both the water and oil binding properties and contributes to the homogeneity of the samples.

When comparing the drying methods with respect to the encapsulation efficiency, it could be seen that SD resulted in higher encapsulation efficiency of RCO in comparison with FD, in agreement with it has been reported in literature (Rezvankhah, Emam-Djomeh, & Askari, 2020). It means that the lipid phase in spray-dried samples was less exposed to the environmental disturbances than the lipid phase entrapped into the freeze-dried matrix (González, Martínez, Paredes, León, & Ribotta, 2016). The atomization of microdroplets and the rapid water removal lead to the formation of rounded capsules with entrapped oil (Section 4.4.3.4.). On the other hand, freezing the samples causes the solid particles to immobilize around the oil and the water crystals' sublimation results in the formation of a porous network of wall material with oil droplets adhered to the matrix. This phenomenon can be slightly more pronounced in CTMO-FD samples due to improved water binding properties of crosslinked chitosan. Since the oil is partially exposed to the environment, the expected lower encapsulation efficiency in freeze-dried samples was confirmed (~44-66%). Regardless the drying method, a higher efficiency was obtained in the present study in relation to some reports in literature that used chitosan as wall material for encapsulating lipid (Esmaeili & Asgari, 2015; Hosseini, Zandi, Rezaei, &

Farahmandghavi, 2013; Kumar et al., 2017). This behavior can be attributed to the presence of maltodextrin as an additional carrier agent and to the emulsification by the Pickering mechanism. Because of the high energy required for detaching the solid particles from the oil-water interface in Pickering emulsions, these solid nanoparticles can form a better barrier against material transfer through the interface (Chevalier & Bolzinger, 2013) – which was confirmed by the increased encapsulation efficiency of the CMO-FD and CTMO-FD samples in comparison with the control without chitosan (MO-FD).

Table 4.4.3 Drying yields, oil retention and encapsulation efficiency of RCO microcapsules.

Sample	Drying yield (%)	Oil retention (%)	Encapsulation Efficiency (%)
MO-FD	89.95 ± 2.56 [a]	76.29 ± 11.41 [b]	43.96 ± 7.53 [d]
CMO-FD	92.69 ± 0.13 [a]	85.15 ± 2.35 [ab]	76.06 ± 2.55 [b]
CTMO-FD	91.16 ± 1.38 [a]	95.36 ± 6.26 [a]	65.60 ± 4.47 [c]
MO-SD	19.16 ± 2.56 [c]	40.18 ± 6.39 [c]	88.14 ± 1.36 [a]
CMO-SD	25.47 ± 0.70 [b]	83.04 ± 8.94 [ab]	84.98 ± 2.51 [a]

CMO-FD = freeze-dried microcapsules of RCO with self-aggregated chitosan and maltodextrin. CTMO-FD = freeze-dried microcapsules of RCO with crosslinked chitosan and maltodextrin. MO-FD = freeze-dried microcapsules of RCO without chitosan. CMO-SD = spray-dried microcapsules of RCO with self-aggregated chitosan and maltodextrin. MO-SD = spray-dried microcapsules of RCO without chitosan. Data are expressed as means values ± standard deviation. Values with different letters within the same column are significantly different ($p < 0.05$) according to the LSD (Fisher) multiple range test.

4.4.3.4 Microstructure

Figure 4.4.2 presents the images obtained by FESEM of the microcapsules formulated with self-aggregated chitosan and crosslinked chitosan nanoparticles after FD or SD. The electronic micrographs showed that SD produced more spherical microcapsules without the presence of apparent fissures, potentially preventing the core oxidation due to the probably lower permeability to oxygen and moisture (Kumar et al., 2017). The observed wrinkled surface is expected as a consequence of the rapid water loss during SD (Fang, Zhao, Liu, Liang, & Yang, 2019).

Although the two spray-dried samples demonstrated similar morphology, the MO samples showed a noticeable number of particles smaller than 4 µm around the bigger ones with particle size of ~15 µm. In fact, this observation is in close agreement with the bimodal particle size distribution in Figure 4.4.1b. Probably, the poor stabilization of emulsions containing exclusively maltodextrin as carrier agent lead to lower oil retention (Table 4.4.3) and the possible production of empty capsules of smaller sizes. By producing smaller particles, the area/volume ratio of spray-dried samples tended to be higher than of freeze-dried ones.
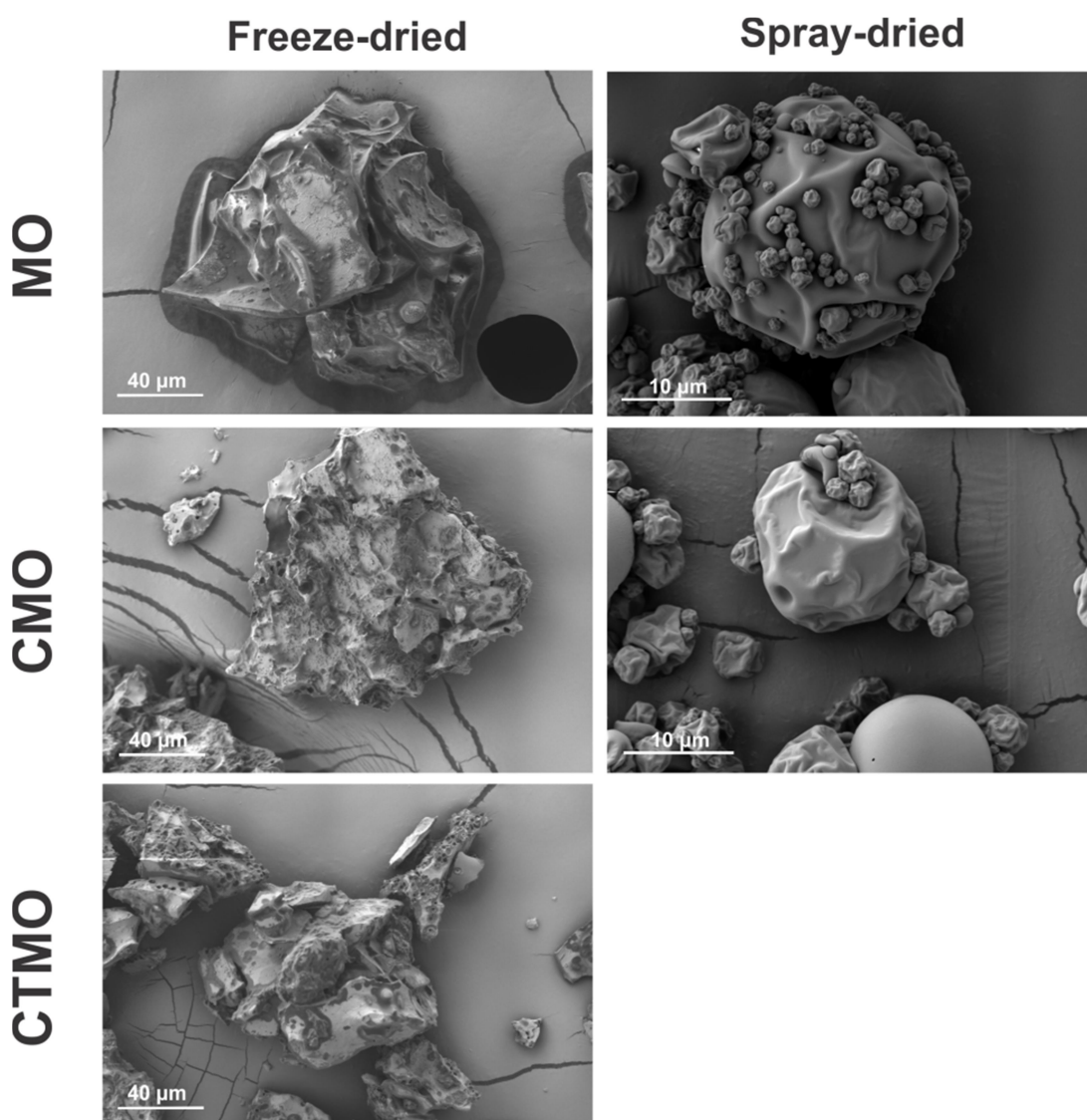

Figure 4.4.2 Field emission scanning electron microscopy for RCO microcapsules obtained by freeze-drying and spray-drying. CMO: self-aggregated chitosan and maltodextrin; CTMO: crosslinked chitosan and maltodextrin; MO: only maltodextrin.

Freeze-drying the RCO emulsions resulted in microparticles with irregular shape and higher particle size than spray-dried samples as previously observed in Figure 4.4.2. These microparticles seemed to be more porous than spray-dried as a consequence of sublimation of the water crystals that are formed between the oil droplets during freezing. In addition, the micrographs showed that these microparticles presented oil as an entrapped phase into the polymeric network.

The morphology of the microparticles obtained by SD or FD affects not only the encapsulation efficiency but also the capacity of the solid matrix for protecting the encapsulated compounds during storage as well as during the human gastrointestinal digestion (Ballesteros, Ramirez, Orrego, Teixeira, & Mussatto, 2017).

4.4.3.5 Total phenolic contents and antioxidant capacity of the microcapsules

RCO is considered a byproduct of the coffee processing industry that is rich in phenolic compounds and antioxidant properties (Ribeiro, Borreani, et al., 2020). The compounds responsible for the antioxidant activity in roasted coffee oil are approximately the same as the ones found in the oil from green coffee beans (Esquivel & Jiménez, 2012). In the group of phenolic compounds, it is pointed out the presence of chlorogenic acid, caffeic acid and tocopherols (Yen, Wang, Chang, & Duh, 2005). It is interesting to note that the chlorogenic acid-chitosan complex contributes for a synergistic antioxidant activity as opposed to the two isolated compounds (Rui et al., 2017). Accounting for the diterpenes, cafestol and kahweol are the main fraction analyzed (Oliveira, Cornelio-Santiago, Fukumasu, & Oliveira, 2018). Besides the creation of flavor and aroma, the roasting process leads to formation of melanoidins – which also contribute to an antioxidant-rich diet (Alves, Xavier, Limoeiro, & Perrone, 2020). The higher antioxidant activity of the lipophilic fraction of roasted coffee beans in comparison with the lipophilic fraction of green beans contributes to a stronger neuronal protection, as seen as the brain is a lipid-rich organ (Chu et al., 2009). Therefore, evaluation of total phenolic content and antioxidant activity as affected by the encapsulation mechanisms and drying method represents an important issue to attest the quality of microcapsules, and the results are presented in Table 4.4.4.

Table 4.4.4 Total phenolic content (TCP) and antioxidant activity by FRAP and DPPH method for freeze-dried and spray-dried samples.

Sample	TPC (meq GA/g of dry matter)	FRAP (µmol of Trolox/g of dry matter)	DPPH (µmol of Trolox/g of dry matter)
MO-FD	60.2 ± 0.2 [a]	11.83 ± 0.82 [a]	3.17 ± 0.03 [a]
CMO-FD	46.3 ± 0.2 [c]	5.08 ± 0.43 [c]	1.49 ± 0.06 [c]
CTMO-FD	50.4 ± 0.3 [b]	8.18 ± 0.97 [b]	1.94 ± 0.02 [b]
MO-SD	18.5 ± 0.2 [d]	3.19 ± 0.55 [d]	0.36 ± 0.01 [d]
CMO-SD	19.4 ± 0.2 [d]	3.43 ± 0.56 [d]	0.38 ± 0.06 [d]

CMO-FD = freeze-dried microcapsules of RCO with chitosan and maltodextrin. CTMO-FD = freeze-dried microcapsules of RCO with crosslinked chitosan and maltodextrin. MO-FD = freeze-dried microcapsules of RCO without chitosan. CMO-SD = spray-dried microcapsules of RCO with chitosan and maltodextrin. MO-SD = spray-dried microcapsules of RCO without chitosan. Data are expressed as means values ± standard deviation. Values with different letters within the same column are significantly different ($p < 0.05$) according to the LSD (Fisher) multiple range test.

Spray-dried samples showed the lowest contents of phenolic compounds and antioxidant properties by FRAP and DPPH methods in comparison with the freeze-dried ones. Even more, there were no significant differences in the total phenolic contents and antioxidant activity in samples formulated with or without self-aggregated chitosan. The lower TPC and antioxidant activity of spray-dried samples are probably related to specific formation of the spherical particles that protects the core and hinders its access during the extract preparation (Šturm et al., 2019).

Among the freeze-dried microparticles, the control samples formulated only with maltodextrin presented the highest TPC and antioxidant activity, followed by the ones produced with TPP-crosslinked chitosan and deprotonated chitosan. A possible explanation for this behavior is that the porous microstructure of FD samples allows a better radical scavenging by the antioxidant compounds entrapped into the matrix. As the microparticles encapsulated better the oil phase by the addition of chitosan nanoparticles, the total phenolic compounds in the corresponding ethanolic extract decreased. Although the increased permeability leads to higher TPC and antioxidant activity in the extract, this reflects a higher exposure of the encapsulated material and a lower stability is expected.

Comparing the CMO-FD and CMO-SD, which resulted close in oil retention and encapsulation efficiency, a higher TPC and antioxidant activity was observed in CMO-FD probably due to the low thermal degradation effects (Rezvankhah et al., 2020).

4.4.3.6 Bioaccessibility

The conditions at which bioactive compounds are more or less accessible provides important information about the protective action of the wall material and the drying method against the action of external agents. In the specific case of simulated gastrointestinal digestion, the higher the phenolic compounds and antioxidant activity in the complete digested phase in comparison with the raw material, the higher is the protection. Due to the carbohydrate-phenolic compounds interaction, lower phenolic compounds are quantified before digestion and this value tended to increase as the digestive enzymes break down these interactions during the simulated gastrointestinal tract (Altin, Gültekin-Özgüven, & Ozcelik, 2018). Moreover, higher presence of bioactive compounds in the IN fraction means that they are more available for intestinal absorption into the systematic circulation. Table 4.4.5 shows the bioaccessibility indexes for the studied samples. Spray-dried microcapsules formulated with self-aggregated chitosan gave rise to the highest bioaccessibility indexes for TPC and FRAP analysis. In addition to a better oil retention capacity, self-aggregated particles showed the best performance in protecting the oil as well as the TPC and antioxidant activity by FRAP method over the in vitro gastrointestinal digestion.

Self-aggregated chitosan also presented higher bioaccessibility in freeze-dried samples, even when comparing with TPP-crosslinked chitosan. In contrast to the crosslinked chitosan, self-aggregated nanoparticles can be reversely solubilized under acidic pH (Akbari-Alavijeh, Shaddel, & Jafari, 2020), which is found during the gastric step. This causes the wall material to partially solubilize and the material of interest is more easily released. Concerning the CTMO-FD samples, the release occurs mainly during the higher pH stages (intestinal phase), at which the ionization of chitosan are lower and the ionic interactions between chitosan and TPP are weakened (Shu & Zhu, 2000). In this condition, the matrix network becomes more flexible to allow the mass transfer.

Table 4.4.5 Bioaccessibility index (%) of the total phenolic content (TPC) and antioxidant activity for RCO microcapsules.

	Bioaccessibility index		
	TPC (%)	FRAP (%)	DPPH (%)
MO-FD	243.75 ± 17.73 [c]	132.50 ± 13.81 [c]	55.13 ± 1.37 [d]
CMO-FD	331.69 ± 1.25 [b]	846.54 ± 37.22 [b]	112.20 ± 4.19 [c]
CTMO-FD	205.05 ± 12.88 [c]	588.78 ± 81.52 [b]	83.66 ± 1.58 [cd]
MO-SD	100.56 ± 21.10 [d]	257.19 ± 63.10 [c]	584.85 ± 2.13 [a]
CMO-SD	548.77 ± 18.14 [a]	1698.91 ± 246.76 [a]	399.13 ± 45.23 [b]

CMO-FD = freeze-dried microcapsules of RCO with chitosan and maltodextrin. CTMO-FD = freeze-dried microcapsules of RCO with crosslinked chitosan and maltodextrin. MO-FD = freeze-dried microcapsules of RCO without chitosan. CMO-SD = spray-dried microcapsules of RCO with chitosan and maltodextrin. MO-SD = spray-dried microcapsules of RCO without chitosan. Data are expressed as means values ± standard deviation. Values with different letters within the same column are significantly different ($p < 0.05$) according to the LSD (Fisher) multiple range test.

In general, the bioaccessibility indexes for the different analysis were lower for freeze-dried samples than for spray-dried ones. From this observation, it can be assumed that the microcapsules produced by SD could act as an efficient barrier to promote a controlled release of bioactive compounds along the digestion. CMO-SD had even higher bioaccessibility because of the lower area/volume ratio from the more spherical and smaller particles obtained in spray-drying process.

On the other hand, freeze-drying was more efficient for preserving the lipids and the bioactive compounds of the raw material during drying as a consequence of the milder conditions of temperature applied (Velasco, Dobarganes, & Márquez-Ruiz, 2003). Thus, relatively lower values for bioaccessibilty indexes are expected for FD samples, reaching values lower than 100% for DPPH analysis in the samples with lower encapsulation efficiency (MO-FD and CTMO-FD).

4.4.4. Conclusions

Microcapsules containing roasted coffee oil were obtained after freeze-drying or spray-drying Pickering emulsions templates using self-aggregated and TPP-crosslinked chitosan nanoparticles. All of the samples presented adequate water activity, moisture content and solubility – being the self-aggregated chitosan-based

emulsions more hydrophobic followed by maltodextrin and crosslinked chitosan-based ones. Spray-drying produced spherical microcapsules with smaller particle size when compared to the freeze-dried microparticles, which showed irregular-shape. Spray-drying oil with maltodextrin yielded lower amounts of powdered RCO with lower oil retention, but the addition of self-aggregated chitosan improved the oil retention and maintained higher encapsulation efficiency (>88%). Encapsulation efficiency of freeze-dried samples also had slightly better scores when the matrix contained crosslinked or self-aggregated chitosan. No significant effects of the wall materials on the morphology of freeze-dried microparticles were observed. Results of total phenolic content and antioxidant activity of the microcapsules were in accordance to the encapsulation efficiency, where the higher was the protection the lower was the bioactive compounds concentration in the ethanolic extract. In addition, freeze-drying tended to preserve the bioactive compounds as a consequence of the low temperature applied. Bioaccessibility of the spray-dried samples formulated with self-aggregated chitosan was higher than the control due to the high oil retention and encapsulation efficiency. Freeze-dried samples had similar bioaccessibility indexes among each other, but the matrix of CMO-SD samples showed better protection of the bioactive compounds until simulated intestinal absorption.

4.4.5. Acknowledgments

4.4.6. References

Akbari-Alavijeh, S., Shaddel, R., & Jafari, S. M. (2020). Encapsulation of food bioactives and nutraceuticals by various chitosan-based nanocarriers. Food Hydrocolloids, 105, 105774.

Altin, G., Gültekin-Özgüven, M., & Ozcelik, B. (2018). Chitosan coated liposome dispersions loaded with cacao hull waste extract: Effect of spray drying on

physico-chemical stability and in vitro bioaccessibility. Journal of Food Engineering, 223, 91-98.

Alves, G., Xavier, P., Limoeiro, R., & Perrone, D. (2020). Contribution of melanoidins from heat-processed foods to the phenolic compound intake and antioxidant capacity of the Brazilian diet. Journal of food science and technology, 57 (8), 3119-3131.

Araiza-Calahorra, A., Akhtar, M., & Sarkar, A. (2018). Recent advances in emulsion-based delivery approaches for curcumin: From encapsulation to bioaccessibility. Trends in Food Science & Technology, 71, 155-169.

Baek, J., Wahid-Pedro, F., Kim, K., Kim, K., & Tam, K. C. (2019). Phosphorylated-CNC/modified-chitosan nanocomplexes for the stabilization of Pickering emulsions. Carbohydrate Polymers, 206, 520-527.

Ballesteros, L. F., Ramirez, M. J., Orrego, C. E., Teixeira, J. A., & Mussatto, S. I. (2017). Encapsulation of antioxidant phenolic compounds extracted from spent coffee grounds by freeze-drying and spray-drying using different coating materials. Food Chemistry, 237, 623-631.

Benzie, I. F. F., & Strain, J. J. (1996). The Ferric Reducing Ability of Plasma (FRAP) as a Measure of "Antioxidant Power": The FRAP Assay. Analytical Biochemistry, 239 (1), 70-76.

Brand-Williams, W., Cuvelier, M. E., & Berset, C. (1995). Use of a free radical method to evaluate antioxidant activity. LWT- Food science and Technology, 28 (1), 25-30.

Burgos-Díaz, C., Opazo-Navarrete, M., Soto-Añual, M., Leal-Calderón, F., & Bustamante, M. (2020). Food-grade Pickering emulsion as a novel astaxanthin encapsulation system for making powder-based products: Evaluation of astaxanthin stability during processing, storage, and its bioaccessibility. Food Research International, 134, 109244.

Cano-Chauca, M., Stringheta, P. C., Ramos, A. M., & Cal-Vidal, J. (2005). Effect of the carriers on the microstructure of mango powder obtained by spray drying and its functional characterization. Innovative Food Science & Emerging Technologies, 6 (4), 420-428.

Carlan, I. C., Estevinho, B. N., & Rocha, F. (2017). Study of microencapsulation and controlled release of modified chitosan microparticles containing vitamin B12. Powder Technology, 318, 162-169.

Chevalier, Y., & Bolzinger, M.-A. (2013). Emulsions stabilized with solid nanoparticles: Pickering emulsions. Colloids and Surfaces A: Physicochemical and Engineering Aspects, 439, 23-34.

Chu, Y.-F., Brown, P. H., Lyle, B. J., Chen, Y., Black, R. M., Williams, C. E., Lin, Y.-C., Hsu, C.-W., & Cheng, I. H. (2009). Roasted Coffees High in Lipophilic Antioxidants and Chlorogenic Acid Lactones Are More Neuroprotective than Green Coffees. Journal of Agricultural and Food Chemistry, 57 (20), 9801-9808.

Costa, A. L. R., Gomes, A., & Cunha, R. L. (2018). One-step ultrasound producing O/W emulsions stabilized by chitosan particles. Food Research International, 107, 717-725.

Eriksen, J. N., Luu, A. Y., Dragsted, L. O., & Arrigoni, E. (2017). Adaption of an in vitro digestion method to screen carotenoid liberation and in vitro accessibility from differently processed spinach preparations. Food Chemistry, 224, 407-413.

Esmaeili, A., & Asgari, A. (2015). In vitro release and biological activities of Carum copticum essential oil (CEO) loaded chitosan nanoparticles. International Journal of Biological Macromolecules, 81, 283-290.

Esquivel, P., & Jiménez, V. M. (2012). Functional properties of coffee and coffee by-products. Food Research International, 46 (2), 488-495.

Ezhilarasi, P. N., Indrani, D., Jena, B. S., & Anandharamakrishnan, C. (2013). Freeze drying technique for microencapsulation of Garcinia fruit extract and its effect on bread quality. Journal of Food Engineering, 117 (4), 513-520.

Fang, S., Zhao, X., Liu, Y., Liang, X., & Yang, Y. (2019). Fabricating multilayer emulsions by using OSA starch and chitosan suitable for spray drying: Application in the encapsulation of β-carotene. Food Hydrocolloids, 93, 102-110.

Freiberger, E. B., Kaufmann, K. C., Bona, E., Araújo, P. H. H., Sayer, C., Leimann, F. V., & Gonçalves, O. H. (2015). Encapsulation of roasted coffee oil in biocompatible nanoparticles. LWT - Food Science and Technology, 64 (1), 381-389.

Gharsallaoui, A., Roudaut, G., Chambin, O., Voilley, A., & Saurel, R. (2007). Applications of spray-drying in microencapsulation of food ingredients: An overview. Food Research International, 40 (9), 1107-1121.

Gómez-Mascaraque, L. G., Perez-Masiá, R., González-Barrio, R., Periago, M. J., & López-Rubio, A. (2017). Potential of microencapsulation through emulsion-

electrospraying to improve the bioaccesibility of β-carotene. Food Hydrocolloids, 73, 1-12.

González, A., Martínez, M. L., Paredes, A. J., León, A. E., & Ribotta, P. D. (2016). Study of the preparation process and variation of wall components in chia (Salvia hispanica L.) oil microencapsulation. Powder Technology, 301, 868-875.

Ho, K. W., Ooi, C. W., Mwangi, W. W., Leong, W. F., Tey, B. T., & Chan, E.-S. (2016). Comparison of self-aggregated chitosan particles prepared with and without ultrasonication pretreatment as Pickering emulsifier. Food Hydrocolloids, 52, 827-837.

Hosseini, S. F., Zandi, M., Rezaei, M., & Farahmandghavi, F. (2013). Two-step method for encapsulation of oregano essential oil in chitosan nanoparticles: Preparation, characterization and in vitro release study. Carbohydrate Polymers, 95 (1), 50-56.

Hurtado-Benavides, A., Dorado A, D., & Sánchez-Camargo, A. d. P. (2016). Study of the fatty acid profile and the aroma composition of oil obtained from roasted Colombian coffee beans by supercritical fluid extraction. The Journal of Supercritical Fluids, 113, 44-52.

Jara-Palacios, M. J., Gonçalves, S., Hernanz, D., Heredia, F. J., & Romano, A. (2018). Effects of in vitro gastrointestinal digestion on phenolic compounds and antioxidant activity of different white winemaking byproducts extracts. Food Research International, 109, 433-439.

Karthik, P., & Anandharamakrishnan, C. (2013). Microencapsulation of Docosahexaenoic Acid by Spray-Freeze-Drying Method and Comparison of its Stability with Spray-Drying and Freeze-Drying Methods. Food and Bioprocess Technology, 6 (10), 2780-2790.

Klinkesorn, U., Sophanodora, P., Chinachoti, P., Decker, E. A., & McClements, D. J. (2006). Characterization of spray-dried tuna oil emulsified in two-layered interfacial membranes prepared using electrostatic layer-by-layer deposition. Food Research International, 39 (4), 449-457.

Kumar, L. R. G., Chatterjee, N. S., Tejpal, C. S., Vishnu, K. V., Anas, K. K., Asha, K. K., Anandan, R., & Mathew, S. (2017). Evaluation of chitosan as a wall material for microencapsulation of squalene by spray drying: Characterization and oxidative stability studies. International Journal of Biological Macromolecules, 104, 1986-1995.

Li, Y., Wu, C., Wu, T., Wang, L., Chen, S., Ding, T., & Hu, Y. (2018). Preparation and characterization of citrus essential oils loaded in chitosan microcapsules by using different emulsifiers. Journal of Food Engineering, 217, 108-114.

Minekus, M., Alminger, M., Alvito, P., Ballance, S., Bohn, T., Bourlieu, C., Carrière, F., Boutrou, R., Corredig, M., Dupont, D., Dufour, C., Egger, L., Golding, M., Karakaya, S., Kirkhus, B., Le Feunteun, S., Lesmes, U., Macierzanka, A., Mackie, A., Marze, S., McClements, D. J., Ménard, O., Recio, I., Santos, C. N., Singh, R. P., Vegarud, G. E., Wickham, M. S. J., Weitschies, W., & Brodkorb, A. (2014). A standardised static in vitro digestion method suitable for food – an international consensus. Food & Function, 5 (6), 1113-1124.

Mwangi, W. W., Ho, K.-W., Ooi, C.-W., Tey, B.-T., & Chan, E.-S. (2016). Facile method for forming ionically cross-linked chitosan microcapsules from Pickering emulsion templates. Food Hydrocolloids, 55, 26-33.

Oliveira, N. A., Cornelio-Santiago, H. P., Fukumasu, H., & Oliveira, A. L. (2018). Green coffee extracts rich in diterpenes – Process optimization of pressurized liquid extraction using ethanol as solvent. Journal of Food Engineering, 224, 148-155.

Rahman, M. S., & Labuza, T. P. (2007). Water activity and food preservation. In M. S. Rahman (Ed.), Handbook of food preservation (2 ed., pp. 465-494). Boca Raton: CRC Press.

Rezvankhah, A., Emam-Djomeh, Z., & Askari, G. (2020). Encapsulation and delivery of bioactive compounds using spray and freeze-drying techniques: A review. Drying Technology, 38 (1-2), 235-258.

Ribeiro, E. F., Barros-Alexandrino, T. T., Assis, O. B. G., Cruz-Jr., A., Quiles, A., Hernando, I., & Nicoletti, V. R. (2020). Chitosan and crosslinked chitosan nanoparticles: synthesis, characterization and their role as Pickering emulsifiers. Carbohydrate Polymers.

Ribeiro, E. F., Borreani, J., Moraga, G., Nicoletti, V. R., Quiles, A., & Hernando, I. (2020). Digestibility and Bioaccessibility of Pickering Emulsions of Roasted Coffee Oil Stabilized by Chitosan and Chitosan-Sodium Tripolyphosphate Nanoparticles. Food Biophysics, 15 (2), 196-205.

Rui, L., Xie, M., Hu, B., Zhou, L., Saeeduddin, M., & Zeng, X. (2017). Enhanced solubility and antioxidant activity of chlorogenic acid-chitosan conjugates due to

the conjugation of chitosan with chlorogenic acid. Carbohydrate Polymers, 170, 206-216.

Schulz, M., Biluca, F. C., Gonzaga, L. V., Borges, G. S. C., Vitali, L., Micke, G. A., de Gois, J. S., de Almeida, T. S., Borges, D. L. G., Miller, P. R. M., Costa, A. C. O., & Fett, R. (2017). Bioaccessibility of bioactive compounds and antioxidant potential of juçara fruits (Euterpe edulis Martius) subjected to in vitro gastrointestinal digestion. Food Chemistry, 228, 447-454.

Shah, B. R., Li, Y., Jin, W., An, Y., He, L., Li, Z., Xu, W., & Li, B. (2016). Preparation and optimization of Pickering emulsion stabilized by chitosan-tripolyphosphate nanoparticles for curcumin encapsulation. Food Hydrocolloids, 52, 369-377.

Shu, X. Z., & Zhu, K. J. (2000). A novel approach to prepare tripolyphosphate/chitosan complex beads for controlled release drug delivery. International Journal of Pharmaceutics, 201 (1), 51-58.

Silva, V. M., Vieira, G. S., & Hubinger, M. D. (2014). Influence of different combinations of wall materials and homogenisation pressure on the microencapsulation of green coffee oil by spray drying. Food Research International, 61, 132-143.

Singleton, V. L., & Rossi, J. A. (1965). Colorimetry of Total Phenolics with Phosphomolybdic-Phosphotungstic Acid Reagents. American Journal of Enology and Viticulture, 16 (3), 144-158.

Šturm, L., Črnivec, I. G. O., Istenič, K., Ota, A., Megušar, P., Slukan, A., Humar, M., Levic, S., Nedović, V., Kopinč, R., Deželak, M., Gonzales, A. P., & Ulrih, N. P. (2019). Encapsulation of non-dewaxed propolis by freeze-drying and spray-drying using gum Arabic, maltodextrin and inulin as coating materials. Food and Bioproducts Processing, 116, 196-211.

Velasco, J., Dobarganes, C., & Márquez-Ruiz, G. (2003). Variables affecting lipid oxidation in dried microencapsulated oils. Grasas y Aceites, 54 (3), 304-314.

Vishnu, K. V., Chatterjee, N. S., Ajeeshkumar, K. K., Lekshmi, R. G. K., Tejpal, C. S., Mathew, S., & Ravishankar, C. N. (2017). Microencapsulation of sardine oil: Application of vanillic acid grafted chitosan as a bio-functional wall material. Carbohydrate Polymers, 174, 540-548.

Yan, H., Chen, X., Song, H., Li, J., Feng, Y., Shi, Z., Wang, X., & Lin, Q. (2017). Synthesis of bacterial cellulose and bacterial cellulose nanocrystals for their

applications in the stabilization of olive oil pickering emulsion. Food Hydrocolloids, 72, 127-135.

Yen, W.-J., Wang, B.-S., Chang, L.-W., & Duh, P.-D. (2005). Antioxidant Properties of Roasted Coffee Residues. Journal of Agricultural and Food Chemistry, 53 (7), 2658-2663.

4.5. CHAPTER 5

Oxidative stability and volatile compounds of microcapsules

Storage stability of dried chitosan-based Pickering emulsion containing roasted coffee oil

Elisa Franco Ribeiro [a,b*], Tiago Carregari Polachini [c], Adilson Roberto Locali Pereira [a], Amparo Quiles [b], Isabel Hernando [b], Vânia Regina Nicoletti [a]

[a] **São Paulo State University (Unesp), Institute of Bioscience, Humanities and Exact Sciences (Ibilce),** Campus São José do Rio Preto, SP, 15054-000, Brazil

[b] **Food Microstructure and Chemistry Research Group, Universitat Politècnica de València (UPV),** 46022, Valencia, Spain

[c] **ONIRIS-GEPEA UMR CNRS,** 6144 Nantes, France

*Corresponding author: elisa.franco@unesp.br

Abstract: Drying Pickering o/w emulsions has been considered a promising strategy to produce oil microcapsules, as long as their quality parameters may be preserved over storage. Thus, freeze- and spray-dried chitosan-based Pickering emulsions of roasted coffee oil were evaluated over 30-day storage at 25 ºC together with the non-encapsulated oil as a control. Water sorption isotherms were determined, whereas color, oxidative stability (peroxide value and conjugated dienes) and volatile compounds were assessed over the storage period. Type II isotherms and Guggenheim–Anderson–Boer (GAB) model parameters showed that water binding was impaired by the surface oil in freeze-dried samples. Oxidation was maintained under acceptable values over the storage for all samples, with slightly higher protection also for volatiles compounds in the spray-dried particles. The powdered emulsions were able to suitably preserve the oil quality over 30 days of storage, enabling its commercialization and application as a food ingredient.

4.5.1. Introduction

Roasted coffee oil (RCO) is a byproduct with high aggregate value that is obtained from the coffee processing industry (Reddy et al., 2019). It can be used as an interesting ingredient in replacement of saturated fats, as well as to incorporate bioactive compounds and antioxidant properties in food products (Ogrodowska et al., 2017). Furthermore, RCO is rich in volatile compounds that are formed during the roasting process of coffee beans (Oliveira et al., 2005). This lipid fraction is responsible to confer interesting flavor to different food products as chocolates, baked goods, dairy products, and beverages such as the own coffee brew (Frascareli et al., 2012). Because of the several health and flavor promoting characteristics attributed to RCO, methods have been developed to encapsulate this byproduct as a manner to improve its stability and to facilitate its application. One main technique is the oil emulsification, which may be accomplished by the aid of natural solid particles instead of surfactants. The principle of the so-called Pickering method is to adsorb solid particles onto the oil droplet to reduce the water/oil interfacial tension. This is carried out not only to avoid droplet coalescence – by the high energy for detachment needed – but also to protect the oil against degrading external agents (Atarian et al., 2019).

Many polysaccharides and/or proteins have been successfully employed to produce Pickering stabilizing particles: soy protein, whey protein, nanocellulose, nanocrystals, starch, and others (Yang et al., 2017). Among these various solid particles, chitosan modification has been explored in order to confer suitable emulsifying properties for the controlled release of bioactive compounds (Garg et al., 2019). The interest in using chitosan is attributed to its biocompatibility, biodegradability, non-toxicity and antioxidant properties, besides being a cleaner alternative to current surfactants (Rizeq et al., 2019). In fact, previous studies demonstrated the ability of both self-aggregate and trypolyphosphate (TPP)-crosslinked chitosan to encapsulate RCO by the Pickering emulsification route (Ribeiro et al., 2020a; Ribeiro et al., 2020b). Nevertheless, the high volume of liquid emulsions hinders their use as a delivery medium for the material of interest. In addition, their high water content has a direct effect in the long-term stability of the oil and its constituents.

Drying is a simple and effective method to reduce the water content of food products. Spray-drying is an easy and simple water removal method in which the product is aspersed in contact with a hot airflow and the dried products are collected in powdered form. On the other hand, freeze-drying is based on water sublimation under vacuum at low temperature, thus following a direct transition from the solid to the vapor phase. In spite of being more complex and slower than spray-drying, the use of low temperatures in freeze-drying prevents degradation of thermo-sensitive compounds. Regardless the technique, drying o/w Pickering emulsions is a novel procedure that might improve oil encapsulation and thus enhance the product quality. Ribeiro et al. (2021) investigated the effects of the type of chitosan modification and drying method on the quality parameters of Pickering emulsions containing RCO. Although both self-aggregated and crosslinked chitosan showed good results, higher oil retention and encapsulation efficiency were obtained for microcapsules formulated with self-aggregated chitosan.

The microencapsulation process should focus on generating final products with efficiency and quality. In addition, it is important that these quality attributes remain less affected as possible over storage. One of the major factors affecting food preservation is the state of water (Fernandes et al., 2014), a reason by which studying sorption isotherms are encouraged. Furthermore, in lipid-rich foods as microencapsulated oils, parameters such as lipid oxidation and color changes are indicative of deterioration (Rodriguez et al., 2019). Such parameters can be affected not only by the wall material used but also by the drying method (Ogrodowska et al., 2017). In the specific case of RCO, the knowledge about how the volatile composition changes over storage may reflect the potential application and shelf life of the encapsulated oil.

This work focused on the storage stability of spray-dried and freeze-dried chitosan-based Pickering emulsions containing RCO. Sorption isotherms were experimentally determined and modeled for samples produced by the different drying methods. Lipid oxidation and volatile compounds were assessed over 30 days of storage under controlled relative humidity.

4.5.2. Materials and Methods

4.5.2.1 Microencapsulation of roasted coffee oil

4.5.2.1.1 Synthesis of chitosan nanoparticles

Chitosan nanoparticles were synthetized by self-aggregation to formulate the Pickering emulsions. Low molecular weight chitosan (deacetylation degree of 77%, Sigma-Aldrich) was dissolved into 1% (w/w) glacial acetic acid (Dinâmica, Brazil) solution. The solution was kept under magnetic stirring at room temperature for 24 h until complete dissolution. Chitosan nanoparticles (CN) were obtained by deprotonating the amino groups of the D-glucosamine units, which was performed by increasing the solution pH from 3.5 up to 6.7 with NaOH 6M (Dinâmica, Brazil). A final dispersion with 0.9% (w/w) of CN was obtained for further application.

4.5.2.1.2 Preparation of Pickering emulsions

Roasted coffee oil, kindly supplied by Companhia Iguaçu de Café Solúvel (Cornélio Procópio, Brazil), was used to formulate emulsions with 10% (w/w) of lipid phase. RCO was dripped into the CN dispersion under homogenization (Ultra-Turrax T25, IKA, Germany) at 12,000 rpm. After the total amount of oil was added to the dispersion, the samples were maintained under homogenization for 5 min more.

4.5.2.1.3 Microencapsulation by spray- and freeze-drying

Microcapsules containing RCO were produced using the previously prepared emulsions. Maltodextrin DE 10 (Dinâmica, Brazil) was added to the emulsions at the ratio of 1:5 [solids in the emulsion]:[maltodextrin]. Maltodextrin was dispersed into the emulsion using an Ultra-turrax stirrer (T25 model, IKA, Germany) at 12,000 rpm for 5 minutes. For comparison purpose, a control system was elaborated by homogenizing RCO and maltodextrin under the same conditions but without CNs in the aqueous phase.

Samples were dried in triplicate using a spray dryer (B-290 model, Büchi, Switzerland). A peristaltic pump was responsible for driving the emulsion to the double-fluid spray nozzle with 0.7 mm of orifice diameter. After fixing the minimum inlet air temperature at which the emulsions could be dried (160 °C), the feed flow rate was established at 2 mL•min^{-1}, atomization air rate at 742 L.h^{-1} and aspiration at

35 $m^3.h^{-1}$. Drying yield (%) was determined as the ratio between the mass of microcapsules and the mass of solids in the emulsion before drying.

For freeze-drying, the emulsions were initially frozen at –40° C in an ultra-freezer for 24 h, followed by drying in a freeze-dryer (model L-101, Liotop, Brazil) for 48 h at an approximated pressure of 200 µmHg. After freeze-drying, samples were finely grinded using the mortar and stored into metallized bags in a desiccator at room temperature.

The microcapsules were conditioned in metallized bags and, then, placed inside desiccators at room temperature.

4.5.2.2 Storage conditions

Freeze-dried and spray-dried microcapsules were stored in opened plastic containers at 25 °C and 54.4% of relative humidity for 30 days. Roasted coffee oil was used as a control. Samples were taken at different time intervals (0, 2, 4, 6, 10, 20 and 30 days) and the oxidation process was monitored via analysis of color, peroxide value, conjugated dienes and volatile composition.

4.5.2.3 Water sorption isotherms

Water sorption behavior was evaluated by the static gravimetric method. Samples were maintained under different relative humidities and periodically weighted until constant weight (<5% of weight variation) – characterizing the moisture content at the equilibrium. In order to reach a wide range of relative humidites (a_w×100), saturated salt solutions of LiCl, $MgCl_2$, K_2CO_3, $Mg(NO_3)_2$, NaCl, $(NH_4)_2SO_4$ and $BaCl_2$ were placed into glass desiccators, reaching a range of water activity from 0.113 up to 0.902 at 25 ºC (Labuza, 1963). Approximately 0.3 g of each sample of microcapsules were placed into small recipients inside desiccators accommodated in a controlled BOD-type temperature chamber (MA415, Marconi, Piracicaba, Brazil) previously set at 25 ºC. The samples were weighted every week using an analytical balance (AUW220D, Shimadzu, Japan). The initial moisture content of the samples was determined in vacuum oven at 70 ºC (AOAC, 2010). After ~3 weeks, the equilibrium moisture content could be determined by the weight difference. Analyses were carried out in triplicate.

Sorption isotherms were obtained by plotting each equilibrium moisture content (X_{eq}, g of water per g of dried matter) against the corresponding water activity

(*a_w*). The Guggenheim–Anderson–de Boer (GAB) model (Equation 1), which is reported to accurately fit sorption isotherms of food products in wide range of water activity (Bastıoğlu et al., 2017), was used to model the experimental data.

$$X_{eq} = \frac{X_m C k a_w}{(1 - k a_w)(1 + (C - 1) k a_w)}$$

(1)

in which X_m, C and k are parameters of the model. The fitting accuracy was evaluated by the adjusted determination coefficient (R^2_{adj}) and by the root mean square error (*RMSE*) (Polachini et al., 2021).

4.5.2.4 Color parameters

The color parameters of the microcapsules were analyzed in a colorimeter CM-5 (Konica Minolta, New Jersey, USA) measuring the coordinates: *L* (brightness) on a 0-100 scale from black to white, *a* (red-green), *b* (yellow-bluish), as well as the total color change (*ΔE*), given by Equation (2):

$$\Delta E = \sqrt{(L - L_0)^2 + (a - a_0)^2 + (b - b_0)^2}$$

(2)

in which the subscript "0" corresponds to the sample before storage (time 0 days).

4.5.2.5 Peroxide value

The oil was extracted according to the method described by Partanen et al. (2008) with some modifications. Briefly, 0.5 g of microcapsules were mixed with 5 mL of acetic acid solution (1%, v/v) in a test tube and the extract was shaken for 1 min on a vortex mixer to disrupt the microcapsules. The phases were separated after adding 1.5 mL of iso-octane/isopropanol solution (2:1) to 400 μL of extract, vortexed for 1 min and then, centrifuged at 1000×g for 4 min. The non-encapsulated oil sample was decoloured according to Anese et al. (2000) in order to avoid the absorbance interference of coloured compounds The peroxide value was determined spectrophotometrically according to IDF standard method 74A:1991 (International Dairy Federation, 1991). The supernatant (0.4 mL) or a droplet of oil (0.1-0.3 g) in the

case of control was added to 9.6 mL of chloroform/methanol solution (7:3, v/v). Then, 50 µL of 3.9 mol/L potassium thiocyanate and 50 µL of 0.072 mol/L Fe^{2+} were added. The mixture was vortexed and reacted in the dark for 5 min. The chloroform/methanol solution was used as a blank and the absorbance was measured at 510 nm using an Multiskan Go Spectrophotometer (Thermo Fisher Scientific, Vantaa, Finland). The concentration of hydroperoxides was determined using a Fe^{3+} standard curve, as described by Frascareli et al. (2012).

4.5.2.6 Conjugated dienes

For measurement of conjugated dienes the oil was extracted from the microcapsules following the method described by Satué-Garcia et al. (2000) with modifications. A powder sample of 1.0 g was mixed with 10 mL of acetic acid solution (1%, v/v) and the extract was vortexed for 1 min. Hexane (7 mL) was used for separating the organic phase through centrifugation at 10.000 rpm for 20 min and the supernatant was evaporated under nitrogen flow. The recovered oil was suspended with 2-propanol in order to obtain measurable absorbance at 234 nm (Drusch et al. 2006). The results obtained spectrophotometrically were expressed as millimoles of hydroperoxides per kilogram of oil using a molar coefficient of 26,000 for methyl linoleate hydroperoxides (Chan & Levett, 1977).

4.5.2.7 Volatile compounds

The content of volatiles compounds of crude and microencapsulated RCO was determined by using Headspace Solid Phase Microextraction-Gas Chromatography-Mass Spectrometry/Flame Ionization Detector (HS-SPME-GC-MS/FID) (Lee et al 2017). Samples were taken from storage at 10-day time intervals to be analysed. The extraction of volatile compounds was carried out in 10 mL vials (hermetically sealed) containing 300 µL of RCO or 2 g of microcapsules, based on oil retention values previously determined. The samples were heated at 70 ºC for 20 min and then SPME fiber (DVB/CarboxenTM/PDMS) was inserted into the headspace for 30 min. After that, the fiber was placed in the GC-FID injection system for 5 min and volatile compounds were desorbed at 250 ºC under splitless mode into Rtx-Wax column (30 m x 0.25 mm x 0.25 µm) using nitrogen as carrier gas at flow rate of 1.2 mL/min. The separation and detection of compounds was performed on a gas chromatograph equipped with flame ionization detector (CF-2014, Shimadzu Scientific Corporation,

Japan) according to the following oven temperature program: 40 ºC for 5 min; heating to 60 ºC at 4 ºC/min; 60 ºC for 5 min; then heating to 250 ºC at 8 ºC/min and 250 ºC for 3 min. The same chromatographic parameters described for GC-FID were used in GC-MS (GC–MS QP2010 SE, Shimadzu, Japan) for identification of volatile compounds. For this, a fused silica capillary column SH-Rtx-Wax (30 m × 0.25 mm × 0.25 μm) was used with helium as carrier gas at a constant flow rate of 1 mL/min. Volatile compounds were identified with Wiley database, linear retention indices derived using C7-C30 alkane standards diluted in hexan (2:1) (Sigma-Aldrich) and semi-quantified with GC-FID peak areas. The linear retention indices were also compared with indices of relative retention reported by the database NIST/2002 Library (National Institute of Standards and Technology, 2002).

4.5.2.8 Statistical analysis

Means of the experimental measurements were subjected to the analysis of variance (ANOVA) and the presence of significant differences was evaluated by the Tukey test at 95% of confidence.

4.5.3 Results and discussion

4.5.3.1 Water sorption isotherms

The equilibrium moisture content (X_{eq}) of spray-dried (SD) and freeze-dried (FD) samples was determined in triplicate for the range of water activity studied. Spray-dried microcapsules showed X_{eq} varying from 0.0187 to 0.2717 g of water·g^{-1} of dry matter, whereas freeze-dried samples had slightly higher X_{eq}, varying from 0.0312 and 0.3061 g of water·g^{-1} of dry matter. The X_{eq} values increased with increasing water activity as it was expected.

Sorption isotherms showed sigmoidal shape (Figure 4.5.1) typical of type II isotherms according to the Brunauer classification (Brunauer et al., 1940). The first zone of low water activity corresponds to the region where water molecules are strongly bound to the matrix, while the latter, of high a_w, is related to free water molecules (Polachini et al., 2016). The intermediate zone of almost constant X_{eq} was barely noticed for both samples. This is probably a consequence of the constituting maltodextrin, which has a trend to confer a type III isotherm (with linear increase in X_{eq} up to a critical a_w) when incorporated in dried products (Bastıoğlu et al., 2017),

but also to the hydrophobicity degree of self-aggregated chitosan (Ribeiro et al., 2020a).

In addition to the mathematical estimation of the sorption behavior, the parameters of GAB model provide important information about the microstructure and water-matrix interactions. Thus, GAB model was fitted to the experimental data and R_{adj}^2 >0.99 and *RMSE*<0.01 was observed (Table 4.5.1). These results give insights about the model accuracy and the reliability of the fitting parameters shown in Table 4.5.1. A requirement of 0.24 < *k* < 1 and 5.4 < *C* < ∞ is reported in literature for GAB parameters to confirm type II isotherms (Lewicki, 1997) – which, in fact, were satisfied in the present study.
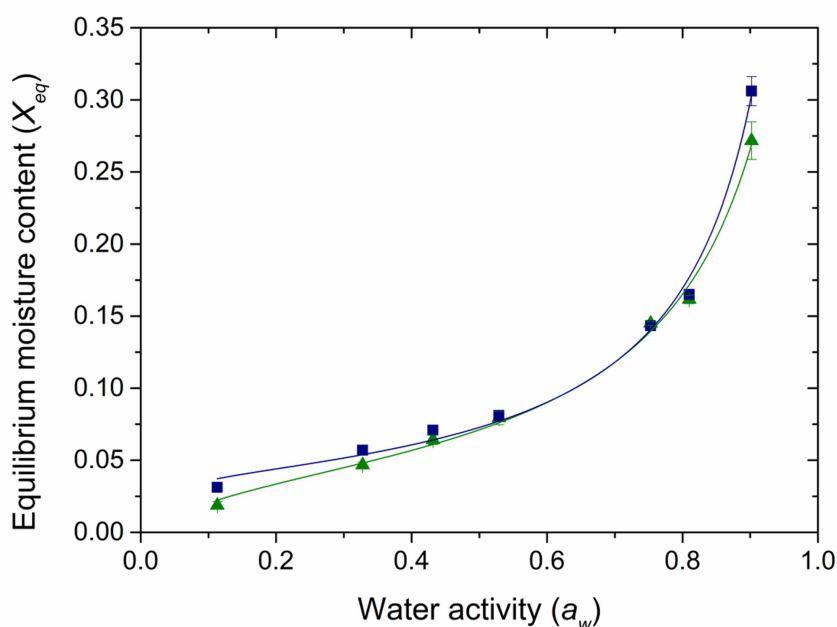
Figure 4.5.1 Water sorption isotherms at 25 ºC for spray-dried (▲,━━) and freeze-dried (■, ━━) samples. Lines represent the fitted GAB model.

The parameter X_m represents the monolayer moisture content, i.e. the moisture content needed to cover the first layer of water molecules bound to the food matrix. Above this value, multilayer water molecules with less strong interactions with the sorbent than the monolayer are found (Quirijns et al., 2005). In these conditions, water molecules are more available for reactions. Monolayer moisture (X_m) has a close agreement with the hydrogen bonding degree (Polachini et al., 2016), which means that freeze-dried samples, presenting smaller X_m values, have less active

sites for water sorption, probably due to the higher particle size with lower surface area (Koc et al., 2020) and to the overlapping of active sites by the higher amounts of surface oil – parameters evaluated in a previous study for the same samples (Ribeiro et al., 2021). On the other hand, Figure 4.5.1 showed slightly higher X_{eq} for freeze-dried than spray-dried samples, mainly at low (< 0.25) and high (> 0.85) water activities. This may be a result of the capacity for entrapping water into the porous structure of freeze-dried samples, although this moisture is not strongly bound to the active site. In summary, spray-dried microcapsules bound water molecules in a stronger way, whereas freeze-dried samples seems to have cavities that are able to entrap water molecules, impairing water removal by steric issues.

Table 4.5.1. Fitting parameters of the GAB model to the sorption isotherms.

Parameters	Samples	
	Spray-dried	Freeze-dried
X_m (g water/g dry matter)	0.044 ± 0.003 [a]	0.038 ± 0.001 [b]
C	7.04 ± 1.08 [b]	29.82 ± 4.34 [a]
k	0.931 ± 0.019 [b]	0.969 ± 0.009 [a]
R^2_{adj}	> 0.991	> 0.990
RMSE	< 0.0064	< 0.0072

Means and standard deviation followed by the same letter in the same line represent no significant difference among the samples by the Tukey test at 95% of confidence.

4.5.3.2 Color parameters

The color of the microcapsules was evaluated over the 30 days of storage at 25 ºC. As expected, color parameters (Table 4.5.2) showed that oil had brown darkened coloration with low brightness, *a* and *b* values. These results are strongly related to the presence of compounds formed from Maillard reaction during roasting of the beans (Anese et al., 2002). On the other hand, both SD and FD samples showed to be brighter than oil tending to yellowish coloration as a consequence of the encapsulant material incorporation. SD samples were slightly brighter and less yellowish than FD samples, probably due to the higher oil retention in the latter (Ribeiro et al., 2021).

Total color variation (ΔE) was used to evaluate possible changes in the coloration of the samples during storage. According to Wibowo et al. (2015), ΔE between 0 – 0.5 is considered to be unnoticeable, between 0.5 – 1.5 slightly noticeable, between 1.5 – 3.0 noticeable, between 3.0 – 6.0 visible, and higher than 6.0 it is greatly visible. Thus, it can be stated that the majority of the changes in the coloration of microcapsules were slightly noticeable. Some slightly variations could be seen in RCO, probably due to homogenization of the samples during measurement.

Table 4.5.2. Color parameters of roasted coffee oil (RCO) and spray- and freeze-dried microcapsules over 30 days of storage at 25 ºC.

Samples	Days	Color parameters			
		a	*b*	*L*	*ΔE*
RCO	0	0.02 ± <0.01 [e]	0.11 ± 0.09 [d]	0.09 ± <0.01 [d]	-
	2	0.44 ± 0.01 [de]	0.13 ± 0.08 [cd]	0.16 ± 0.04 [cd]	0.45 ± <0.01 [d]
	4	1.66 ± 0.46 [bcd]	0.42 ± 0.09 [bcd]	0.40 ± 0.10 [bc]	1.71 ± 0.44 [bcd]
	6	1.56 ± 0.71 [cd]	0.38 ± 0.21 [bcd]	0.38 ± 0.21 [bc]	1.61 ± 0.77 [cd]
	10	4.21 ± 0.38 [a/a]	1.15 ± 0.09 [a]	0.85 ± 0.09 [a]	4.39 ± 0.35 [a]
	20	2.60 ± 0.61 [bc]	0.65 ± 0.13 [bc]	0.58 ± 0.12 [ab]	2.69 ±0.63 [bc]
	30	2.87 ± 1.07 [ab]	0.72 ± 0.39 [ab]	0.57 ± 0.18 [ab]	2.97 ± 1.12 [b]
Spray-dried	0	0.94 ± 0.05 [c]	12.43 ± 0.40 [ab]	86.54 ± 0.31 [ab]	-
	2	0.89 ± 0.04 [c]	11.63 ± 0.08 [c]	85.45 ± 0.05 [c]	1.35 ± 0.03 [a]
	4	0.87 ± 0.01 [bc]	11.71 ± 0.03 [c]	85.52 ± 0.04 [c]	1.25 ± 0.05 [ab]
	6	0.95 ± 0.02 [bc]	12.35 ± 0.16 [b]	86.78 ± 0.08 [a]	0.29 ± 0.02 [d]
	10	0.99 ± 0.01 [b]	12.36 ± 0.13 [b]	86.63 ± 0.07 [ab]	0.17 ± 0.04 [d]
	20	1.15 ± 0.02 [a]	12.91 ± 0.06 [a]	86.32 ± 0.16 [b]	0.59 ± 0.12 [c]
	30	1.17 ± 0.02 [a]	12.65 ± 0.23 [ab]	85.49 ± 0.13 [c]	1.11 ± 0.09 b
Freeze-dried	0	2.9 ± 0.01 [b]	21.63 ± 0.04 [a]	77.19 ± 0.04 [ab]	-
	2	2.75 ± 0.08 [c]	20.51 ± 0.52 [c]	76.84 ± 0.29 [c]	1.18 ± 0.58 [b]
	4	2.90 ± 0.01 [b]	21.28 ± 0.04 [ab]	77.02 ± 0.07 [bc]	0.39 ± 0.06 [c]
	6	2.93 ± 0.01 [b]	21.03 ± 0.13 [abc]	76.69 ± 0.04 [cd]	0.78 ± 0.10 [bc]
	10	2.95 ± 0.04 [b]	20.88 ± 0.10 [bc]	76.91 ± 0.08 [bc]	0.81 ± 0.12 [bc]
	20	2.86 ± 0.01 [b]	19.25 ± 0.02 [d]	77.49 ± 0.05 [a]	2.40 ± 0.02 [a]
	30	3.19 ± 0.01 [a]	20.81 ± 0.01 [bc]	76.38 ± 0.09 [d]	1.19 ± 0.07 [b]

Means and standard deviation followed by the same letter in the same column represent no significant difference among the days for a same sample by the Tukey test at 95% of confidence.

In general, RCO tended to become slightly brighter over the storage days, which can be attributed to be more related to sedimentation of unsaponificable matter than to oxidation itself (see Sections 4.5.3.3 and 4.5.3.4). Regarding the dried samples, FD samples were darker than SD probably due to the higher amount of surface oil (Ribeiro et al., 2021). Both powders became slightly darker over the storage, which can be related to the moisture gain during the equilibration with the controlled relative humidity.

4.5.3.3 Peroxide value

The formation of hydroperoxides as primary compounds of lipid degradation products was determined as an indicative of the product quality and its safety. As the hydroperoxides are degraded, compounds such as aldehydes, ketones and hydrocarbons are released and technological properties of the oil starts to be affected (Menin et al., 2018). Thus, the peroxide value of the non-encapsulated and encapsulated roasted coffee oil was determined over the 30 days of storage at 25 ºC. Means and standard deviations are shown in Figure 4.5.2 for all of the samples.

At the beginning of the storage experiments, the non-encapsulated oil showed slightly lower peroxide (~1.5 meq/kg of oil) value when compared to the encapsulated oil by both drying methods (~2.4 meq/kg of oil). These differences can be attributed to the air incorporation into the oil during emulsification and drying, being in accordance to literature for other lipid sources (Ferreira et al., 2016; Hoyos-Leyva et al., 2019).

Up to 10 days of storage, the samples showed approximately similar peroxide value. After that, the oil from SD microcapsules showed slightly lower peroxide values when compared to the non-encapsulated oil, although this difference was not significant due to the heterogeneity of the samples. The possible trend of SD samples for decreasing oil peroxide values can be attributed to the reduction of hydroperoxide precursors and secondary degradation compounds, which may occur by the steric and chitosan wall thickness hindrance against pro-oxidant penetration into the microcapsules (Chang et al., 2018). On the other hand, the oil in the FD microparticles presented peroxide value higher (~4.5 meq/kg of oil) than the non-encapsulated oil (~3.4 meq/kg of oil) and the oil in SD microcapsules (~2.4 meq/kg of oil). Because FD microparticles had much higher particle size than SD microcapsules (Ribeiro et al., 2021), the bed porosity of FD microparticles tend to be higher than for

SD microcapsules. In addition to the higher amounts of external oil observed in FD sample and its more porous structure (Ribeiro et al., 2021), the higher bed porosity might have allowed oxygen to diffuse more easily in FD samples, consequently causing the slightly higher lipid oxidation than in SD samples. In fact, the bed porosity plays an important role during storage of microcapsules due to the increased oil accessibility from the microcapsules (Drusch & Schwarz, 2006). Moreover, according to the sorption isotherms (see Section 4.5.3.1), water molecules are more freely available in FD samples than in SD ones, which might had an important role in accelerating the oxidation reactions.

In which concerns the non-encapsulated oil, the oxidation occurred only onto the surface of the samples and the oxygen was not able to penetrate the samples – bringing the peroxide content per kg of oil to lower levels. Moreover, the roasting process leads to the formation of colored Maillard reaction compounds as melanoidins with antioxidant properties. These compounds act against oxidation and explain the low oxidation rate of the lipid fraction of roasted coffee beans (Anese et al., 2002).
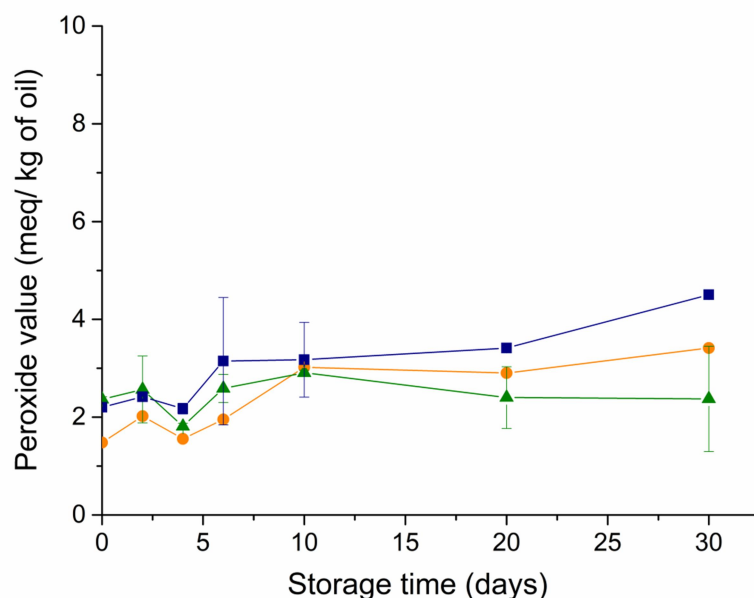

Figure 4.5.2 Peroxide value (meq/kg of oil) for spray-dried (——), freeze-dried (——) and non-encapsulated RCO (——) over 30 days of storage at 25 ºC.

In spite of the observed differences, all of the samples showed acceptable peroxide value with less than 15 meq/kg of oil – within the safety range

recommended by the *Codex Alimentarius* for cold-pressed oils. The way by how lipid oxidation proceeds in each sample should be carefully evaluated over longer periods in order to observe if this trend remains similar over time.

4.5.3.4 Conjugated dienes

The content of conjugated dienes in the samples was evaluated as a manner of measuring the rearrangement of the hydroperoxide double bonds during lipid oxidation. Results are shown in Figure 4.5.3 for all samples over the 30 days of storage. The obtained data over storage time were in accordance to the peroxide value determinations, confirming the analyses dependence (Talón et al., 2019). At day 0, samples had similar concentration of conjugated dienes of 1.2 mmol/kg of oil. Nevertheless, the oil in FD samples was slightly more affected by lipid oxidation than non-encapsulated oil and the oil in SD samples.
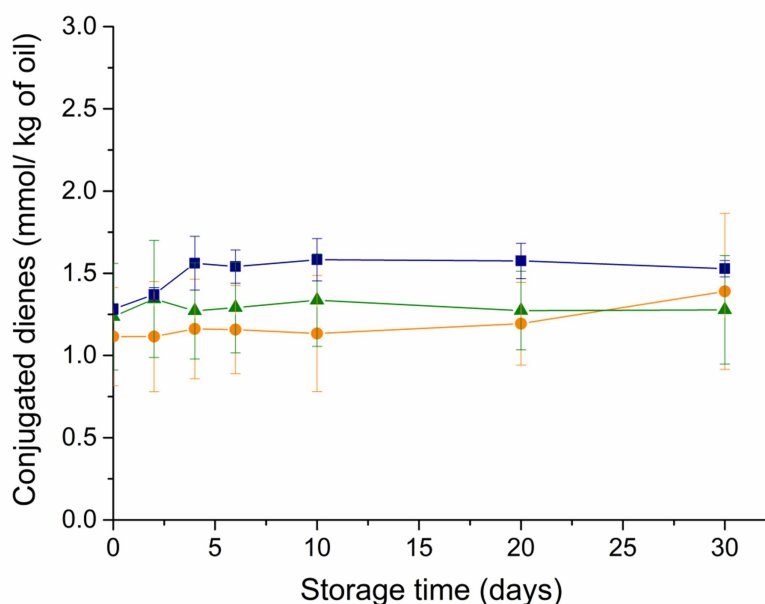
Figure 4.5.3. Conjugated dienes for spray-dried (—), freeze-dried (—) and non-encapsulated RCO (—) over 30 days of storage at 25 ºC.

It is important to highlight that at the day 30, non-encapsulated oil started to show a trend to increase up to the values of FD samples. This can be an indicative of the lower protection of non-encapsulated oil under longer storage periods, mainly after 30 days. Analogously, the presence of chitosan nanoparticles as wall material seemed to present a protective effect that scavenge free radicals and interrupt lipid oxidation under long term storage (Ding et al., 2019). Although there was a subtle

distinction among the samples, conjugated dienes did not exceed 1.6 mmol/kg of oil for the whole period analyzed. These values were lower than the ones found for different oils subjected to oxidative stress (Kenari et al., 2020; Moser et al., 2020; Talón et al., 2019), which can be attributed to the colored compounds from Maillard reaction formed during roasting process. Together with the results of peroxide value, lipid oxidation during 30 days may not be a restriction for application of the microcapsules in food products.

4.5.3.5 Volatile compounds

Changes in the content of volatile compounds during storage were observed using the SPME sampling method applied to microcapsules and non-encapsulated RCO. The 27 major compounds detected in the headspace and their respective GC-FID peak areas are shown in Table 4.5.3. Aroma description was reported based on the literature.

In addition to protecting RCO against lipid oxidation it is important that the microcapsules contain the desired compounds that compose roasted coffee aroma. SD and FD microcapsules presented similar values for total content of volatile compounds at the end of storage. Higher impact of storing could be observed for non-encapsulated oil which presented a decrese of about 50% in total volatile content (Figure 4.5.4).
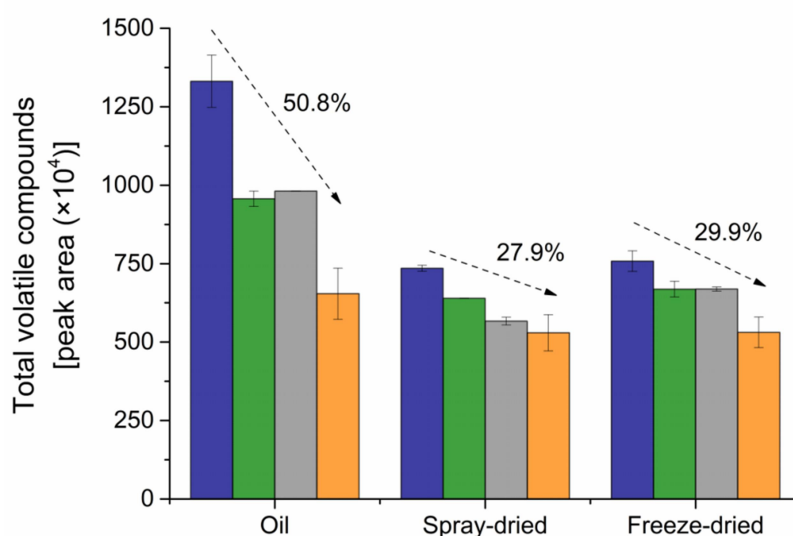

Figure 4.5.4 The effects of drying methods for encapsulation of RCO on the peaks areas of total volatile compounds detected in the samples under storage. Analysis were carried out at day 0 (blue), day 10 (green), day 20 (gray) and day 30 (orange).

1 **Table 4.5.3.** Volatile aroma compounds of non-encapsulated roasted coffee oil (RCO) and microcapsules of RCO produced by spray-
2 drying (SD) and freeze-drying (FD)

Volatile compounds	Linear retention index (LRI)		GC-FID peak area (x10^4)												Aroma description
			t = 0			t = 10			t = 20			t = 30			
	Rtx-Wax	Literature	Coffee oil	SD	FD	Coffee oil	SD	FD	Coffee oil	SD	FD	Coffee oil	SD	FD	
Pyridine	-	1194[2]	13,4 ± 4,8[a]	1,1 ± 0,3[b]	0,3 ± 0,1[c]	18,3 ± 1,8[a]	0,5 ± 0,1[c]	0,8 ± 0,1[b]	7,2 ± 0,2[a]	1,4 ± 0,3[b]	1,3 ± 0,2[b]	7,4 ± 0,2[a]	0,8 ± 0,2[b]	0,6 ± 0,0[b]	Roasted[3]
Pyrazine															
Pyrazine	-		4,5 ± 0,5[a]	0,5 ± 0,4[c]	2,4 ± 1,4[b]	1,9 ± 0,8[a]	0,4 ± 0,1[b]	0,5 ± 0,2[b]	1,5 ± 0,4[a]	0,4 ± 0,0[b]	0,3 ± 0,1[b]	0,5 ± 0,1[a]	0,1 ± 0,1[b]	0,2 ± 0,0[b]	Rancid peanuts[3]
2,5- Dimethylpyrazine	1314	1329[2]	15,4 ± 1,2[a]	2,8 ± 0,9[b]	1,4 ± 0,4[b]	17,0 ± 0,9[a]	1,2 ± 0,3[b]	0,6 ± 0,1[c]	7,8 ± 3,7[a]	1,5 ± 0,3[b]	2,3 ± 1,7[b]	10,2 ± 1,3[a]	1,9 ± 0,3[b]	3,6 ± 2,5[b]	Nuts[3]
2,6- dimethylpyrazine	1337	1335[2]	0,1 ± 0,1[b]	0,5 ± 0,2[a]	0,7 ± 0,1[a]	0,0 ± 0,0[b]	0,1 ± 0,0[a]	0,0 ± 0,0[b]	0,0 ± 0,0[c]	0,1 ± 0,0[b]	0,3 ± 0,0[a]	0,0 ± 0,0[a]	0,0 ± 0,0[a]	0,0 ± 0,0[a]	Roasted[3]
2-Ethyl-5-Methylpyrazine	1432	1428[2]	2,6 ± 0,1	4,8 ± 0,1	16,1 ± 1,2	1,0 ± 0,7[c]	4,2 ± 0,8[a]	2,7 ± 0,2[b]	2,6 ± 2,0[a]	0,1 ± 0,1[b]	1,4 ± 1,2[ab]	0,1 ± 0,0[b]	4,6 ± 0,1[a]	0,1 ± 0,1[b]	Nuts, peanut[2]
Aldehyde															
Pyrrole-2-carboxaldehyde	2040	2017[2]	9,8 ± 0,6[a]	6,2 ± 0,6[b]	5,6 ± 0,4[b]	9,0 ± 0,2[a]	5,8 ± 0,6[b]	5,0 ± 0,4[b]	10,5 ± 0,4[a]	5,3 ± 0,3[b]	6,3 ± 0,8[b]	8,1 ± 1,6[a]	5,6 ± 0,4[b]	4,1 ± 0,1[c]	Roasted, smoky[2]
Nonanal	1397	-	1,2 ± 0,1[a]	0,3 ± 0,0[c]	0,8 ± 0,2[b]	3,2 ± 0,2[a]	0,6 ± 0,0[b]	0,5 ± 0,0[b]	0,6 ± 0,0[b]	0,4 ±0,0[c]	0,8 ± 0,1[a]	0,0 ± 0,0[b]	0,2 ± 0,1[a]	0,0 ± 0,0[b]	-
Furans															
2- Furancarboxaldehyde	1467	1465[2]	1,6 ± 0,1[a]	1,8 ± 0,1[a]	1,6 ± 0,0[a]	1,2 ± 0,1[a]	0,8 ± 0,0[b]	0,4 ± 0,0[c]	0,8 ± 0,0[b]	4,3 ± 0,3[a]	3,9 ± 1,8[a]	2,4 ± 0,1[a]	0,9 ± 0,1[b]	0,7 ± 0,1[b]	Caramellic, cinnamon, almond[2]
Furfural; 2-Furaldehyde	1484	1485[1]	4,8 ± 2,1[a]	0,0 ± 0,0[c]	0,2 ± 0,0[b]	13,4 ± 0,9[a]	0,2 ± 0,1[b]	0,2 ± 0,0[b]	1,8 ± 0,5[a]	0,4 ± 0,0[b]	0,5 ± 0,1[b]	0,0 ± 0,0[b]	0,2 ± 0,2[a]	0,1 ± 0,1[a]	Caramellic, woody[1]
2-Furanmethanol Acetate	1538	1539[2]	0,2 ± 0,0[b]	0,3 ± 0,1[b]	1,4 ± 0,3[a]	0,2 ± 0,0[b]	0,4 ± 0,1[a]	0,4 ± 0,1[a]	1,0 ± 0,2[a]	0,1 ± 0,0[c]	0,2 ± 0,0[b]	0,2 ± 0,0[b]	0,8 ± 0,3[a]	0,0 ± 0,0[b]	Roasted nut, floral[2]
3-Furanmethanol	1677	1673[2]	2,8 ± 0,1[a]	2,6 ± 0,4[a]	3,2 ± 0,3[a]	1,8 ± 0,0[c]	2,0 ± 0,0[b]	2,3 ± 0,0[a]	1,8 ± 0,0[a]	1,6 ± 0,1[b]	1,3 ± 0,7[ab]	1,6 ± 0,1[b]	1,7 ± 0,0[b]	1,9 ± 0,1[a]	Carmellic[3]
Ketones															
4-Cyclopentene-1,3-dione	1574	-	64,5 ± 2,8[a]	40,8 ± 2,7[b]	44,1 ± 4,0[b]	19,6 ± 0,6[a]	14,0 ± 0,6[b]	19,3 ± 1,5[a]	24,7 ± 2,1[a]	10,2 ± 3,3[c]	19,8 ± 2,1[b]	5,0 ± 0,6[c]	7,2 ± 0,3[b]	13,6 ± 1,3[a]	-
1,2-Cyclopentanedione	1748	-	123,9 ± 5,3[c]	196,0 ± 13,9[b]	226,5 ± 6,7[a]	67,6 ± 1,8[c]	172,2 ± 4,8[b]	207,0 ± 8,5[a]	59,7 ± 2,4[c]	159,3 ± 0,3[b]	210,2 ± 15,4[a]	48,9 ± 8,8[b]	112 ± 39,7[a]	116,8 ± 29,3[a]	-
2-hydroxy-3-methyl-2-cyclopenten-1-one	1855	1857[1]	5,0 ± 0,2[a]	4,1 ± 0,9[b]	5,0 ± 1,1[a]	4,2 ± 0,1[a]	3,4 ± 0,3[b]	2,9 ± 0,1[b]	4,2 ± 0,1[a]	2,4 ± 0,2[b]	3,1 ± 0,1[a]	2,7 ± 0,3[a]	2,6 ± 0,0[a]	2,8 ± 0,1[a]	Caramellic[1]
3-Ethyl-2-hydroxy-2-cyclopenten-1-one	1920	1909[1]	646,3 ± 50,0[a]	152,4 ± 14,6[b]	139,7 ± 3,2[b]	422,0 ± 7,5[a]	144,7 ± 7,5[b]	130,5 ± 3,8[c]	411,8 ± 2,0[a]	92,9 ± 5,5[c]	124,5 ± 1,7[b]	207,2 ± 25,5[a]	119,0 ± 4,4[b]	103,3 ± 14,5[b]	Caramellic, smoky[1]
Maltol; 3-Hydroxy-2-Methyl-4-Pyrone	1965	1955[2]	13,4 ± 0,9[b]	16,3 ± 1,4[a]	16,6 ± 2,9[a]	12,1 ± 0,2[c]	16,5 ± 1,3[a]	14,1 ± 0,6[b]	15,2 ± 0,4[c]	17,5 ± 0,8[b]	20,1 ± 0,3[a]	11,3 ± 1,5[b]	17,4 ± 0,4[a]	16,8 ± 0,1[a]	Caramel

Compound	RI	RI[ref]	1	2	3	4	5	6	7	8	9	10	11	12	Descriptor
2-Pentadecanone	2143	-	33,5 ± 1,7a	32,9 ± 5,8a	24,7 ± 2,2b	25,2 ± 0,5c	39,8 ± 3,2a	32,3 ± 0,8b	40,0 ± 1,0a	37,4 ± 0,9b	33,3 ± 4,9ab	35,0 ± 6,2ab	39,1 ± 2,6a	34,2 ± 0,6b	Waxy[2]
Acids															
3-Methyl-2-butenoic acid	1772	1777[2]	33,4 ± 0,2a	22,1 ± 0,9b	24,8 ± 3,8b	16,4 ± 0,6b	21,8 ± 0,1a	21,1 ± 1,9a	23,3 ± 1,1b	33,4 ± 1,9a	31,4 ± 1,1a	13,4 ± 1,5b	23,3 ± 0,1a	23,3 ± 1,4a	Dairy, fermented[3]
Caproic acid	1844	-	88,6 ± 3,5b	102,4 ± 3,5a	95,1 ± 11,5ab	69,6 ± 2,2b	83,5 ± 4,0a	78,0 ± 1,7a	61,8 ± 0,6b	58,2 ± 2,8c	63,8 ± 0,6a	37,7 ± 4,9b	66,9 ± 0,4a	67,7 ± 1,2a	-
Acetic acid	1451	1458[1]	4,3 ± 0,2	4,7 ± 0,5	5,6 ± 0,5	0,8 ± 0,1a	0,2 ± 0,0b	0,2 ± 0,0b	1,2 ± 0,0b	7,8 ± 0,1a	6,6 ± 4,5a	0,6 ± 0,1c	5,1 ± 3,6a	1,9 ± 0,2b	Acidic, pungent[1]
Butanoic acid	1630	1632[1]	29,3 ± 1,1a	22,8 ± 0,7b	25,1 ± 1,6b	16,5 ± 0,3a	13,6 ± 0,1c	15,5 ± 0,2b	15,9 ± 0,1a	8,7 ± 0,8c	14,8 ± 0,2b	6,5 ± 0,7c	9,4 ± 0,2b	13,1 ± 0,8a	Sharp, buttery[1]
Benzoic acid	2443	2443[2]	23,9 ± 4,7a	4,3 ± 0,4b	4,9 ± 0,8b	23,1 ± 0,2a	3,7 ± 0,2c	7,1 ± 0,5b	27,0 ± 0,4a	4,2 ± 0,0b	5,0 ± 0,9b	25,6 ± 3,5a	3,1 ± 0,1c	5,7 ± 0,7b	-
Linoleic acid	2511	-	156,9 ± 10,9a	79,4 ± 7,0b	79,7 ± 5,3b	171,7 ± 4,6a	84,6 ± 1,3	104,6 ± 13,6b	200,6 ± 4,2a	85,2 ± 1,0b	83,5 ± 2,3b	180,6 ± 16,3a	72,2 ± 5,7c	88,1 ± 2,0b	-
Palmitic acid	2900	-	0,9 ± 0,1a	0,4 ± 0,0b	0,4 ± 0,0b	3,0 ± 0,2a	0,3 ± 0,0c	0,9 ± 0,0b	2,4 ± 0,0a	0,3 ± 0,0b	0,4 ± 0,0b	1,8 ± 0,0a	1,9 ± 0,1a	0,7 ± 0,1b	-
Phenolics															
4-ethyl-2-methoxy-phenol	2048	2044[2]	20,7 ± 0,7a	17,3 ± 1,2b	15,3 ± 0,6c	8,3 ± 0,4a	6,7 ± 0,9b	5,3 ± 0,7c	22,3 ± 0,3a	15,9 ± 0,8b	16,9 ± 0,7b	17,2 ± 3,0a	15,5 ± 0,6a	15,6 ± 0,0a	Spicy; smoky[1]
4-Methoxyphenol	2098	2099[2]	17,1 ± 0,3a	10,3 ± 0,7b	8,8 ± 0,4c	16,1 ± 0,5a	9,4 ± 0,7b	8,3 ± 0,8c	19,4 ± 0,1a	9,1 ± 0,3b	9,4 ± 0,0b	15,8 ± 3,1a	9,7 ± 0,6b	8,8 ± 0,2b	-
2-Methoxy-4-vinylphenol	2215	2219[2]	12,6 ± 1,0a	7,8 ± 1,0b	7,7 ± 0,0b	13,2 ± 0,3a	8,8 ± 0,8b	8,2 ± 0,2b	15,5 ± 0,3a	8,4 ± 0,1b	7,6 ± 0,1c	14,3 ± 2,9a	8,6 ± 0,8b	7,3 ± 0,0b	Sipcy, peanut[2]
Total			1330,6 ± 83,4a	735,2 ± 9,8b	757,8 ± 32,8b	956,0 ± 24,3a	639,5 ± 0,6c	668,6 ± 25,1b	980,8 ± 0,1a	566,8 ± 12,5c	669,0 ± 6,7b	654,1 ± 81,4a	529,7 ± 57,6c	530,9 ± 48,7b	

Lee et al. (2017)[1]; Hurtato-Benavides et al. (2016)[2]; Cincotta et al (2020)[3]. Data expressed as mean ± standard deviation. Different letters in the same period and in the same line indicate significant difference (p < 0.05).

Despite most of the volatile compounds present in RCO have been identified to contribute to coffee flavor, ketones, pyrazines, aldehydes and furans showed the highest impact on the aroma of samples in the present study. Figure 4.5.5 shows the behavior of each group along 4 weeks of storage.
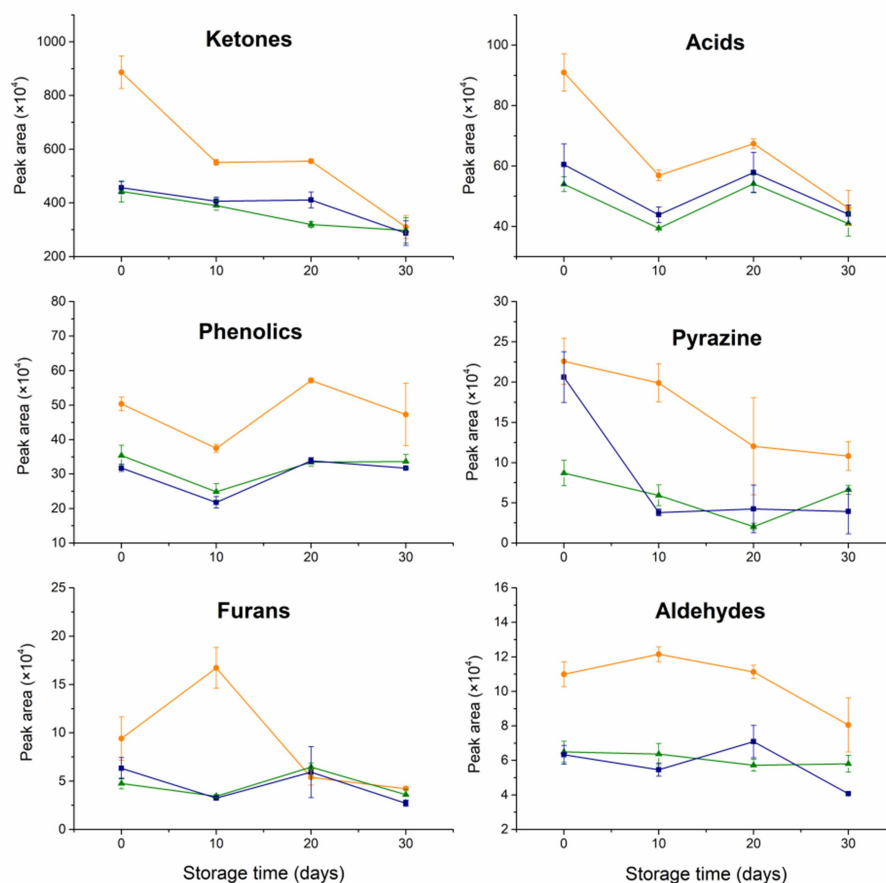

Figure 4.5.5 The effects of storage on spray-dried (—), freeze-dried (—) and non-encapsulated RCO (—) on the peak areas of specific compounds.

According to reported by Hurtado-Benavides et al. (2016), Lee et al. (2017) and Akiyama et al. (2005), ketones and pyrazines are the main and more potent odorants of coffee due to caramelic and nutty flavor. In the current study ketones corresponded to approximately 60% of total compounds present in the samples, with no significant difference between microcapsules, and the main aromatic compound responsible to the coffee flavor could be attributed to 3-ethyl-2-hydroxy-2-cyclopenten-1-one. There was a reduction of 19% in this important group throughout the storage of non-encapsulated RCO. On the other hand, both SD and FD microcapsules showed a protective effect since more than 90% of total ketones were

maintained during storage. As aforementioned for lipid oxidation, factors as porosity and heterogeneity of encapsulant matrix also contribute to diffusion of core material. Although higher content of compounds was found in the non-encapsulated oil, chitosan nanoparticles demonstrated high efficacy on retention of volatiles compounds, since the loss of compounds during storage was lower for microcapsules than for the oil, considering the content initially present in each sample. The effect of encapsulating methods for protecting volatile compounds of RCO is in close agreement with the oxidation parameters analyzed. Freeze-drying also showed accelerate oxidation of fish oil when compared to spray-drying as reported by Anwar et al. (2011), since the particle morphology obtained by that method enables the oxygen diffusivity. In summary, spray-drying and freeze-drying were considered important drying techniques to be utilized for preserving the volatile content of RCO and prevent lipid oxidation throughout 30 days of storage.

4.5.4. Conclusions

Pickering emulsion templates of roasted coffee oil were produced using self-aggregated chitosan nanoparticles by freeze-drying and spray-drying techniques. Storage stability of the non-encapsulated oil and the resulting powders was performed over 30 days at 25 ºC under controlled relative humidity. Sorption isotherms of type II showed a better capacity for binding water molecules in spray-dried samples than in freeze-dried ones. The GAB model fitted well the experimental data, and the monolayer moisture content showed lower sorption sites in freeze-dried particles. Roasted coffee oil showed a strong dark color and, as a consequence of the carrier agents, the powdered samples had a yellowish coloration. In spite of slight differences in color parameters over the storage, the color variation compared to the day 0 was not visible. Because freeze-dried particles were bigger than spray-dried ones, with higher content of surface oil and with lower water binding properties, oxidation was slightly favored. However, peroxide value and conjugated dienes were maintained under acceptable values over the 30 days of storage for all of the samples and the volatile compounds were preserved in the microcapsules.

4.5.5. Acknowledgments

4.5.6. References

Anese, M., De Pilli, T., Massini, R., Lerici, C.R. 2002. Oxidative stability of the lipid fraction in roasted coffee. Italian Journal of Food Science, 12(4), 457-462.

Akiyama, M., Murukami, K., Ikeda, M., Iwatsuki, K., Kokubo, S., Wada, A., Tokuno, K., Onishi, M., Iwabuchi and Tanaka, K. 2005. Characterization of Flavor Compounds Released During Grinding of Roasted Robusta Coffee Beans. Food Science Technology Research, 11(3), 298-307.

AOAC. 2010. Official Methods of Analysis International. Association of Official Analytical Chemists, Washington D. C.

Atarian, M., Rajaei, A., Tabatabaei, M., Mohsenifar, A., Bodaghi, H. 2019. Formulation of Pickering sunflower oil-in-water emulsion stabilized by chitosan-stearic acid nanogel and studying its oxidative stability. Carbohydrate Polymers, 210, 47-55.

Bastıoğlu, A.Z., Koç, M., Ertekin, F.K. 2017. Moisture sorption isotherm of microencapsulated extra virgin olive oil by spray drying. Journal of Food Measurement and Characterization, 11(3), 1295-1305.

Brunauer, S., Deming, L.S., Deming, W.E., Teller, E. 1940. On a Theory of the van der Waals Adsorption of Gases. Journal of the American Chemical Society, 62(7), 1723-1732.

Chan, H.W.-S., Levett, G. 1977. Autoxidation of methyl linoleate. Separation and analysis of isomeric mixtures of methyl linoleate hydroperoxides and methyl hydroxylinoleates. Lipids, 12(1), 99-104.

Chang, H.W., Tan, T.B., Tan, P.Y., Abas, F., Lai, O.M., Wang, Y., Wang, Y., Nehdi, I.A., Tan, C.P. 2018. Microencapsulation of fish oil using thiol-modified β-lactoglobulin fibrils/chitosan complex: A study on the storage stability and in vitro release. Food Hydrocolloids, 80, 186-194.

Ding, J., Xu, Z., Qi, B., Cui, S., Wang, T., Jiang, L., Zhang, Y., Sui, X. 2019. Fabrication and characterization of soybean oil bodies encapsulated in maltodextrin and chitosan-EGCG conjugates: An in vitro digestibility study. Food Hydrocolloids, 94, 519-527.

Drusch, S., Schwarz, K. 2006. Microencapsulation properties of two different types of n-octenylsuccinate-derivatised starch. European Food Research and Technology, 222(1), 155-164.

Fernandes, R.V.B., Borges, S.V., Botrel, D.A. 2014. Gum arabic/starch/maltodextrin/inulin as wall materials on the microencapsulation of rosemary essential oil. Carbohydrate Polymers, 101, 524-532.

Ferreira, C.D., Conceição, E.J.L., Machado, B.A.S., Hermes, V.S., Rios, A.O., Druzian, J.I., Nunes, I.L. 2016. Physicochemical Characterization and Oxidative Stability of Microencapsulated Crude Palm Oil by Spray Drying. Food and Bioprocess Technology, 9(1), 124-136.

Frascareli, E.C., Silva, V.M., Tonon, R.V., Hubinger, M.D. 2012. Effect of process conditions on the microencapsulation of coffee oil by spray drying. Food and Bioproducts Processing, 90(3), 413-424.

Garg, U., Chauhan, S., Nagaich, U., Jain, N. 2019. Current Advances in Chitosan Nanoparticles Based Drug Delivery and Targeting. Advanced pharmaceutical bulletin, 9(2), 195-204.

Hoyos-Leyva, J.D., Bello-Perez, L.A., Agama-Acevedo, J.E., Alvarez-Ramirez, J., Jaramillo-Echeverry, L.M. 2019. Characterization of spray drying microencapsulation of almond oil into taro starch spherical aggregates. LWT, 101, 526-533.

Kenari, R.E., Amiri, Z.R., Motamedzadegan, A., Milani, J.M., Farmani, J., Farahmandfar, R. 2020. Optimization of Iranian golpar (Heracleum persicum) extract encapsulation using sage (Salvia macrosiphon) seed gum: chitosan as a wall materials and its effect on the shelf life of soybean oil during storage. Journal of Food Measurement and Characterization, 14(5), 2828-2839.

Koc, B., Isleroglu, H., Turker, I. 2020. Sorption behavior and storage stability of microencapsulated transglutaminase by ultrasonic spray–freeze–drying. Drying Technology, 1-15.

Labuza, T. 1963. Creation of moisture sorption isotherms for hygroscopic materials. Sorption isotherm methods. in: International Symposium on Humidity and Moisture.

Lewicki, P.P. 1997. The applicability of the GAB model to food water sorption isotherms. International Journal of Food Science & Technology, 32(6), 553-557.

Menin, A., Zanoni, F., Vakarelova, M., Chignola, R., Donà, G., Rizzi, C., Mainente, F., Zoccatelli, G. 2018. Effects of microencapsulation by ionic gelation on the oxidative stability of flaxseed oil. Food Chemistry, 269, 293-299.

Moser, P., Nicoletti, V.R., Drusch, S., Brückner-Gühmann, M. 2020. Functional properties of chickpea protein-pectin interfacial complex in buriti oil emulsions and spray dried microcapsules. Food Hydrocolloids, 107, 105929.

Ogrodowska, D., Tańska, M., Brandt, W. 2017. The Influence of Drying Process Conditions on the Physical Properties, Bioactive Compounds and Stability of Encapsulated Pumpkin Seed Oil. Food and Bioprocess Technology, 10(7), 1265-1280.

Oliveira, A.L., Cruz, P.M., Eberlin, M.N., Cabral, F.A. 2005. Brazilian roasted coffee oil obtained by mechanical expelling: compositional analysis by GC-MS. Food Science and Technology, 25, 677-682.

Partanen, R., Raula, J., Seppänen, R., Buchert, J., Kauppinen, E., Forssell, P. 2008. Effect of Relative Humidity on Oxidation of Flaxseed Oil in Spray Dried Whey Protein Emulsions. Journal of Agricultural and Food Chemistry, 56(14), 5717-5722.

Polachini, T.C., Betiol, L.F.L., Lopes-Filho, J.F., Telis-Romero, J. 2016. Water adsorption isotherms and thermodynamic properties of cassava bagasse. Thermochimica Acta, 632, 79-85.

Polachini, T.C., Hernando, I., Mulet, A., Telis-Romero, J., Cárcel, J.A. 2021. Ultrasound-assisted acid hydrolysis of cassava (Manihot esculenta) bagasse: Kinetics, acoustic field and structural effects. Ultrasonics Sonochemistry, 70, 105318.

Quirijns, E.J., Van Boxtel, A.J.B., Van Loon, W.K.P., Van Straten, G. 2005. Sorption isotherms, GAB parameters and isosteric heat of sorption. Journal of the Science of Food and Agriculture, 85(11), 1805-1814.

Reddy, M.N.P., Ishwarya, S.P., Anandharamakrishnan, C. 2019. Nanoencapsulation of roasted coffee bean oil in whey protein wall system through nanospray drying. Journal of Food Processing and Preservation, 43(3), e13893.

Ribeiro, E.F., Barros-Alexandrino, T.T., Assis, O.B.G., Cruz-Jr., A., Quiles, A., Hernando, I., Nicoletti, V.R. 2020a. Chitosan and crosslinked chitosan nanoparticles: synthesis, characterization and their role as Pickering emulsifiers. Carbohydrate Polymers.

Ribeiro, E.F., Borreani, J., Moraga, G., Nicoletti, V.R., Quiles, A., Hernando, I. 2020b. Digestibility and Bioaccessibility of Pickering Emulsions of Roasted Coffee Oil Stabilized by Chitosan and Chitosan-Sodium Tripolyphosphate Nanoparticles. Food Biophysics, 15(2), 196-205.

Ribeiro, E.F., Polachini, T.C., Alvim, I.D., Quiles, A., Hernando, I., Nicoletti, V.R. 2021. Dried chitosan-based Pickering emulsions: effect of wall material and drying method. Food Research International.

Rizeq, B.R., Younes, N.N., Rasool, K., Nasrallah, G.K. 2019. Synthesis, Bioapplications, and Toxicity Evaluation of Chitosan-Based Nanoparticles. . International Journal of Molecular Sciences, , 20(22), 5776.

Rodriguez, E.S., Julio, L.M., Henning, C., Diehl, B.W.K., Tomás, M.C., Ixtaina, V.Y. 2019. Effect of natural antioxidants on the physicochemical properties and stability of freeze-dried microencapsulated chia seed oil. Journal of the Science of Food and Agriculture, 99(4), 1682-1690.

Satué-Gracia, M.T., Frankel, E.N., Rangavajhyala, N., German, J.B. 2000. Lactoferrin in Infant Formulas: Effect on Oxidation. Journal of Agricultural and Food Chemistry, 48(10), 4984-4990.

Talón, E., Vargas, M., Chiralt, A., González-Martínez, C. 2019. Antioxidant starch-based films with encapsulated eugenol. Application to sunflower oil preservation. LWT, 113, 108290.

Wibowo, S., Vervoort, L., Tomic, J., Santiago, J.S., Lemmens, L., Panozzo, A., Grauwet, T., Hendrickx, M., Van Loey, A. 2015. Colour and carotenoid changes of pasteurised orange juice during storage. Food Chemistry, 171, 330-340.

Yang, Y., Fang, Z., Chen, X., Zhang, W., Xie, Y., Chen, Y., Liu, Z., Yuan, W. 2017. An Overview of Pickering Emulsions: Solid-Particle Materials, Classification, Morphology, and Applications. Frontiers in Pharmacology, 8(287).

5. General discussion

The application of roasted coffee oil as a food ingredient requires adequate processing in order to preserve its properties and to facilitate its incorporation. The current literature review presented the use of several polyssacharides and proteins for emulsifying lipid phases by different methods. The main mechanisms proposed in this work aimed at emulsifying roasted coffee oil, a by product of the coffee industry, by using chitosan after modifications. The studied chitosan modifications (self-aggregation and crosslinking) demonstrated to act differently as Pickering particles. Depending on the modification method, the produced particles tend to show distinct adsorption mechanisms onto the oil droplets. It reinforces the need for evaluating their performance in each system separately in order to verify the best application in a given process.

In this way, this doctoral thesis evaluated methods of producing chitosan nanoparticles capable to formulate emulsions containing roasted coffee oil to be subjected to drying processes with the aim of protecting important compounds of oil and improving nutritional and sensory aspects of food products.

Firstly, a previous study determined how the roasted coffee oil emulsification is affected by different concentrations of lipid phase and chitosan nanoparticles in aqueous phase. Emulsions that presented no phase separation after 24 hours under resting were selected as potential systems for encapsulation. The addition of a crosslinking agent, sodium tipolyphosphate (TPP), was used as a mechanism to reinforce the layer of chitosan particles at the oil/water interface.

Data about lipid digestibility showed that free fatty acids release and bioaccessibility of phenolic compounds were influenced by the rheological properties of the emulsions as well as by the droplet size distributions. More viscous emulsions presented lower lipid digestibility and lower bioaccessibility, which was probably related to the presence of phenolic compounds entrapped within the non-digested oil droplets. On the other hand, higher extent of lipid digestion was obtained for emulsions with lower lipid content. It contributed to higher concentration of bioactive compounds in the micellar phase and, thus, higher bioaccessibility.

The way by how each type of chitosan nanoparticles stabilized the emulsions of roasted coffee oil was reported to be dependent on the method of nanoparticles preparation as well as on their concentration in the final emulsions. Suspensions of TPP-crosslinked nanoparticles showed to be more stable due to the higher zeta potential. It means that the electrostatic repulsion among the particles avoided their

aggregation and contributed to a more homogeneous particle size distribution. In addition, smaller nanoparticles were obtained by the resulting particle shrinkage when the short-range attraction occurred between opposite charges of amino groups of chitosan and the TPP phosphates (Wilk et al., 2010). In fact, CS-TPP showed to be adhered to the oil/water interface of separated droplets in the emulsions. Even with an increasing CS-TPP nanoparticle concentration in the suspension, there was no pronounced changes in the apparent viscosity. However, deprotonated chitosan nanoparticles stabilized the emulsions by forming a network in the dispersed phase. It occurred due to the intra- and inter-molecular interactions by the lower repulsion forces between chitosan chains. Increasing the concentration of deprotonated particles interfered in the molecular movement by setting up physical barriers against the flow (Maskan & Göğüş, 2000), suggesting that the chitosan network was reinforced by adsorption in multilayers. This stronger network may be related to the enhanced bioaccessibility to the phenolic compounds in the previous emulsions formulated with deprotonated chitosan, which allowed better protection of the oil droplet against environmental agents.

In order to produce low fat systems, emulsions containing 10% (w/w) of roasted coffee oil were formulated using a nanoparticle concentration of 0.9 g/g in the continuous phase. Emulsions stabilized with deprotonated and crosslinked chitosan in such conditions were subjected to spray-drying and freeze-drying with the aid of maltodextrin as carrier agent. The resulting powders were evaluated concerning the the physical properties, encapsulation parameters and simulated *in vitro* digestibility of the microcapsules. The use of boh chitosan nanoparticles as encapsulating matrix demonstrated high impact on the drying processes, since they improved emulsions stabilization. Consequently, drying well-defined Pickering emulsions increase the drying yield and oil retention in the resulting microcapsules. More hydrophobic powders were obtained from deprotonated chitosan-based emulsions. By the contact angle measurement in the Chapter 3, it was showed that the deprotonation method of chitosan led to particles with higher hydrophobicity than for the crosslinked ones. It caused a decrease in the polar interaction between water molecules and the wall material, reducing the moisture content. However, higher water activity values were obtained for the same microcapsules. The hydrophobic property of the deprotonated chitosan nanoparticles aforementioned weakens the hydrogen bound between water molecules and the matrix, increasing water availability for reactions.

The microstructure of microcapsules containing chitosan nanoparticles showed some aspects to be considered. Microcapsules formed by spray-drying presented more rounded shape, which was able to better entrap the oil and to improve the encapsulation efficiency. On the contrary, the irregular shape of freeze-dried samples tended to form a porous network by the water crystals' sublimation – making the lipid phase partially exposed. This effect is supposed to be greater for the powders produced with crosslinked chitosan. The high ability of those particles to bind the water molecules probably generated more porous in the dried samples, exposing free oil and reducing the encapsulation efficiency. Regardless the type of chitosan nanoparticles, their use as wall material had an important impact in binding the oil to create microcapsules with high oil-loading capacity.

Roasted coffee oil is reported to be as an interesting source of phenolic and volatiles compounds. Thus, the development of methods to improve its protection is highly recommended. Furthermore, important conclusions could be taken based on remained oil inside and out of microcapsules. The content of phenolic compounds and antioxidant activities were higher for freeze-dried samples than spray-dried ones. It may have occurred as a consequence of lower temperature applied during the drying process.

Moreover, a gastrointestinal *in vitro* digestion was simulated in order to verify the release of these compounds and their avalilability to be absorbed into the systematic circulation. During the gastric phase of digestion, the samples are inserted in an acidic pH medium. This condition is suitable for the partial resolubilization of the deprotonated nanoparticles and the consequent release of the oil content during this step (Akbari-Alavijeh, Shaddel, & Jafari, 2020). In spite of that, the amount of bioactive compounds that were able to reach the intestinal phase was higher due to the protective effect attributed to the deprotonated chitosan nanoparticles. Additionally, spray-dried microcapsules had higher bioacessibility was in comparison with freeze-dried ones. It was probably related to their capacity to retain the major amount of initial coffee oil into their spherical structure.

Finally, the protective property of the wall material can be evidenced not only by their ability to control the release of bioactive compounds but also by their capacity for preventing deterioration during storage. For this reason, lipid oxidation and release of volatile compounds over 30 days of storage were evaluated for freeze-dried and spray-dried samples formulated with deprotonated chitosan. The

results showed to be in close aggrement with the previous findings. Spray-dried samples were more efficient for protecting oil compounds against the action of external agents such as oxygen and moisture. The presence of a porous microstrucure and higher content of surface oil in freeze-dried samples promoted a slightly higher oxidation and less effective protection of the volatile compounds. However, the oil encapsulation in both matrices retained a higher percentage of volatile compounds (~70%) over the 30 days of storage when compared to the non-encapsulated oil (~50%).

6. General conclusions

The main conclusions extracted by this doctoral thesis are presented in five different sections according to the different approaches addressed:

6.1. Protein- and polysaccharide-based particles used for Pickering emulsion stabilisation

- Sustainable solid particles have been of interest for stabilization of food emulsions as alternative to surfactants.
- Biopolymer particles must have desired features to be able to act as stabilizers. The partial wettability by oil and water is an important property for the adsorbing at W/O interface.
- Proteins, polysaccharides and protein-polysaccharide complexes have been reported provide Pickering stabilization. However, changes in theis structure are often required to achieve the ideal feature to act as Pickering stabilizers.
- An effective steric structural barrier against coalescence depends on factors as concentration of particles, pH values, protein to polysaccharide ratio, particles sizes as well as processing conditions for emulsifying.
- The three dimensional network in the continuous phase is a good sign to prevent creaming and sedimentation.

6.2. Digestibility and bioaccessibility of Pickering emulsions of roasted coffee oil stabilized by chitosan and chitosan-sodium tripolyphosphate nanoparticles

- Roasted coffee oil concentration plays an important role in rheological behavior, oil droplet size distributions, microstructure of emulsions as well as on their lipid digestibility and bioaccessibility along in vitro digestion.
- The presence of TPP as a crosslinked agent influenced the whole structure of emulsions. Certain process conditions must be taken into account to obtain the desired result.
- Higher viscosity may have an effect on the movement of molecules such as lipase toward droplet surface, which hinders the lipid digestion.

- No correlation between FFAs and surface area of fresh emulsions was found. Structural characteristics throughout gastrointestinal tract may be important factors contributing to the rate and extent of lipid digestion.

- High bioaccessibility of phenolic compounds showed to be related to the high extent of free fatty acids released throughout the gastrointestinal tract.

6.3. Chitosan and crosslinked chitosan nanoparticles: Synthesis, characterization and their role as Pickering emulsions

- Chitosan nanoparticles were produced by self-assembly from deprotonation or by crosslinked from an electrostatic interaction with TPP.

- High zeta potential of solution, partial wettability and biomadal particle size distribution were obtained by both self-assembly and crosslinked chitosan nanoparticles.

- TPP crosslinking enables to obtain smallest particle sizes and greater stability of nanoparticles suspensions.

- Smaller and more spherical droplets were formed in emulsions stabilized by CS-TPP nanoparticles.

- Low repulsion forces of CN particles led to an interaction among them providing the sharing of same particles by oil droplets in the emulsions. The emulsion stabilization occourred due to an interconnected network obtained from the spreading of chitosan in the continuous phase.

- Emulsions formulated with TPP-crosslinked nanoparticles presented lowest viscosity, thus being suitable for processes subjected to high shear rates.

6.4. Roasted coffee oil microcapsules from chitosan-based Pickering emulsions: effect of nanoparticle synthesis and drying methods on physicochemical properties and *in vitro* bioaccessibility

- Freeze-drying was used to obtain microcapsules contained roasted coffee oil stabilized by both self-aggregated and TPP-crosslinked

chitosan nanoparticles whereas spray-drying was suitable only for self-aggregated nanoparticles.

- Chitosan nanoparticles were essential to both drying methods.

- High oil retention and encapsulating efficiency were related to an effective stabilization.

- Microcapsules obtained from self-aggregated chitosan-based emulsions showed more hydrophobic property.

- Spray-drying produced spherical microcapsules with smallest size particles.

- The highest encapsulation efficiency of RCO was achieved by spray-drying process.

- Throughout freeze-drying method the RCO was partially exposed to the environment.

- The porous microstructure of FD samples may allow a better radical scavenging by the antioxidant compounds entrapped into the matrix.

- The higher phenolic compounds and antioxidant activity in the complete digested phase in comparison with the raw material, the higher is the protection.

- Microcapsules formulated with self-aggregated chitosan showed the best performance in protecting the oil providing highest bioaccessibility indexes.

- CMO-SD samples showed better protection of the bioactive compounds until simulated intestinal absorption.

6.5. Storage stability of dried chitosan-based Pickering emulsion containing roasted coffee oil

- Type II sorption isotherms showed that spray-dried samples presented the best capacity for binding water molecules.

- The monolayer moisture content showed lower sorption sites in freeze-dried particles probably due to the higher surface oil content.

- As a consequence of the carrier agentes the powdered samples had a yellowish coloration and slight differences in color parameters occoured during storage.

- Oxidation was slightly favored in freeze-dried particles due to the content of surface oil and water binding properties.
- The period of storage showed an oxidation process but acceptable values of oxidation products were obtained for all samples and volatiles compounds were preserved by microcapsules.

As a general conclusion of this work, it can be stated that emulsification and encapsulation processes can be considered an interesting technology for preventing important compounds of roasted coffee oil. In addition, chitosan-based Pickering emulsions and dried capsules can work as a delivery system for controling the release of lipophilic bioactives and increasing their bioacessibility.

7. Recommendations

As seen as chitosan nanoparticles played an important role in the emulsification of roasted coffee oil by the Pickering method, some additional studies can be carried out to provide a wide kwnoledge about the obtained systems and their applications. Therefore, as recommendations for future works, it is proposed to evaluate:

- A deeper understanding of the mechanisms of particle adsorption onto the oil droplet surface by microfluid assays;

- The performance of the studied chitosan nanoparticles in the emulsification and bioaccessibility of bioactive-rich lipid phase from alternative vegetable sources than coffee beans;

- Different methods for chitosan modification and possible complexation with proteins and their performance in emulsifying the lipid phase;

- The application of additional technologies for emulsification, such as ultrasound application and high pressure homogenization;

- Antimicrobial properties of the encapsulated roasted coffee oil using the different modified chitosan nanoparticles as carrier agents;

- A long-term stability (>30 days) of the microcapsules produced by the different methods and drying techniques in which concerns lipid oxidation, volatile compounds release and physicochemical properties;

- The application of the produced emulsions and/or microcapsules into food products (chocolates, ice creams, baked goods, beverages, etc.) to confer roasted coffee flavor and to replace saturated fats by healthier lipids; and how their addition affect the consumer's sensory perception;

8. Scientific contributions

8.1. Research papers

Ribeiro, E. F.; Borreani, J.; Moraga, G.; Nicoletti, V. R.; Quiles, A.; Hernando, I. Digestibility and bioaccessibility of pickering emulsions of roasted coffee oil stabilized by chitosan and chitosan-sodium tripolyphosphate nanoparticles. *Food Biophysics* 15, 196–205, 2020.

Ribeiro, E. F.; de Barros-Alexandrino, T. T.; Assis, O. B. G.; Junior, A. C.; Quiles, A.; Hernando, I.; Nicoletti, V. R. Chitosan and crosslinked chitosan nanoparticles: Synthesis, characterization and their role as Pickering emulsifiers. *Carbohydrate Polymers,* v. 250, p. 116878. 2020.

Ribeiro, E.F.; Morell, P.; Nicoletti, V.R.; Quiles, A.; Hernando, I. Protein- and polysaccharide-based particles used for Pickering emulsion stabilization. *Submitted to Critical Reviews in Food Science and Nutrition.*

Ribeiro, E. F.; Polachini, T. C.; Alvim, I. D.; Quiles, A.; Hernando, I.; Nicoletti, V. R. Roasted coffee oil microcapsules from chitosan-based Pickering emulsions: effect of nanoparticle synthesis and drying methods on physicochemical properties and in vitro bioaccessibility. *Submited to LWT - Food Science and Technology.*

Ribeiro, E. F.; Polachini, T. C.; Pereira, A. R. L.; Quiles, A.; Hernando, I.; Nicoletti, V. R. Storage stability of dried chitosan-based Pickering emulsion containing roasted coffee oil. *(To be submitted to Food Chemistry)*

8.2. Conference papers

Ribeiro, E. F.; Polachini, T. C.; Quiles, A.; Hernando, I.; Nicoletti, V. R. Influência da reticulação e da concentração de nanopartículas de quitosana na microestrutura e reologia de emulsões contendo óleo de café torrado. 17 de maio de 2019. *Simpósio Comemorativo dos 40 anos da Área de Pesquisa em Sistemas Particulados*, São Carlos.

Silva, J. T. P.; Ribeiro, E. F.; Nicolett, V. R. Crosslinked-biopoplymer nanoparticles stabillizing Pickering emulsions containing rosated-coffee oil. 12-14 de novembro de 2019. *33rd EFFoST International Conference*, Rotterdam, Holanda

Ribeiro, E. F.; Borreani, J. ; Quiles, A. ; Hernando, I. ; Nicoletti, V. R. Pickering emulsions of roasted coffee oil stabilized by chitosan nanoparticles: in vitro lipid digestibility and structure. In: *3rd Foof Structure and Functionality Forum Symposium & IDF Symposium on Microstructure of Dairy Products*. From 3 - 6 June 2018, Montreal, Canada.

Ribeiro, E. F.; Nicoletti, V. R. Comportamento reológico de emulsões de óleo de café estabilizadas por partículas de quitosana. In: *VI Simpósio de Engenharia e Ciência de Alimentos*. De 03 a 07 de dezembro de 2018, São José do Rio Preto.

9. References

Akbari-Alavijeh, S., Shaddel, R., & Jafari, S. M. (2020). Encapsulation of food bioactives and nutraceuticals by various chitosan-based nanocarriers. Food Hydrocolloids, 105, 105774.

Anese, M.; de Pilli, T.; Massini, R.; Lerici, C. R. (2000). Oxidative stability of the lipid fraction in roasted fraction in roasted coffee. Italian Journal of Food Science, 12, 4, 457-462.

Araiza-Calahora, A., Akhtar, M., & Sarkar, A, (2018). Recent advances in emulsion-based delivery approaches for curcumin: From encapsulation to bioaccessibility. Trends in Food Science & Technology, 71, 155-169.

Berton-Carabin, C. C., and K. Schroën. (2015). Pickering Emulsions for Food Applications: Background, Trends, and Challenges. Annual Review of Food Science and Technology: 6(1), 263–297.

Cárdenas, C.; Quesada, A. R., Medina, M. Á. Kahweol, a coffee diterpene with anti-inflammatory properties. In: PREEDY, V.R. (Ed.). Coffee in Health and Disease Prevention, 1 Ed. UK: London, 2015, p. 627-632.

Casas, M. I., Vaughan, M. J., Bonello, P., Gardener, B., M., Grotewold, E., Alonso, A. (2017). Identification of biochemical features of defective *Coffea arabica* L. beans. Food Research International, 95, 59-67.

Hatzold, T. Coffee: Emerging health effects and disease prevention. In: Y. -F. Chu (Ed.). Introduction. New York: John Wiley & Sons, Ltd, 2012, p. 1-20.

Jian, H., Sheng, Y., Ngai, T. (2020) Pickering emulsions: Versatility of colloidal particlesand recent applications. Current Opinion in Colloid & Interface Science, 49: 1-15

Lamothe, S., Guérette, C., & Britten, M. 2020. Nutrient release and oxidative stability during in vitro digestion of linseed oil emulsions produced from cow milk, soy drink, and green tea extract. LWT, 134, 110137.

Liu, Q., Huang, H., Chen, H., Lin, J., Wang, Q. (2019). Food-grade nanoemulsions: preparation, stability and application in encapsulation of bioactive compounds. Molecules, 24, 4242.

Low, L. E., Teng-Hern, T. L., Goh, B-H, Tey, B. T., Boon, H. O., Tang, S. Y. (2019). Magnetic cellulose nanocrystal stabilized Pickering emulsions for enhanced bioactive release and human colon cancer therapy. International Journal of Biological Macromolecules, 127, 76-84.

Maskan, M. & Göğüş, F. (2000). Effect of sugar on the rheological properties of sunflower oil–water emulsions. Journal of Food Engineering, 43(3), 173-177.

McClements, D. J. (2007). Critical review of techniques and methodologies for characterization of emulsion stability. Critical Reviews in Food Science and Nutrition, 47:7, 611-649.

Raba, D. N., Poiana, M-A., Borozan, A. B., Stef, M., Radu, F., Popa, M-V. (2015). Investigation on crude and high-temperature heated coffee oil by ATR-FTIR spectroscopy along with antioxidant and antimicrobial properties. Plos One, 10, 9, 1-20.

Sarkar, A. & Dickinson, E. (2020) Sustainable food-grade Pickering emulsions stabilized by plant-based particles. Current Opinion in Colloid & Interface Science, 49: 69–81

Singh, C. K. S. S., Lim, H-P., Chan, E-S. (2021). Spray-dried alginate-coated Pickering emulsion stabilized by chitosan for improved oxidative stability and in vitro release profile. Carbohydrate Polymers, 251, 117110.

Stasse, M., Laurichesse, E, Vandroux, M., Ribaut, T., Hérogueza, V., Schmitt, V. (2010) Cross-linking of double oil-in-water-in-oil emulsions: A new way for fragrance encapsulation with tunable sustained release. Colloids and Surfaces A: Physicochemical and Engineering Aspects, 607, 125448.

Wilk, A., Huißmann, S., Stiakakis, E., Kohlbrecher, J., Vlassopoulos, D., Likos C. N., Meier, G., Dhont, J. K. G., Petekidis, G. & Vavrin, R. (2010). Osmotic shrinkage in star/linear polymer mixtures. European Physical Journal E, 32, 127-134.